PB2001-105577

Final Report

ENHANCEMENT OF FLORIDA HIGHWAYS USING RESULTS FROM AN IMPROVED FIELD PERMEABILITY TEST DEVICE (FPTD)

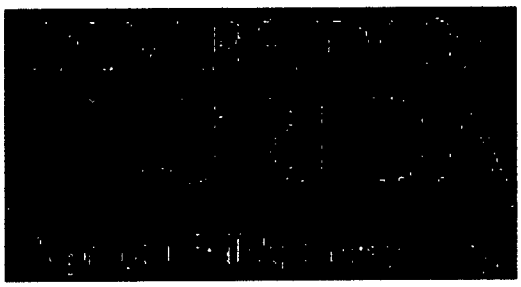

Contract Number BB-896

UF 4504660-12

Submitted from:
University of Florida
Department of Civil and Coastal Engineering

Submitted by:

David Bloomquist, Ph.D., P.E.
Department of Civil and Coastal Engineering
345 Weil Hall
PO Box 116580
Gainesville, FL 32611

TABLE OF CONTENTS

page

APPENDICES

LIST OF TABLES

LIST OF FIGURES

EXECUTIVE SUMMARY

Each year the Florida Department of Transportation (FDOT) spends millions of dollars maintaining the state's roads and highways. These costs are anticipated since all pavement systems are exposed to harsh environmental conditions jeopardizing their integrity and serviceability. Thus, the FDOT has invested their resources in providing a quality system that will minimize the public's cost in road repairs and maintenance, which will lead to a reduction in traffic delays and accidents.

Estimates indicate that the long term cost of poorly drained roads is more than double the cost of roads constructed over well draining material. It is also estimated that the service life of roads constructed over well draining material can exceed that of poorly drained roads by as much as three times. Even with this statistic, primary emphasis in current pavement design continues to focus on strength rather than drainability.

The FDOT recognizes the importance of providing adequate drainage to pavements and in 1995 initiated a two-year research project with the University of Florida. The objective was to design and build a device capable of measuring the insitu permeability of base, sub-base, and subgrade material. In 1998, the project was reinstated with the University of Florida to address safety and time saving issues.

The Field Permeability Testing Device consists of a trailer-mounted probe that is hydraulically pushed into the ground. Located at the end of the probe is a 1.74 cm cylindrical porous element. Once inserted, water is forced out through the element and either a constant or falling head test can be conducted. The device is ballasted with twin polyethylene water tanks and is equipped with hydraulic leveling jacks. A coring device and a portable generator are also included.

Results to date indicate a trend may exist between standard field and this insitu permeability device. However, due to the dissimilarity in the test procedure and boundary conditions, a strong correlation may not exist. Thus, the FDOT plans to conduct field tests on a variety of new and existing pavement bases in order to develop a correlation between pavement performance and the insitu permeability. These would include pavements that have failed as well as those performing well. The FDOT plans to establish a database where the following information could be assessed:

1. New pavement designs in terms of stability, density, and permeability.
2. Recently constructed pavements for QA/QC verification.
3. The condition of existing pavements. The location of potential drainage problem areas could result in more efficient use of funds for preventive maintenance as opposed to repair expenditures.

CHAPTER 1
INTRODUCTION

Each year the Florida Department of Transportation (FDOT) spends millions of dollars maintaining the state's roads and highways. Since all pavement systems are exposed to harsh environmental conditions, regularly scheduled maintenance costs are always anticipated. Because of these high costs, the FDOT has invested their resources into combating these issues with the intent of producing long lasting pavement systems.

Most damages and failures are associated with prolonged exposure to heavy traffic loads along with changing environmental conditions such as temperature fluctuations and precipitation. The focus of this research is to develop a device that could be used to analyze the effect that soils, with poor draining characteristics, have on pavement performance. The amount of rainfall that seeps through the cracks and joints and is retained is dependent on the permeability of the underlying material. If water is retained for a significant period, then a negative impact could result.

Retained water can lead to pavement failure in three ways. First, a pumping effect can occur under the cyclic action of heavy wheel loads. Water is forced to escape through the cracks and joints in response to the sudden increase in pressure while eroding supporting material in the process. Second, the pressure distribution acting along the sub-grade does not reduce to its idealized magnitude. It is assumed during design that the pressure decreases with increasing depth. Under saturated conditions, the pressure acting on the surface will be equivalent to the pressure acting on the sub-grade. Therefore, excess deformations will occur. Third, freezing conditions will cause the retained water

to expand, resulting in upward deflections of the pavement surface. A further discussion of these three effects is presented in Chapter 2.

The Florida Department of Transportation has recognized the need to provide adequate drainage to pavement systems, and in mid 1995 initiated a two-year research project with the University of Florida to design and build a field permeability testing device (FPTD). The objective was to develop a device that measures the permeability of base and a sub-base material while being operationally simple, repeatable, cost effective, and reliable. After 1996, an initial prototype was completed and operational. At that time, the FDOT inherited the device for their own use until 1998 when the project was reinstated at the University of Florida.

The renewed contract called for several modifications and enhancements to the device. After some experience was gained, a few shortcomings were discovered therefore improvements were called for. Since late 1998, the device (Figure 1-1) has been under reconstruction to satisfy the FDOT requirements with several changes being made. Chapter 3 discusses all of the main features of the device and Chapter 4 discusses the modifications that have been implemented under the new contract.

The extended time with the FPTD has provided the opportunity to reevaluate the theory associated with determining the permeability of the soil with a porous probe. The original theory by Hvorslev was discussed and compared with the Packer/Lugeon equation and a finite element analysis. A discussion of this topic is presented in Chapter 5.

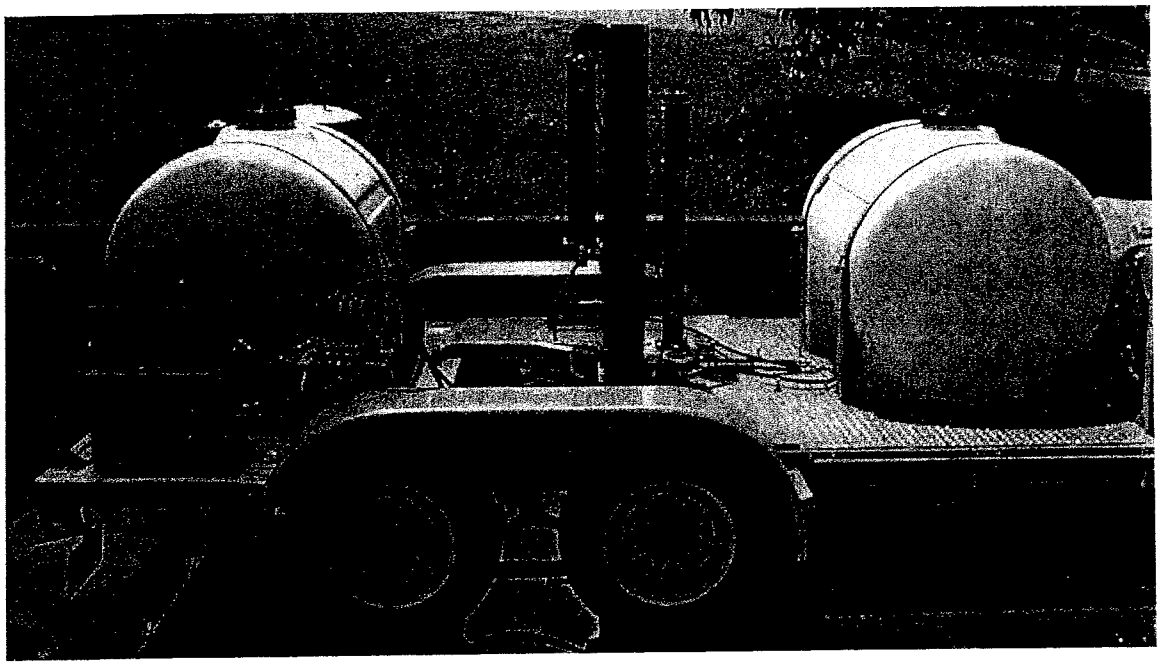

Figure 1-1: Field Permeability Testing Device (FPTD).

To verify that the device was indeed measuring the permeability with reasonable accuracy, a study was conducted that compares the results from the device to another field method. The other method chosen was the ASTM standardized double ring infiltrometer test. The verification procedure called for a double ring test over a location with uniform soil immediately followed by a test using the FPTD. The probe was positioned exactly over the center of the double ring test location to eliminate any effects of variability. Results from this study are discussed in Chapter 6. An overview with concluding comments is made in Chapter 7.

CHAPTER 2
REVIEW OF LITERATURE

Influence of Drainage on Pavement Performance

Prior design guidelines emphasize the strength of the pavement system rather than the potential for rapid internal drainage as the key factor for a long design life. Roadways constructed under this criterion are susceptible to major distress when water, infiltrated through cracks and joints, is retained. Under saturated conditions, three events can occur leading to failure or costly damages. The first event is when water is pumped through cracks and joints under heavy wheel loads. This discharge has the potential to erode fine material leaving the pavement unsupported. The second event is when the pressure distribution acting on the sub-grade material does not reduce to its idealized value as assumed during the design. The pressure experienced by the sub-grade is equivalent to the pressure acting on the surface thereby increasing the potential for excess deformations to occur. The third event occurs under frost action. The expansion of water in freezing conditions will result in upward vertical deflections of the pavement leading to failure. These three critical events are discussed in further detail below.

Effect of Pumping

Figure 2-1 illustrates the influence of water on pavements under heavy dynamic wheel loads. In saturated conditions, water will exit through the path of least resistance under an applied instantaneous pressure caused by heavy wheel loads. Since most base and sub-grade materials are not free flowing, water is forced through the cracks and joints

in the pavement as a means to relieve the excess pore pressure. After prolonged cycles of discharge, erosion will begin to occur reducing the amount of supporting base material directly underneath the surface pavement. Eventually, the pavement will fail when it can no longer bridge the expanding voids.

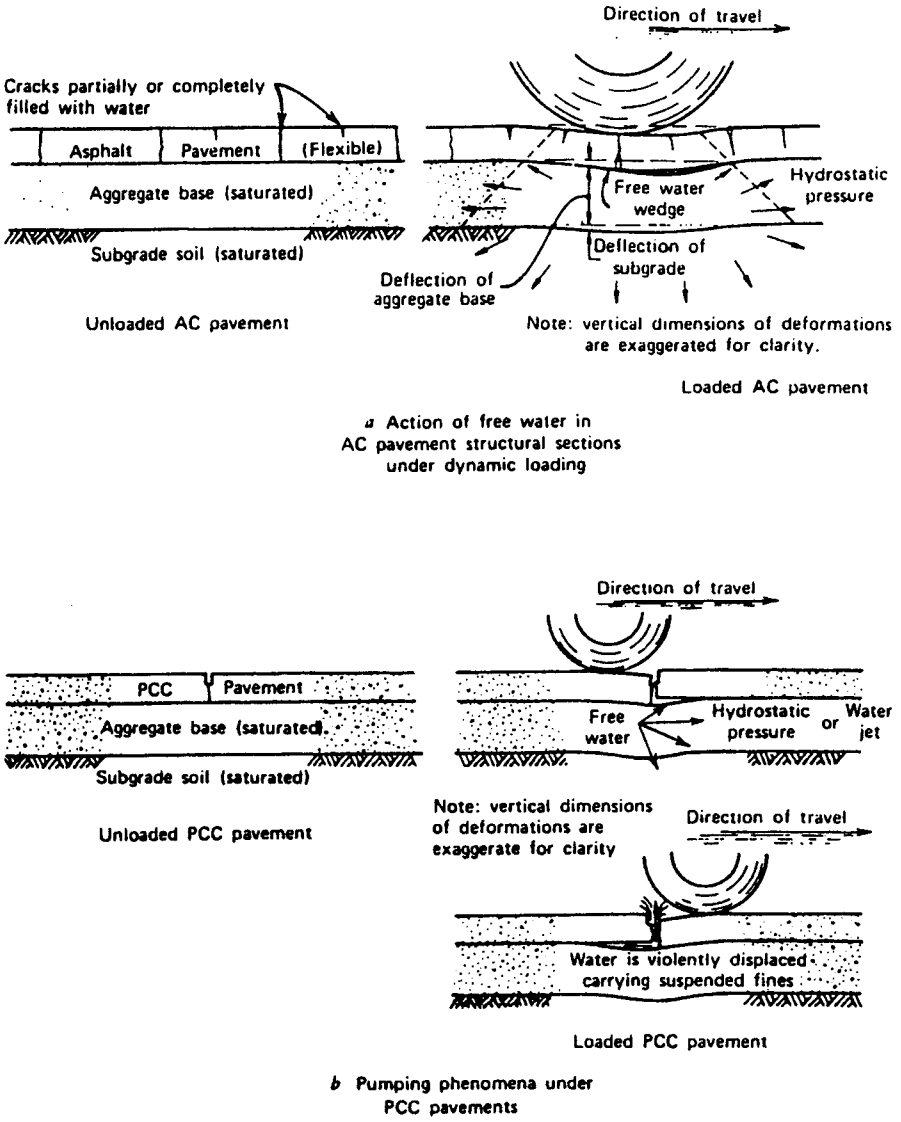

Figure 2-1: Traffic impact on saturated pavements (Cedergren, 1987).

Effect of Saturated Conditions on the Pressure Distribution Acting on the Subgrade

Pavement base and sub-base materials perform several functions for the entire roadbed structure. One of the tasks involved is to reduce the pressure acting on the sub-grade by expanding the pressure distribution. This effect is minimized as the base material becomes fully saturated (Figure 2-2). Since the sub-grade typically does not have the strength capacity to carry such loads, excess deflections will result.

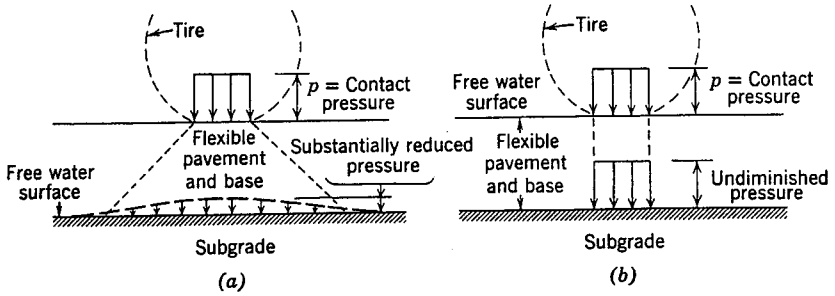

Figure 2-2: (a) Normal design assumption is that the subgrade is saturated but the structural section is well drained. (b) Idealized condition existing in flooded structural sections (Cedergren, 1989).

Effect of Frost Action

The first and second events involved a failure of the pavement due to loss of material or excess deflections. The third event, frost action, is associated with an expansion of the material. As water freezes, the volume increases therefore applying a stress on the pavement from below.

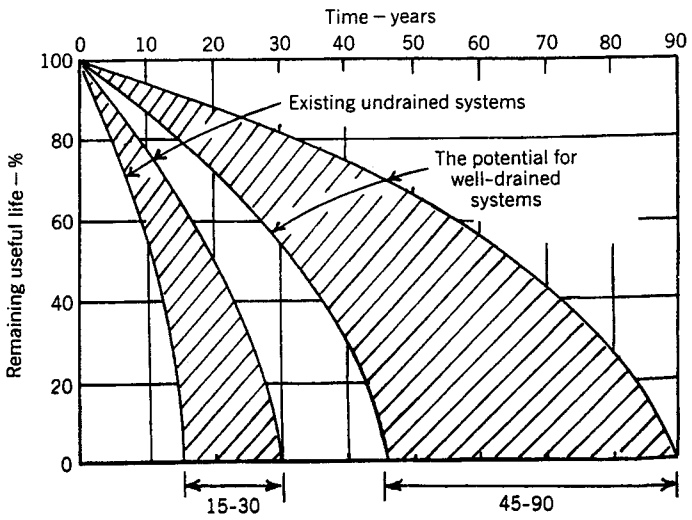

Figure 2-3: Potential life expectancies of drained and un-drained pavements (Cedergren, 1989).

Cost Comparison

Only recently have pavement designers considered the importance of adequate drainage in roadbeds. Changes are being made in standard design guidelines, but millions of miles of existing roads and highways with poor drainage capacities are in use today. Billions of dollars are spent each year in maintenance and repairs of such roads. Estimates indicate that the long-term cost of poorly drained roads is more than double the cost of roads constructed over well-draining material. It is also estimated that the service life of roads constructed over well-draining material can exceed that of poorly drained roads by as much as three times (Figure 2-3).

Coefficient of Permeability

The coefficient of permeability defines the relationship between the rate of flow of water through a unit area of soil and the driving forces. Most disciplines refer to it as the hydraulic conductivity but is simply referred to as the permeability by most civil

engineers. Other names include the engineer's coefficient as well as Darcy's coefficient. Darcy was the first to suggest through experimental observation that a linear relationship existed between the rate of flow of water through a soil and the driving forces. The most common form of Darcy's law used in soil mechanics is written as

$$q = -k\,i\,A \tag{2-1}$$

where q = flow rate (L^3 / T)

i = hydraulic gradient (L / L)

A = total cross-sectional area of flow (L^2)

k = coefficient of permeability (L / T).

Based on Darcy's law, the coefficient of permeability is defined as the discharge velocity under a unit hydraulic gradient. Alternative descriptions include the ease with which a fluid passes through a porous medium.

Factors Influencing the Permeability

The permeability is not dependent on soil type and composition alone, it is a function of several factors widening the variability encountered even within the same site. For this same reason, it is difficult to accurately assess the field permeability from laboratory tests. Samples extracted from the field are always disturbed. The lab technician is then expected to remold the sample into the same soil structure – highly improbable. Even if the composition of the sample is maintained the other factors are unlikely to be as well. These factors include (Cedergren, 1989):

1. The viscosity of the flowing fluid (water).
2. The size and continuity of the pore spaces or joints through which the fluid flows, which depends in soils on:

(a) The size and shape of the soil particles,

(b) The density,

(c) The detailed arrangement of the individual soil grains called the structure.

3. The presence of discontinuities.

Not only does the soil lose its structure when extracted, but also the same density and any discontinuities present are lost. Each factor is further discussed in detail below.

Viscosity

Viscosity is the measurement of resistance or drag of a fluid when in motion. It is equivalent to an internal friction; acting within the fluid as each layer slips and move in relation to one another. Viscosity of any fluid is a function of temperature. As the temperature increases, the viscosity of the fluid decreases (Figure 2-4). Thus, the permeability of the fluid through a porous media increases.

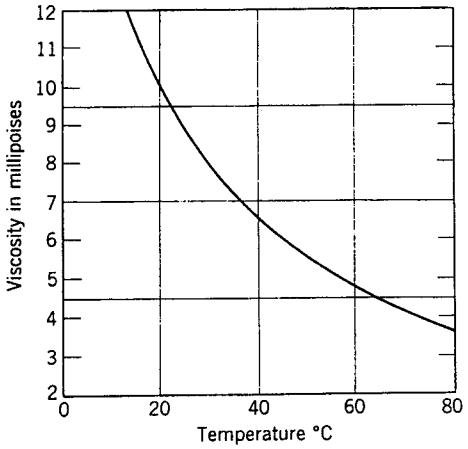

Figure 2-4: Viscosity of water as a function of temperature.

It is then customary to standardize the permeability values in relation to temperature to eliminate the effect of viscosity. 20° C or 70° F is the accepted standard in

practice. To standardize the permeability from any temperature, the following ratio is used:

$$k_{20} = k_T \frac{\eta_T}{\eta_{20}} \tag{2-2}$$

where k_{20} = coefficient of permeability at 20°C

k_T = coefficient of permeability at the test temperature

η_T = viscosity of the fluid at the test temperature

η_{20} = viscosity of the fluid at 20°C.

Size and Shape of the Soil Particles

Theoretical solutions have suggested that the permeability is proportional to the square of the diameters of the pore spaces and the square of the diameters of the soil particles. Figure 2-5 correlates the permeability to the soil type and density. The quantity, characteristic, and distribution of the finest fractions significantly impact the permeability of the soil.

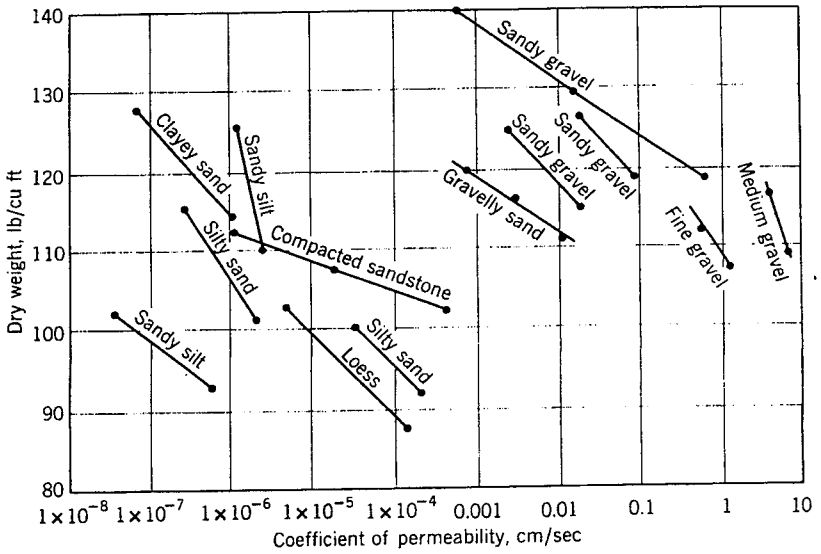

Figure 2-5: Coefficient of permeability as a function of the dry unit weight and soil type (Cedergren, 1989).

Table 2-1 relates the effect of fines with the permeability. A seven- percent increase in the quantity of fines passing the No. 100 sieve, after no fines were present, reduces the permeability by as much as 99 percent.

Table 2-1: Influence of fines on permeability (Cedergren, 1989).

Percentage Passing Number 100 Sieve	Permeability, ft/day
0	80 to 300
2	10 to 100
4	2 to 50
6	0.5 to 20
7	0.2 to 3

Density of the Soil

Density variations do not influence the permeability as much as the particle size. Although less important, it can have a substantial influence (Figure 2-5). The denser a soil, the smaller the pores, thus the lower the permeability. However, this relationship loses strength as the range of particle sizes narrows (typically associated with "uniform soils").

Structure of the Soil

The soil structure or particle arrangement affects the permeability in two ways:

1. By sorting or stratification,
2. By detailed orientation of the particles.

The most illustrative example of the effect of stratification occurs in water-deposited soils. Such soils are slowly deposited over long periods of time in horizontal layers with each layer varying in grain-size distribution and permeability. Water-deposited soils and

other natural soil deposits are generally more permeable in the horizontal direction when contrasted to the vertical. Contrary examples include windblown sands and silts whose permeability profile is greater in the vertical than the horizontal. In these cases it is believed that tubular voids left behind by rotted plants and grass roots provides a quicker route for the water in the vertical direction.

Small particles and fines should be emphasized when focusing on particle orientation. As tabulated in Table 2-1, a small increase in the amount of fines has a drastic effect on the permeability of the soil. Besides the amount of fines present, the location of such fines is important as well. The permeability of a soil would be much greater if all the fines were balled up than if the same amount were evenly dispersed.

Presence of Discontinuities

The detection of discontinuities within a large soil mass is unlikely when laboratory or small-scale insitu permeability tests are performed. Discontinuities can be categorized as joints, seams, cracks, or channels allowing water to flow at higher quantities than the soil or rock in-between. Thus tests performed on small samples or individual cores can be misleading.

Large-scale pumping tests are the only permeability methods available that account for discontinuities. Such tests are only performed when necessary and are not required in every situation.

Methods for Determining Permeability

The methods available to determine the coefficient of permeability can be categorized into three sections:

1. Laboratory methods

2. Field or insitu methods
3. Indirect methods.

Laboratory Methods for Determining the Coefficient of Permeability

The advantage to laboratory methods for permeability measurement is that all variables of Darcy's law are easily controlled. In most cases the length and area of the sample and the applied head are predetermined while the exit flow rate is measured. The permeability is then easily calculated for the laboratory sample. Another advantage is the ability to model variable conditions in the laboratory; which would otherwise be impossible using insitu methods. For example, if the permeability of a soil mass would be of interest after the construction of a dam, then the effective stress acting on the sample could easily be altered to model expected conditions. Such modeling is important since a change in the void ratio is proportional to the change in effective stress. Field measurements prior to the construction of the dam would incorrectly reflect the field conditions after completion.

In spite of these advantages, there are several sources of errors that must be considered.

1. Soil samples are always disturbed to some degree. Once extracted from the field, a relief from confining pressures would result in increasing void ratios. Thus, particle arrangement and structure is never identical.
2. Most soils encountered in the field are anisotropic (the permeability in the vertical direction is not equal to the permeability in the horizontal direction). The problem arises in orientation. The flow direction in the field may not be the same as during laboratory testing.

3. Larger gradients are often applied to lab samples than are encountered in the field. As the gradient increases, the pressure acting on the sample increases thus reducing the void ratio and decreasing the permeability.
4. If the soil in the field is fully saturated, then entrapped air in the lab sample could provide misleading results.
5. The flow path along the smooth walls of the permeameter will encounter less resistance than through the body of the sample.
6. Some hydraulic head is lost through the porous stones and in the water lines. It is common practice to assume otherwise.
7. Leakage from the permeameter and tubing is a common source of error. Water is also lost due to evaporation during long test durations.

Laboratory methods that will be discussed in this section include the flexible wall permeameter along with the constant and falling head standard test methods.

Flexible wall permeameter. This test method is ideal for undisturbed or compacted specimens with a coefficient of permeability of less than or equal to 1×10^{-3} cm/s. The advantage of this method is in the ability to vary the effective stress on the specimen, thus having a broad range of applications that spans from dam construction to landfill liner analysis. Guidelines for this test method are outlined in ASTM 5084.

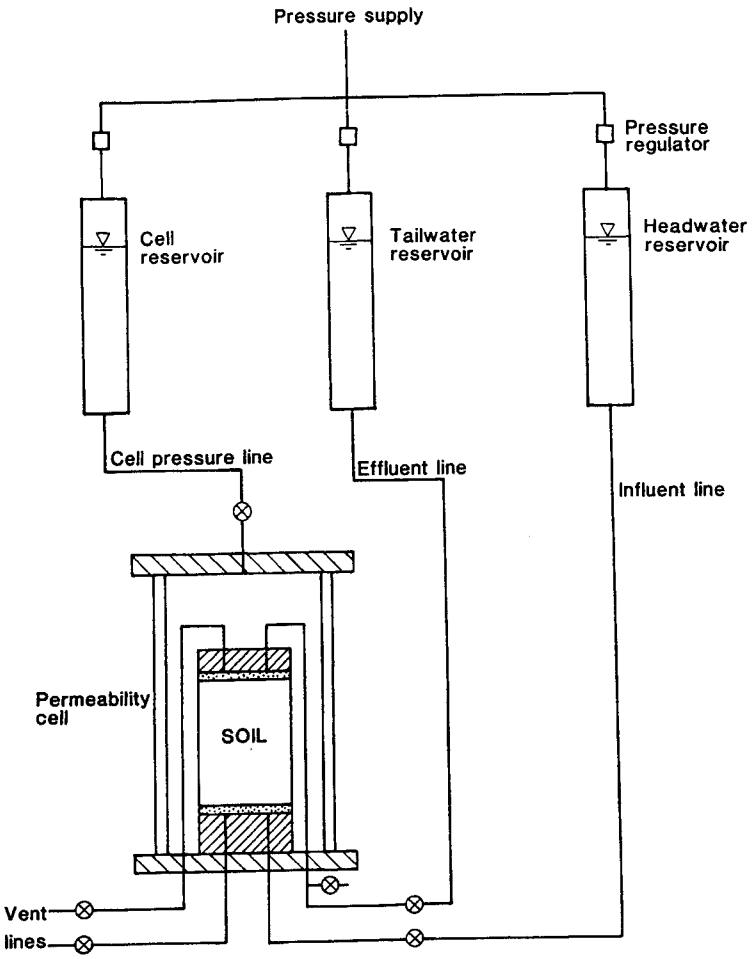

Figure 2-6: Flexible wall permeameter (ASTM D 5084).

A schematic of the apparatus is shown in Figure 2-6. A specimen is placed in a permeameter cell where the inlet, outlet, and surrounding pressures are controlled. During the test, the water levels in the burettes are recorded as water flows from one burette, then through the sample, and into the other.

Constant and falling head test. Either is used for cohesionless soils, but the expected permeability is the determining factor for choosing between the constant head or the falling head test. The constant head test is more applicable to relatively permeable soils since long test durations can result in evaporation losses. In contrast, the falling head test

may be unsuitable for permeable soils because of the inaccuracy in time measurement as the water column drops rapidly. It is suggested by Terzaghi and Peck that the constant head test is applicable for soils with a coefficient of permeability not less than 10^{-3} cm/s, and the falling head test for soils with a coefficient of permeability not greater than 1 cm/s.

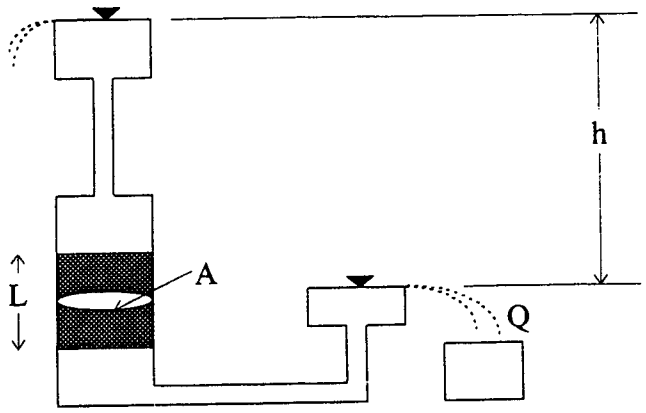

Figure 2-7: Constant head test.

Figure 2-7 illustrates the concept of the constant head test. A constant head of water is applied to a soil mass inside a cylindrical mold. The volume of water collected as it passes through the soil and the time duration is recorded. The permeability of the soil is then calculated using Darcy's law.

The falling head test concept and parameters are illustrated in Figure 2-8. The setup is almost identical to the constant head test expect for the addition of a standpipe in which the hydraulic head will be allowed to fall. Time is measured from an initial height until the water level reaches a predetermined final height. The permeability of the soil is then calculated by integrating Darcy's relationship and applying the following relationship:

$$k = \frac{a \cdot L}{A \cdot t} \log_e \frac{h_i}{h_f} \qquad (2\text{-}3)$$

where t is the time between h_i and h_f, and all other terms are defined in Figure 2-8. It should be noted that this test is not designed for undisturbed sample testing and that procedures should follow ASTM D 2434 guidelines.

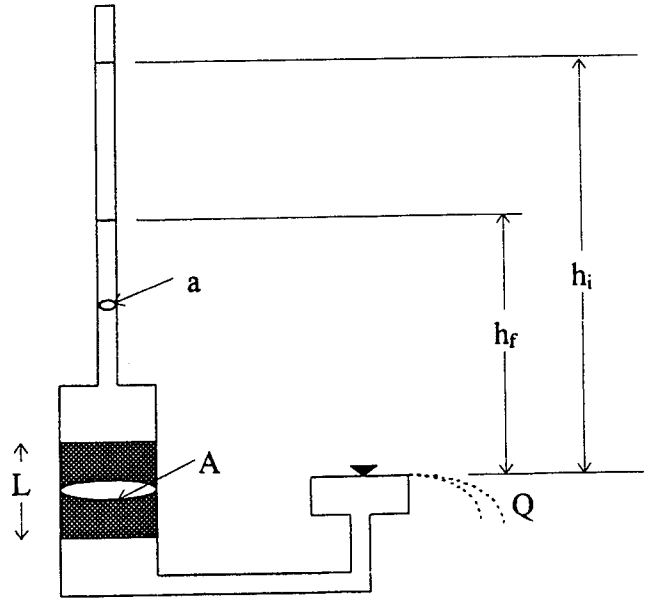

Figure 2-8: Falling head test

Insitu Methods for Determining the Coefficient of Permeability

Field permeability tests have the advantage of representing actual conditions, which might otherwise be difficult to replicate in the laboratory, and the advantage of accounting for possible anomalies present within the soil mass. However, an uncertainty lies in the analysis method when calculating the permeability. It is difficult to assess the hydraulic gradient acting on the soil mass and therefore difficult to assess the effective area under influence. Most methods of calculation are based on theoretical conclusions and modified using correlation studies.

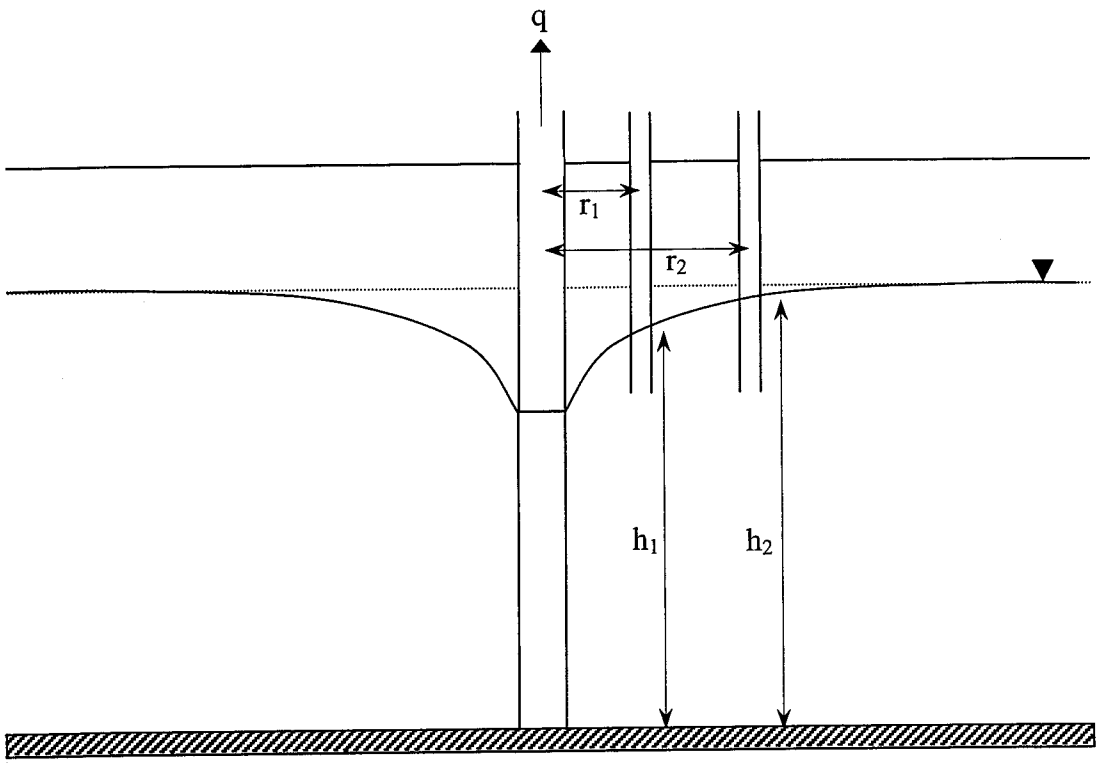

Figure 2-9: Well-pumping test

Field methods that will be discussed in this section include the well-pumping test, packer test, infiltrometers, and the open-end borehole test.

Well-pumping test. The well pumping test is a large-scale test, in which water is drawn out of a well while ground water level readings are made in several nearby locations. Figure 2-9 illustrates the arrangement of the well-pumping test. At least two observation wells at different radial distances are required. The permeability is determined using the following formula:

$$k = \frac{2.3 \cdot q \cdot \log_{10} \cdot (r_2/r_1)}{\pi \cdot (h_2^2 - h_1^2)} \qquad (2\text{-}4)$$

The well formula is based on the following assumptions (Cedergren, 1989):

1. The well penetrates the full thickness of the water-bearing formation.

2. A steady-state flow condition exists.
3. The water-bearing formation is homogeneous and isotropic and extends an infinite distance in all directions.
4. The Dupuit assumption is valid.

The Dupuit assumption assumes that the hydraulic gradient is constant at any point from the top to the bottom of the water-bearing layer and is equal to the slope of the water surface. The accuracy of this assumption increases with the radial distance from the well.

Reliability of results depends on how well the above assumptions are met. True equilibrium may require extremely long periods of pumping, however satisfactory results can be obtained by pumping at a steady state for periods that range from a few hours to a few days.

Packer test. The packer test is primarily used to test in bedrock above or below the water table. The packers are designed to isolate the section being tested. Figure 2-10 details the test arrangement and identifies the variables used for computation. The Permeability is calculated from the following formulas:

$$k = \frac{q}{2 \cdot \pi \cdot L \cdot h} \sinh^{-1}\left(\frac{L}{2r}\right), \text{ for } r \leq L < 10r \qquad (2\text{-}5)$$

$$k = \frac{q}{2 \cdot \pi \cdot L \cdot h} \ln\left(\frac{L}{r}\right), \text{ for } L \geq 10r \qquad (2\text{-}6)$$

The most frequent causes of error include (Cedergren, 1989):

1. Leakage around the packers.
2. Clogging due to sloughing of fines or sediment in the test water.

3. Air locking due to gas bubbles in soil or water.
4. Flow of water into cracks in soft rocks that are opened by excessive head in test holes.

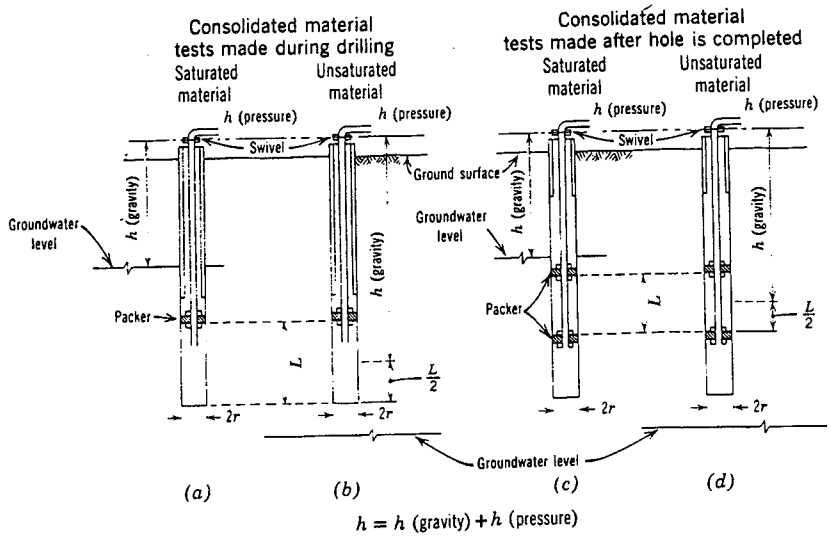

Figure 2-10: Packer test (Cedergren, 1989).

Infiltrometers. Four infiltrometers, shown in Figure 2-11, will be briefly discussed. Infiltrometers are used to conceptually model ponding effects from rainfall. They are primarily tested on clay liners and retention ponds were insitu measurements are required by environmental agencies. They also offer a simple and low cost solution to obtain the surface infiltration rate in any situation.

Infiltration rates are determined by dividing the quantity of water absorbed by the area and time. Driving head is not considered during calculations but should be reported with final results. Typically, the head of water applied is selected on the basis of what is expected to occur under assumed conditions.

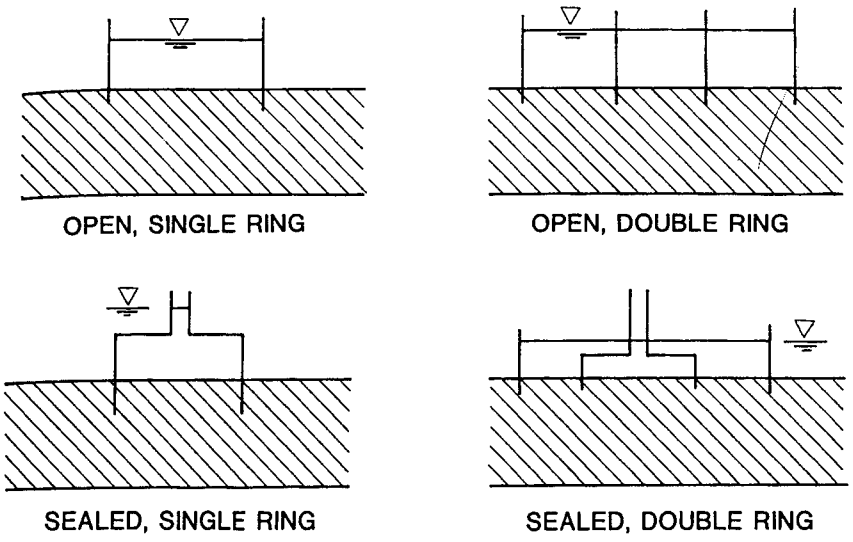

Figure 2-11: Four basic types of infiltrometers (Daniel, 1989).

Choosing between the four methods is guided by soil type and the quality of the information required. For permeable materials (> 10^{-5} cm/s), the open single or double ring method is adequate. For low permeable materials, the closed method types provide greater accuracy. In both cases, the double ring method has one advantage over the single ring in that lateral flow is minimized from the center ring.

Open-end borehole test. This test consists of measuring the rate of flow of water through an open-end casing drilled to the desired depth (Figure 2-12). It can be performed above or below the water table.

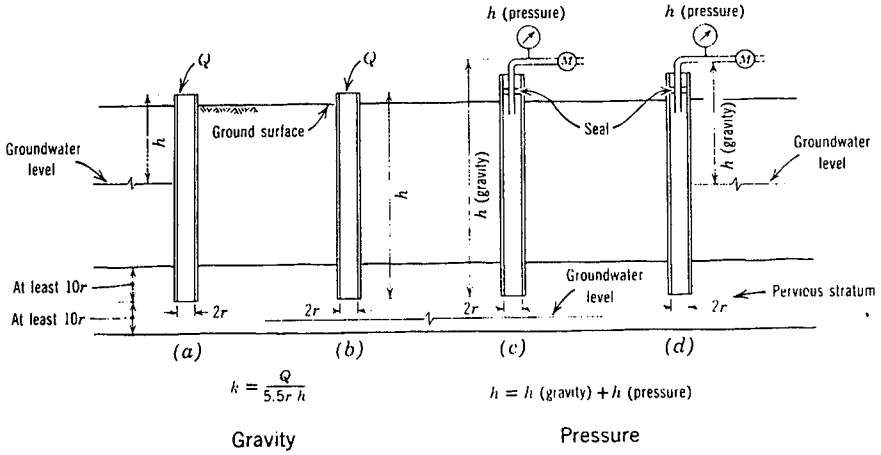

Figure 2-12: The open-end borehole test (Cedergren, 1989).

Since steady state flow is seldom obtained above the water table, the Bureau of Reclamation considers surging of a few tenths of a foot for about five minutes as satisfactory. The relationship of the permeability to the constant rate of flow through the bottom of the casing was determined from electric analog tests. From USBR 67, the coefficient of permeability is determined as follows:

$$k = \frac{q}{5.5 \cdot r \cdot h} \tag{2-7}$$

Indirect Methods for Determining the Coefficient of Permeability

Indirect methods provide an approximation of the coefficient of permeability that may be used for preliminary analysis or estimations. The most common indirect methods make use of an extension of the one-dimensional consolidation test and a grain size distribution analysis.

One-dimensional consolidation test. Although ASTM guideline (D 4186) for the one-dimensional consolidation test does not provide an indirect method for permeability calculations, the vertical permeability can be approximated using the following formula:

$$k_v = \frac{-0.434 \cdot \Delta H \cdot \overline{H} \cdot \gamma_w}{2 \cdot \overline{\sigma}_v' \cdot \Delta t \cdot \left(1 - \frac{\overline{U}_b}{\overline{\sigma}_v}\right)} \tag{2-8}$$

where ΔH = change in height of the specimen between time steps

$\overline{H}$ = average height between time steps

Δt = elapsed time between time steps

γ_w = unit weight of water

$\overline{\sigma}_v'$ = average effective stress between time steps

$\overline{U}_b$ = average change in pore water pressure at the bottom of the sample between time steps.

The consolidation cell permeameter is shown in Figure 2-13.

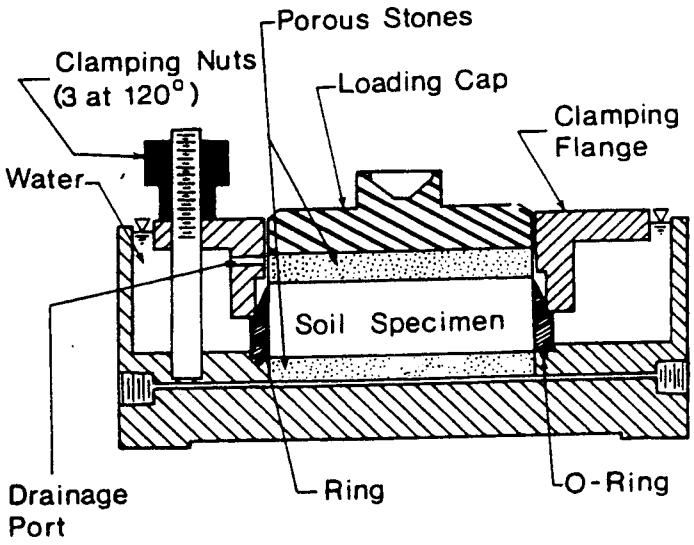

Figure 2-13: One-dimensional consolidation cell (Olson and Daniel, 1981).

Sieve analysis. In 1911, Hazen developed a relationship for clean filter sands between the grain size distribution (ASTM D 422) and the coefficient of permeability:

$$k = C_1 D_{10}^2 \tag{2-9}$$

where $k =$ permeability in cm/s.

$D_{10} =$ effective size in millimeters corresponding to 10% passing.

$C_1 =$ from 0.4 to 1.2. A value of 1.0 is often used.

CHAPTER 3
DEVICE CONFIGURATION

In chapter five, several theories will be discussed that relate the exit flow rate through a porous probe at an applied head with the permeability of the soil. This chapter will discuss the means and equipment necessary to penetrate the probe through base and sub-base layers and then control and measure the variables associated with determining the permeability.

Each major component will be discussed in detail identifying its purpose, location within the device, and limitations. The location relative to the device is graphically shown in Figure 3-1.

Trailer

The trailer provides a stable platform during testing and was selected based on its size and load capacity. After placement of other components, enough space remains for an operator to comfortably maneuver about.

The trailer is supported on two 3500-lb capacity axels with 15-inch tires and installed with a brake system for smoother control. The brake system is a four-wheel surge hydraulic system with breakaway capabilities.

The trailer deck has dimensions of 6 x 12 feet and lies between two 1-foot wheel wells. The deck is divided into three (4 x 6 ft) sections with the outer panels made of quarter-inch thick diamond plate steel and the center with a one-inch thick steel

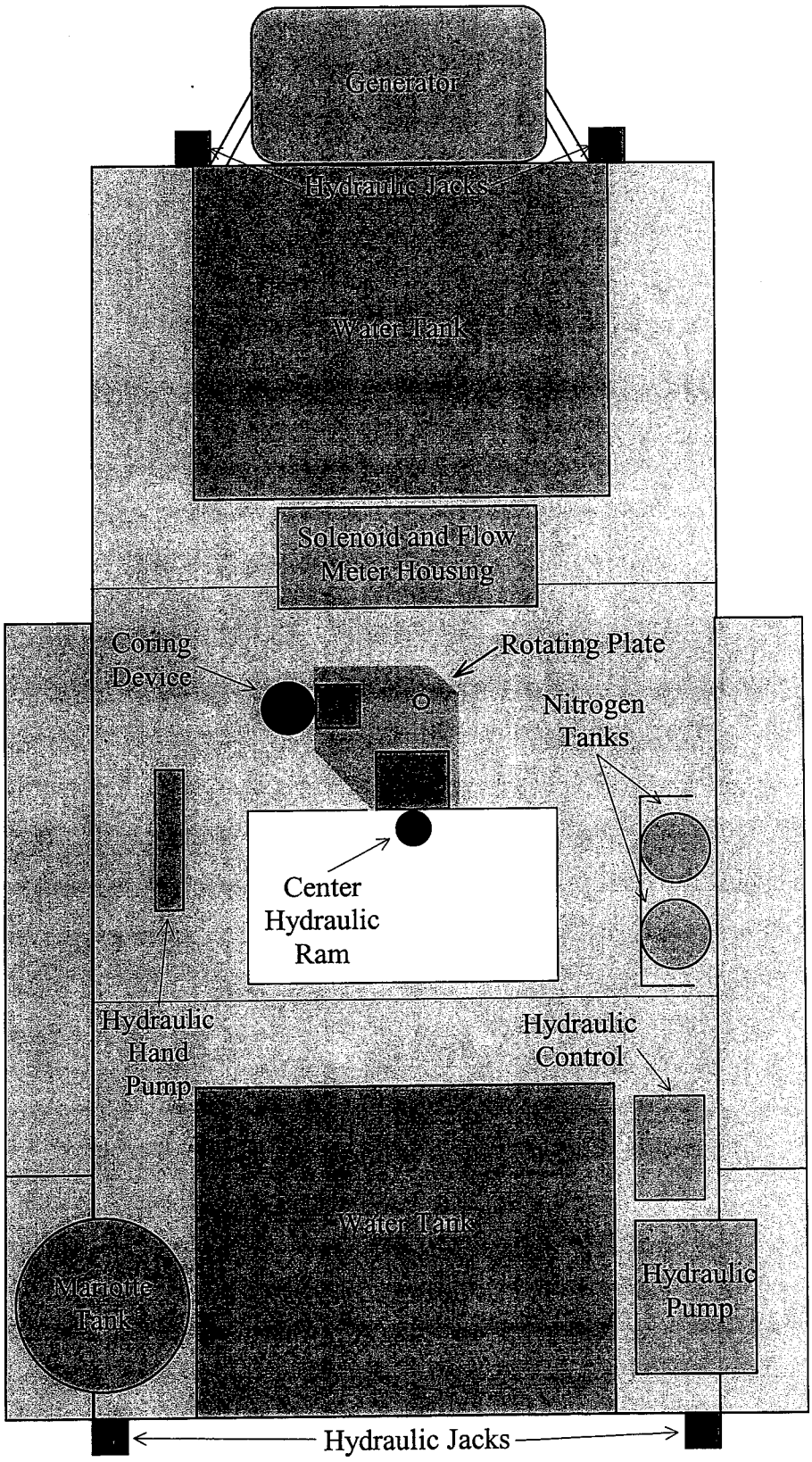

Figure 3-1: Device Configuration

plate. The center plate was installed to provide additional reaction weight and the width of the rear panel was expanded to eight-feet to supply extra space.

Water Tanks

The water tanks (Figure 3-2) provide the option of expanding the reaction weight if necessary. They can be filled near or at the testing site so that the weight is at its minimum as it is being towed, therefore the stress applied to the towing vehicle is reduced.

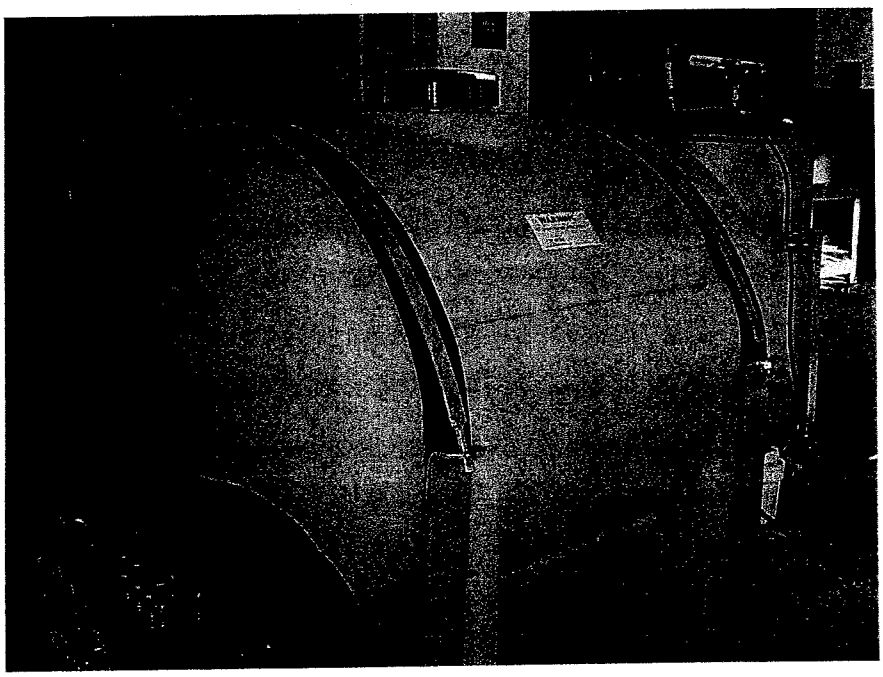

Figure 3-2: One of two water tanks.

Each polyethylene tank has a storage capacity of 230 gallons. When filled, a combined 3840 pounds of reaction is supplied. In addition, the water can be used to refill the Mariotte tank when other sources are not available, and can be used during coring

operations (a pump is necessary in both cases). Both tanks are secured with two steel straps anchored to the trailer deck.

Hydraulic System

To raise and lower the trailer, hydraulic cylinders (Figure 3-3) are placed at each corner. A center ram (Figure 3-4) is used to penetrate the probe into the ground. All cylinders are powered by a 12-volt Bosch motor with a pump rating of 1.4 gallons per minute at 2000-psi. Attached to the pump is a 2.5-gallon reservoir of transmission fluid. Due to the size of the cylinders, an additional 5-gallon reservoir was installed. The hydraulic pump and reservoir is shown in Figure 3-5.

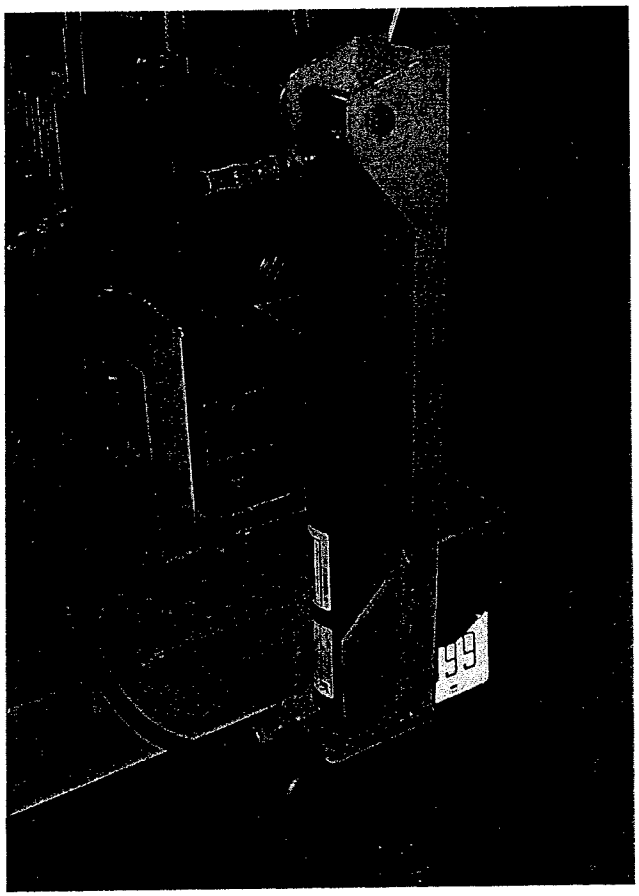

Figure 3-3: One of four hydraulic leveling jacks.

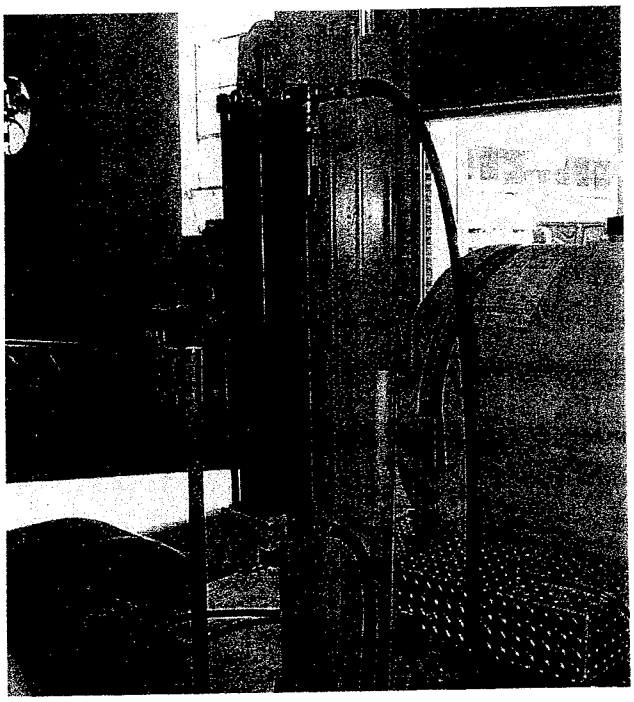

Figure 3-4: Center hydraulic ram.

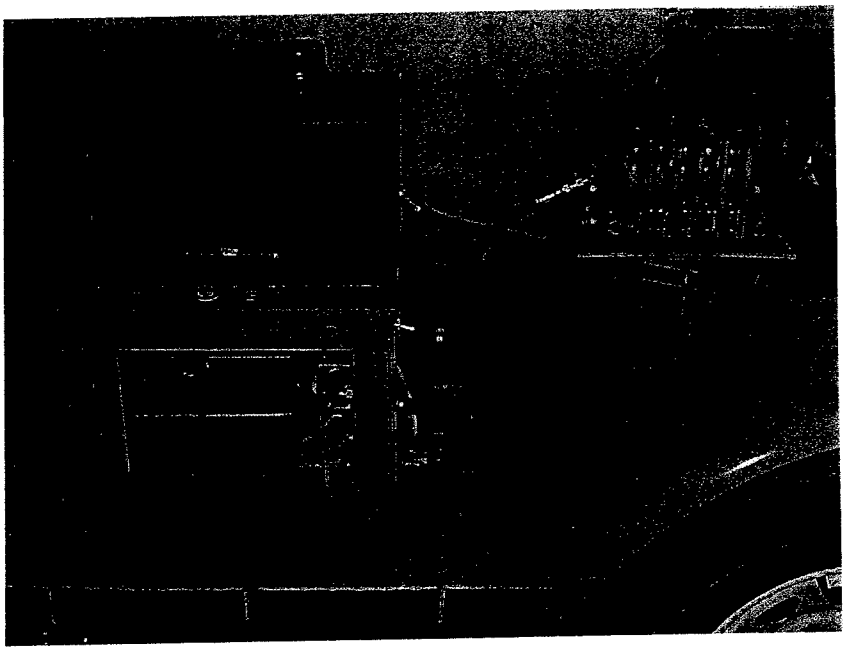

Figure 3-5: Hydraulic pump, controls, and reservoir.

All cylinders are controlled by five spring-centered valves (Figure 3-5). The center ram has a 26-inch stroke and is mounted on an H-beam fixed to a rotating plate. The four leveling cylinders have an 18-inch stroke with a base plate that can rotate to account for uneven ground.

Coring Device

In the case where a test is to be performed over existing pavement, a coring device is used to bore a hole through the pavement to allow access for the probe. The device purchased was a Hilti DD 250E coring system (Figure 3-6) using a 20-amp motor at 115 VAC. Four speeds are available enabling the use of a wide range of coring diameters. Currently, the bit in use is four inches in diameter and 44 inches long. There is also a starting mode switch that reduces the motor speed by one-third for easy hole starting.

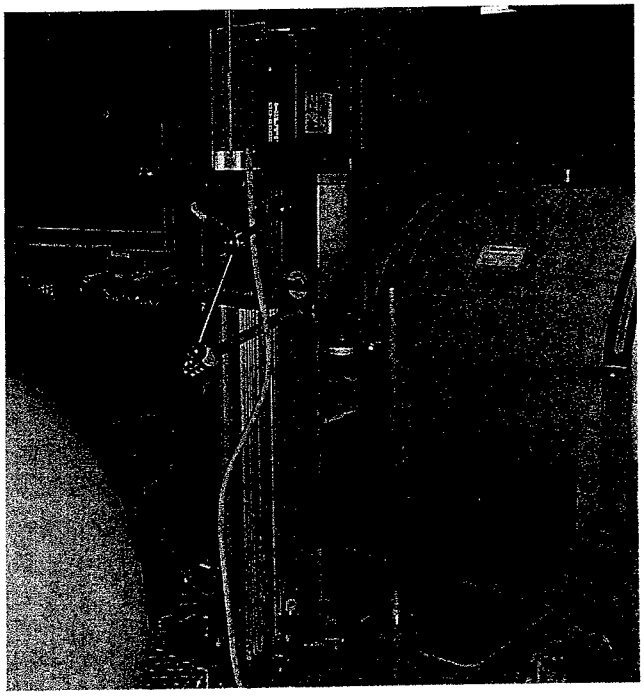

Figure 3-6: Hilti coring device.

The stand for the coring device is fixed on the same rotational plate as the H-beam. This allows for operation of the coring device and the probe without ever realigning the trailer. The Hilti coring system is powered by the generator and water is supplied from the water tanks with the aid of a 12-volt pump.

Generator

The generator (Figure 3-7) is a primary source of power for the coring device and a secondary source for the hydraulic and flow system. It is a 10,000-watt Dyna LLC9000E generator powered by a Briggs & Stratton Vanguard engine with an electric start. Four 15-amp, 120-volt receptacles and one 30-amp, 240-volt twist lock are available for output.

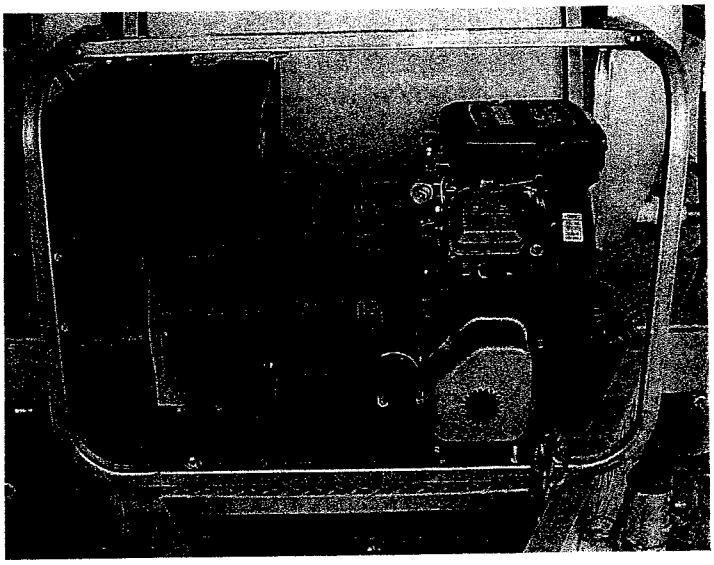

Figure 3-7: Onboard generator.

Because the coring device requires 20 amps at 115 volts, a transformer was required. The transformer also protects the coring device from surges.

Flow System

The components of the flow system include the electronic measuring devices and solenoid switches. It is the system that allows water to flow from the Mariotte tank to the probe while measuring the corresponding pressures and flow rates.

For the system to be capable of performing the constant or falling head test, solenoid valves were installed to route the water through the appropriate flow path. A schematic of the flow system, including solenoids and flow meters, is shown in Figure 3-8.

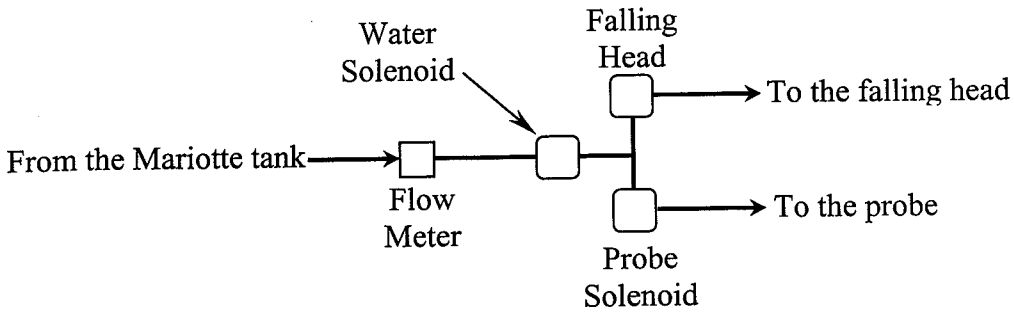

Figure 3-8: Flow system diagram.

There are three possible flow paths for the configuration shown in Figure 3-8. The first flow path is configured to perform a constant head test. The water is routed from the Mariotte tank through the flow meter and then through the probe. If the flow rate is below 50 ml/min, then the system is switched to perform a falling head test. Figure 3-9 highlights the constant head flow path through the flow meter.

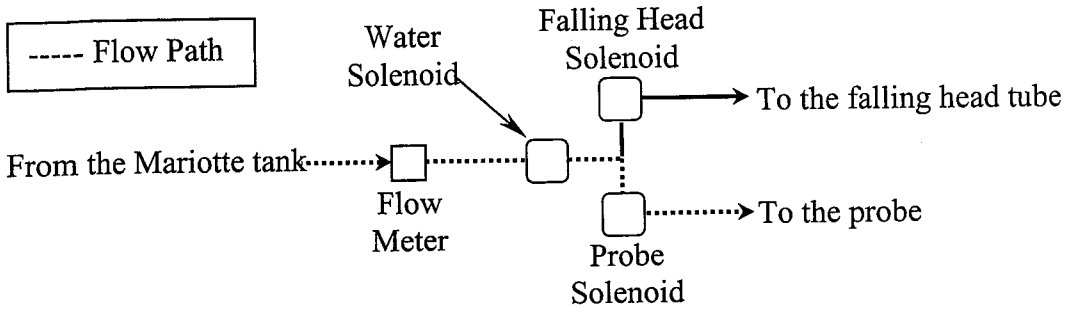

Figure 3-9: Constant head test flow path.

The second flow path is configured to fill the falling head tube. In this case, the probe solenoid is switched off and the falling head solenoid is opened. Thus water will flow from the Mariotte tank to the falling head tube (Figure 3-10).

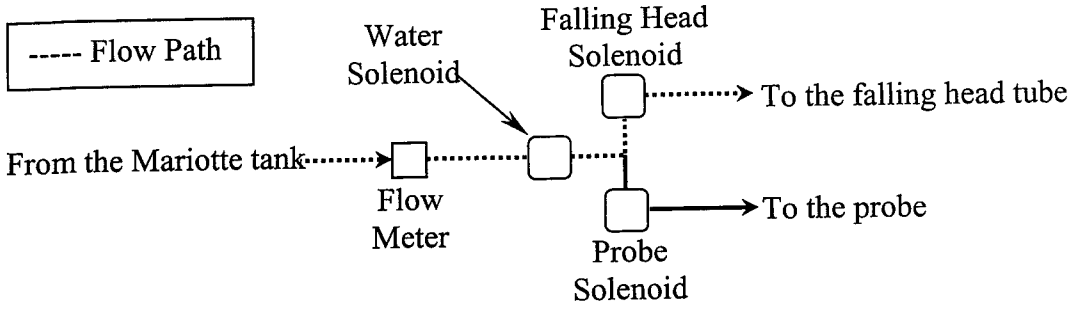

Figure 3-10: Flow path to fill the falling head tube.

The third flow path (Figure 3-11) is configured to run the falling head test. The water in the falling head tube is directly routed to the probe. For this to occur, the water solenoid is switched off, and the falling head and probe solenoids are opened.

The flow meter is only functional when the constant head test is performed. Values are reported in ml/min (or cm^3/min) and are read from the LCD display on the control panel or from the data acquisition software.

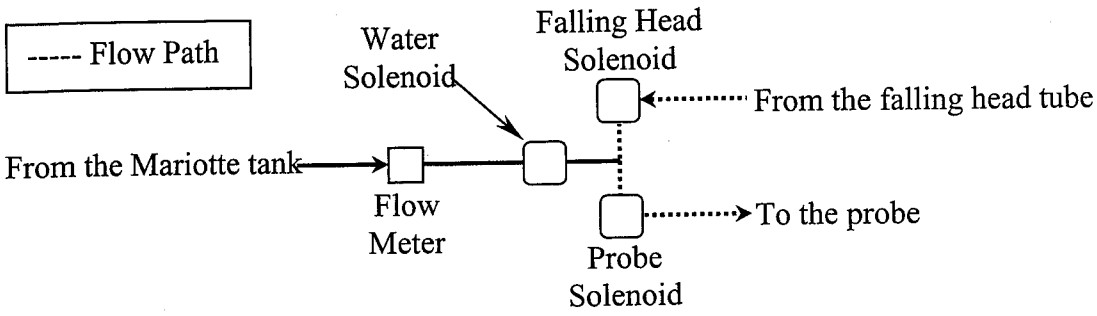

Figure 3-11: Falling head test flow path.

During the constant head test, the pressure is read from an electronic pressure transducer located on the Mariotte tank. The pressure output is automatically converted to an equivalent height of water in units of centimeters. The total head is then calculated as the reading from the transducer plus the height from the transducer to the porous stone on the probe. The falling head tube is instrumented as well. The pressure transducer located on the falling head tube (Figure 3-12) tracks the height of water as the level drops. Initial and final heads are calculated in the same fashion as in the constant head test.

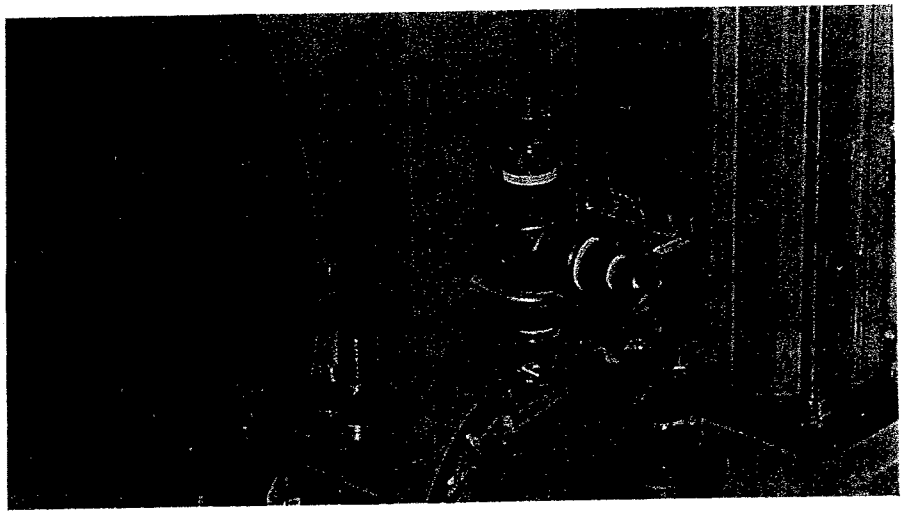

Figure 3-12: Pressure transducer located on the falling head tube.

Mariotte Tank

The Mariotte tank (Figure 3-13) is designed to provide a constant head of water to the flow system even as water levels decline. A schematic of the tank is shown in Figure 3-14. It is made of galvanized steel with a 42-gallon capacity. The tank is sealed except for a small tube open to the atmosphere and extending below the water level. This tube is usually referred to as the Mariotte tube. The head of water acting on the exit port of the tank does not begin at the water surface but rather from the bottom of the tube. It is important that the water level is always above the bottom of the tube or else a constant head of water will not be maintained.

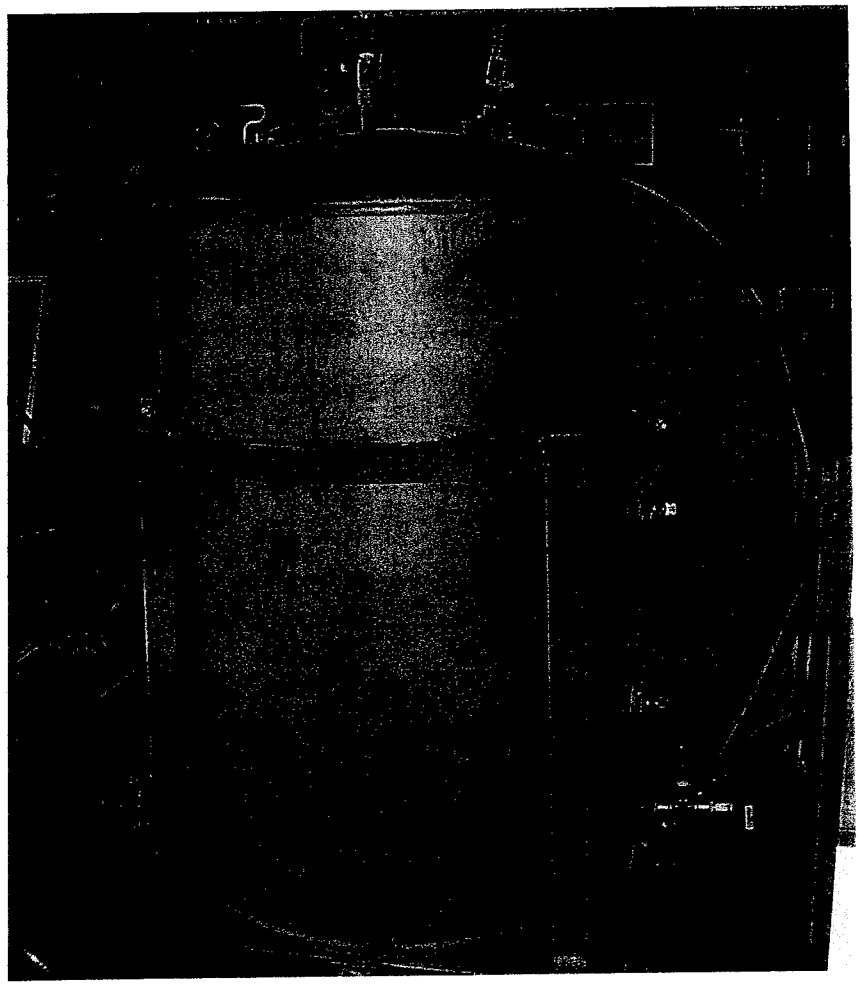

Figure 3-13: Mariotte tank.

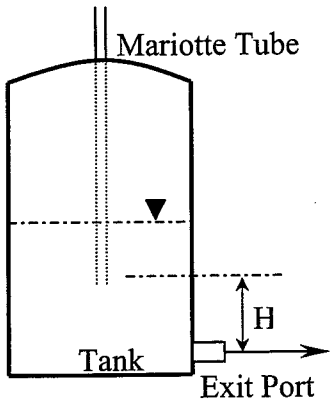

Figure 3-14: Mariotte tank diagram.

The tank is operated through three valves located on the top. Referring to Figure 3-15, the release valve seals the tank from the atmosphere when closed. This valve must be closed if a constant head of water is desirable. The air supply is controlled with a solenoid valve and either opens the Mariotte tube to the atmosphere or it allows pressure to be drawn in from a nitrogen source. The fill valve is used to refill the tank when supplies are depleted.

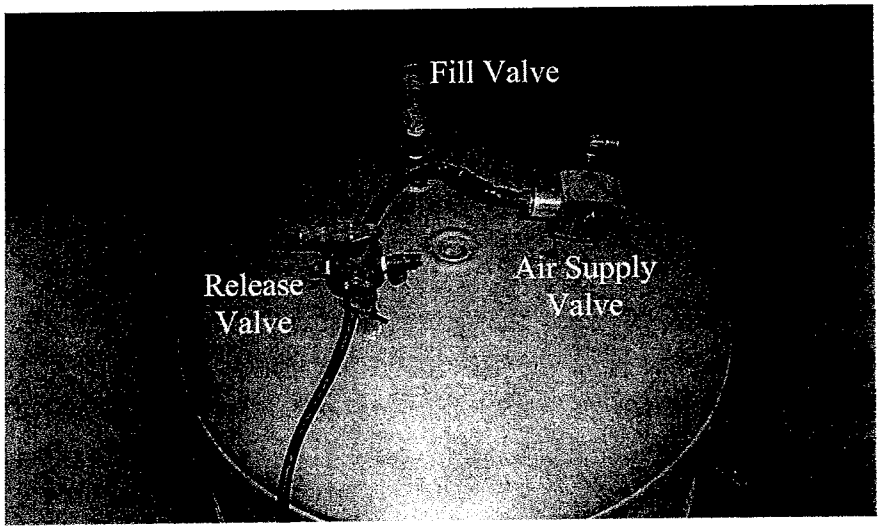

Figure 3-15: Tank control valves.

Nitrogen Pressure System

The nitrogen system supplies pressure to the Mariotte tank when an increase in the constant head is desired. The system consists of a nitrogen tank, regulator, and a check valve. The check valve is used to eliminate any back flow that would damage the pressure regulator.

Probe and Extension Rod

The flow system routes water from the Mariotte tank to the extension rod and probe where it is then introduced into the surrounding soil. The extension rod (Figure 3-16) serves two purposes. First, it eliminates any initial extension of the center hydraulic ram for the probe to make contact with the ground, and second it de-airs the flow system and probe through a bleed valve located near the top. It is best to operate the bleed valve after the probe has been penetrated to the specified depth.

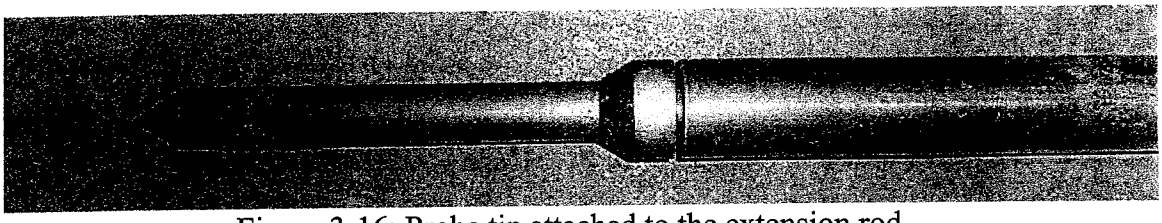

Figure 3-16: Probe tip attached to the extension rod.

A detailed diagram of the probe is presented in Figure 5-1. From Figure 3-16, it is apparent that the extension rod has a larger diameter than the tip of the probe. It was purposely designed in this fashion so that any upward flow of water along the sides of the shaft will be eliminated. The probe is made of three parts: the tip, sleeve and cone as shown in Figure 3-17. The sleeve is a porous element made from stainless steel and purchased from the Mott Metallurgical Corporation. The material was purchased in two

foot segments and cut down to 0.67 inch pieces. The outside diameter of the porous element is approximately 0.75 inches with an inside diameter of 0.65 inches.

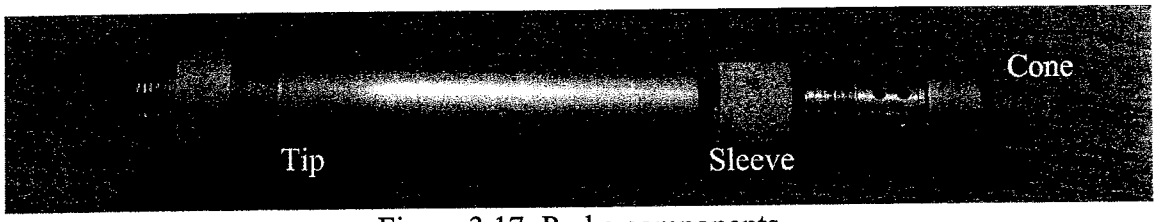

Figure 3.17: Probe components.

Rotating Platform System

The coring device stand and the H-beam, which supports the center hydraulic ram, rests on a rotating plate (Figure 3-18) at the center of the device. The plate rotates about a steel pin and maneuvers easily on three high capacity steel rollers. The rotating plate concept was derived from the necessity of being able to core the pavement and then perform a test without repositioning the device.

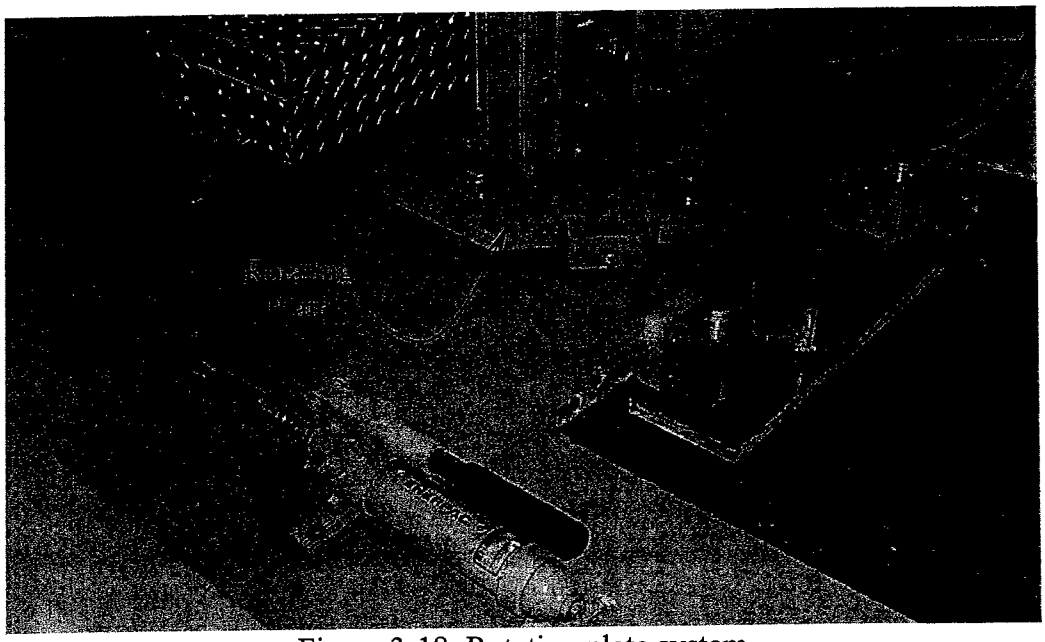

Figure 3-18: Rotating plate system.

To account for the uplift force acting on the plate, three additional steel studs were installed. These studs can resist extremely high loads with a tensile strength of 125,000-psi. Once the device is in position for a test, the plate is locked up with the aid of three five-ton flat-jacks operated by a hydraulic hand pump.

Control Panel

The control box (Figure 3-19) houses the switches and LCD displays that control the flow system. It is not attached to the device thus allowing the operator to place it in the most convenient location. This can either be anywhere about the device or within the tow vehicle. The control box connects with the solenoid and flow meter housing box through two thirty-foot cables. Twelve volts (DC) of supply power are required.

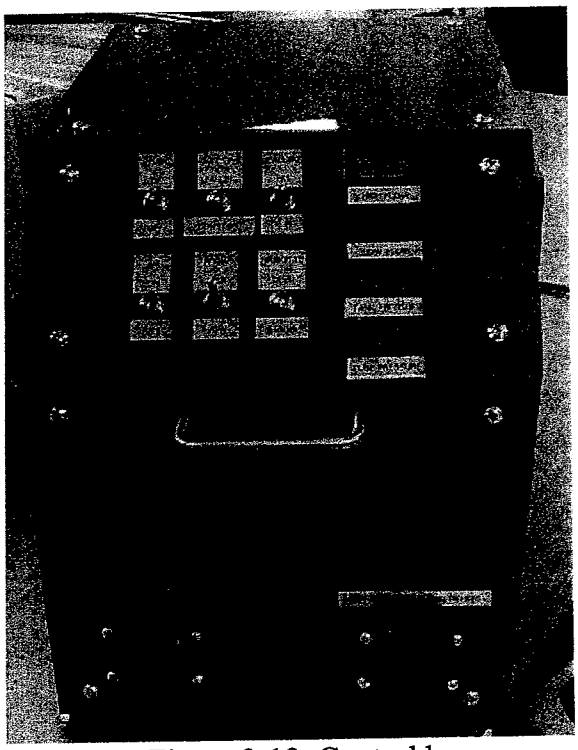

Figure 3-19: Control box

The LCD displays provide the output data from each of the electronic measuring devices as a test is in progress. Recording the values from the displays at equal increments of time can become an extensive task. Therefore, data acquisition capabilities were installed in the control box. A laptop computer connects through a port and records all the pressure and flow measurements at prescribed time increments. This feature relieves the operator from recording the data and allows greater attention to be focused on the entire operation. The same computer is also equipped with global positioning hardware and software that assigns coordinates to each test location. This feature is especially helpful if a database catalog is to be maintained.

CHAPTER 4
DEVICE MODIFICATION AND ENHANCEMENTS

As the frequency of usage of the original device increased, several shortcomings became apparent. In mid 1998, the Florida Department of Transportation contracted the University of Florida to address and eliminate those deficiencies. The original device functioned properly but safety and time saving improvements were requested. A schematic of the original layout is presented in Figure 4-1. Safety improvements were addressed first since it was the primary concern of both parties. The next step was to improve the efficiency and reduce the operating time of the device.

Safety Improvements

Referring to Figure 4-1, all operational controls were located on the left side of the device. In most instances, a test would be performed on the far right lane of a road, which would require the operator in a position between the device and the next passing lane. This situation was dangerous since the possibility of an incoming vehicle colliding with the device existed.

In response, the hydraulic controls were moved to the right side and the control box was redesigned so that it could be positioned at the operator's discretion. The control box communicates with the flow system through two 30-foot cords allowing the box to be placed inside the tow vehicle or outside away from the device.

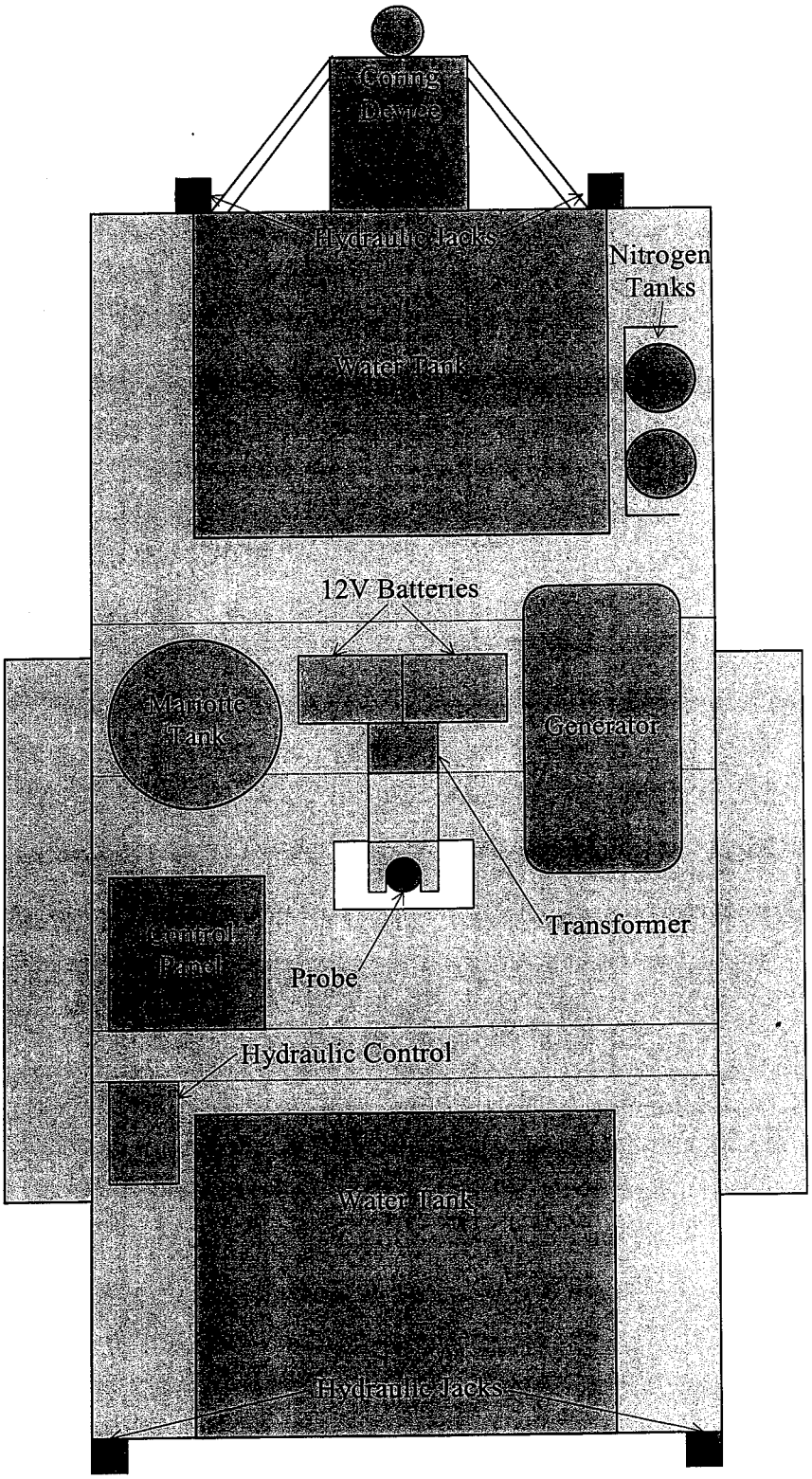

Figure 4-1: Original device configuration.

Efficiency and Time Improvements

Rotating Plate System

When performing a test over an existing pavement, the coring device is used to allow access for the probe into the base and sub-base layers. In the original setup, the coring device was located in the front while the probe was at the center. Problems were encountered while attempting to reposition the trailer to align the probe directly over the cored hole. A solution was needed that would allow the coring device to cut through the pavement and then operate the probe without realigning the device.

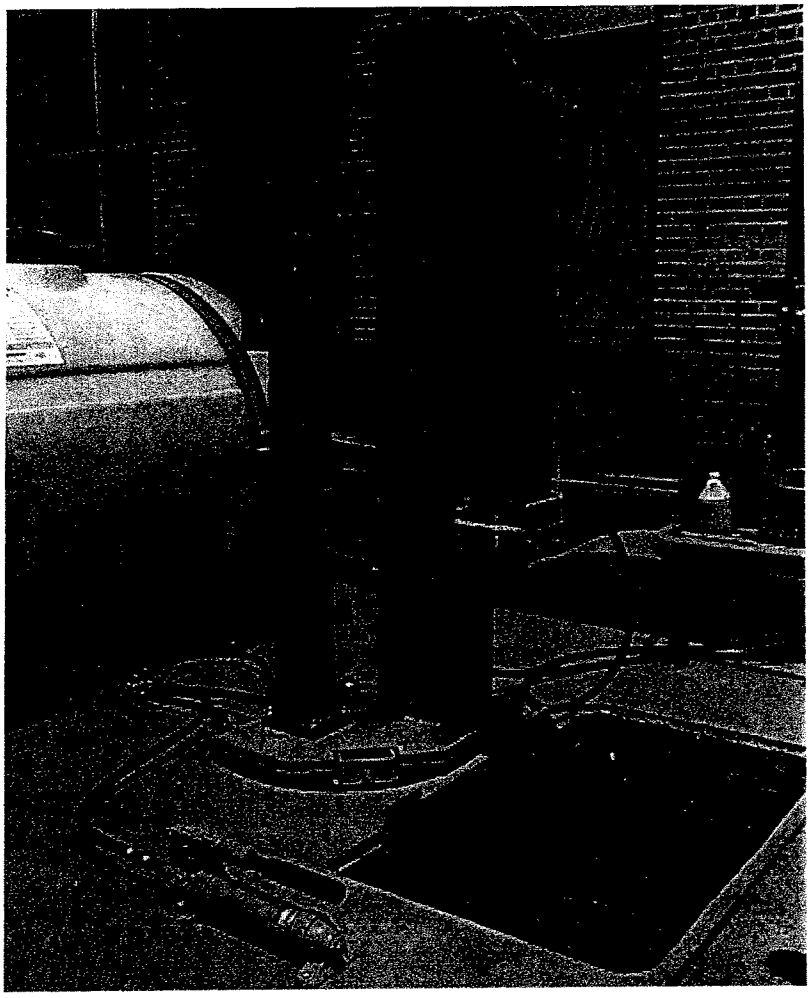

Figure 4-2: Rotational plate system.

The problem was solved with a rotating plate system (Figure 4-2). Resting on the rotating plate is the coring device stand and the H-beam that supports the center hydraulic ram where the probe is attached. After the coring device is used, the plate is rotated 90 degrees to align the probe. The plate pivots about a steel pin and maneuvers on three high strength cast-iron wheels.

Hydraulic Stabilizing System

The hydraulic jacks located on each corner of the trailer are used to levitate the device for support and stabilization. The original system used cylinders that were swung up and chained when traveling (Figure 4-3). The time required to approach each cylinder, unhook the chain and release it into the operating position was too consuming. It was then decided to replace each cylinder with ones having a greater length of stroke thus being able to place them in a higher position (Figure 4-4). Now the jacks are raised and lowered without adjusting their orientation.

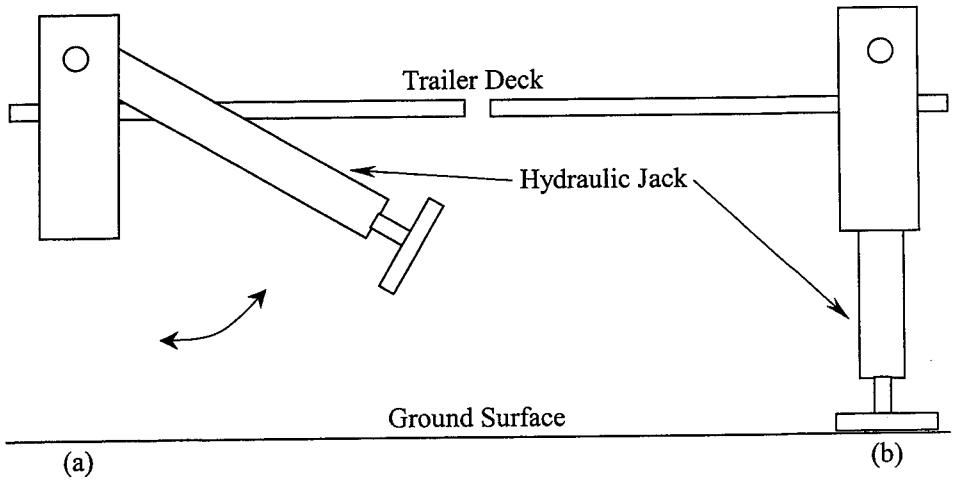

Figure 4-3: Original leveling system. (a) Stabilizing jacks in the traveling position. (b) Stabilizing jacks in the operational position.

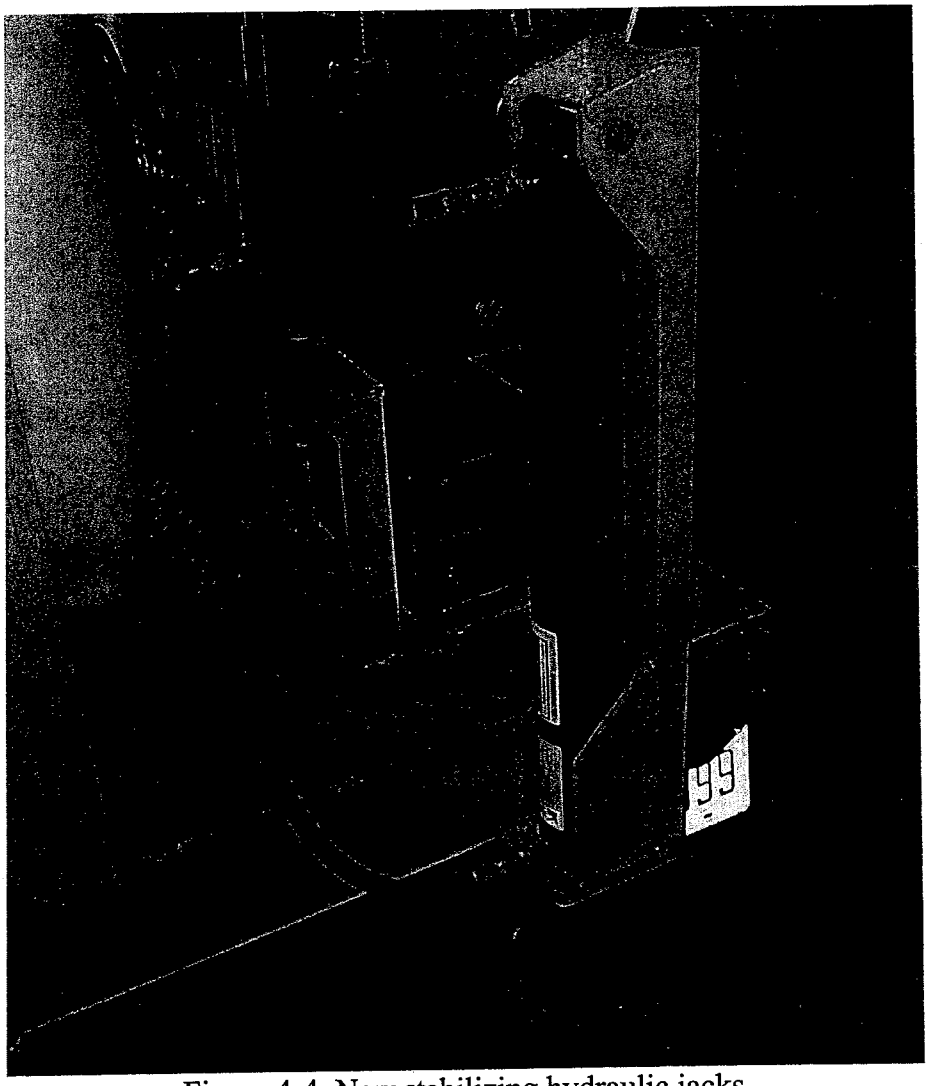

Figure 4-4: New stabilizing hydraulic jacks

Power Supply

The original device relied on a 12 VDC marine deep cycle battery to supply power to the control and hydraulic system. Consistent maintenance was required since each test was dependent on the batteries supplying uninterruptible power. The possibility that a test could prematurely end resulted in the installation of a more reliable source. This source is found in the tow vehicle. A direct line from the device to the tow vehicle provides reliable power with a reduction in maintenance time and cost.

Operational Improvements

The most significant operational improvement was the installation of a data acquisition system. No longer is the operator required to provide their full attention to recording the data during a test. Instead, a computer acquires the pressure and flow data and stores it for later analysis. Implementation of the system began by linking the existing flow meters to the computer. Pressure readings required the installment of new electronic pressure transducers on the Mariotte tank and on the falling head tube.

The laptop computer used for data acquisition also has GPS capabilities to obtain coordinates for each test location. This will provide the opportunity to easily reference each test for database usage.

While advancements were made in acquiring data, changes were also made to the flow system itself. Initial usage of the device produced results that were known to contain inaccuracies since the relationship between the flow, pressure and permeability did not behave as expected. Darcy's law states that permeability is constant even as the applied head and corresponding flow rates vary. Results from the original device (Figure 4-5) showed that the permeability was not constant which is inconsistent with the governing laws of flow.

When the flow system was inspected to determine the cause of such discrepancies, two possible sources were identified and resolved to eliminate these shortcomings. The first alteration was made to the location of the pressure gauge within the system. The gauge was moved from the control box to the Mariotte tank to obtain static head readings. The second alteration was made by installing a bleed valve that would remove any trapped air.

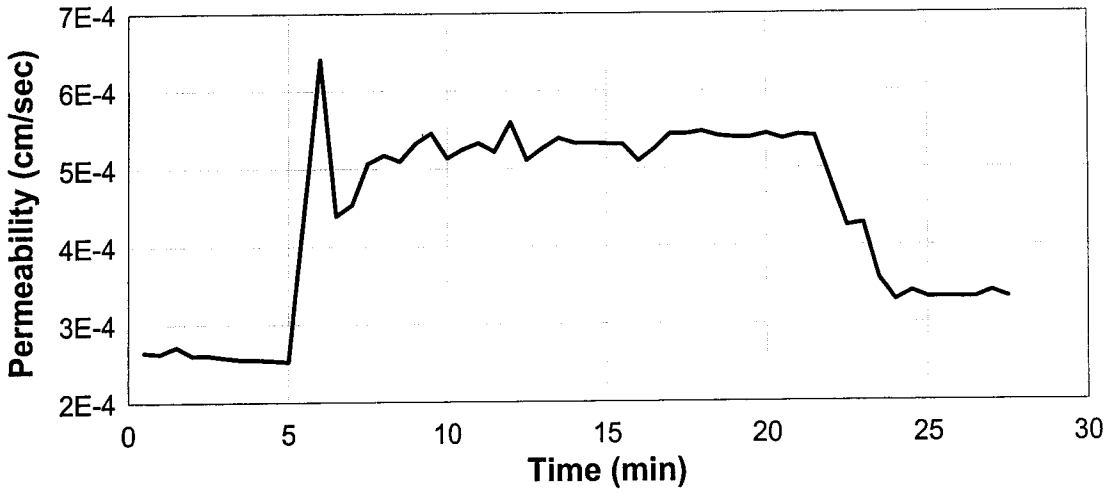

Figure 4-5: Initial permeability results.

Trapped air causes fluctuations and a reduction in the flow under equivalent pressure heads. A bleed valve (Figure 4-6) was installed on the probe extension rod. Once the probe is inserted to the desired depth, the bleed valve is opened and water is allowed to flow through the system. When water is visibly seen exiting the bleed valve, it is assumed that the system is air free and the bleed valve can be closed.

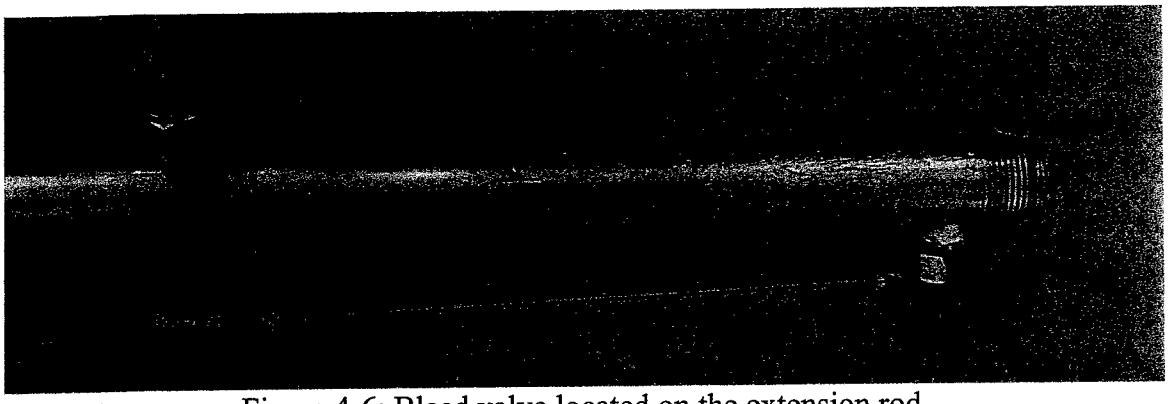

Figure 4-6: Bleed valve located on the extension rod.

Repositioning the pressure gauge and installing a bleed valve has altered the results to correspond with Darcy's law. Even when the pressure is raised two or three times during a test, the permeability remains relatively constant (Figure 4-7).

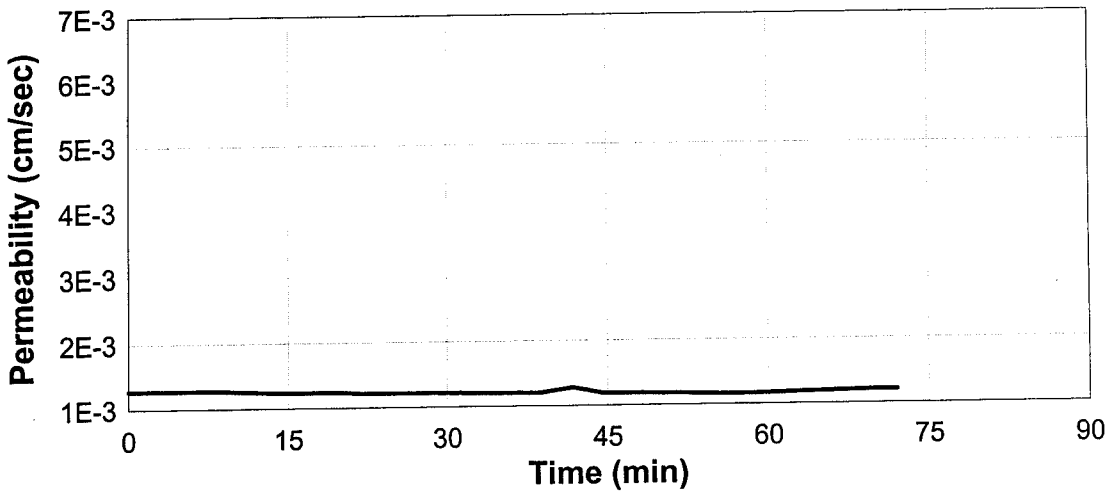

Figure 4-7: Permeability results after enhancements were made.

Other changes to the flow system have been made to the water lines. The original device used thin plastic tubing that became brittle after prolonged exposure to sunlight. The new lines are larger, more flexible tubing that is specifically designed to resist damage caused by the outside environment.

CHAPTER 5
FUNDAMENTALS OF FLOW THROUGH A POROUS PROBE

The focus of the research is to identify the relationship between a known quantity of water exiting through a porous probe at a corresponding head to the permeability of the surrounding soil. During the early stages of soil mechanics, several charts were published correlating the permeability with the flow rate, applied head, and dimensions and shape of a piezometer or observation-well. Darcy's law states that the coefficient of permeability is the discharge velocity under a unit hydraulic gradient. It is easily applied to laboratory methods, however the application in field tests is more difficult. In most cases, the area under influence is difficult to assess as well as the hydraulic gradient. For field permeability tests, a variation of Darcy's law was necessary. Equation 5-1 is an expanded form of Darcy's law:

$$k = \frac{q}{i \cdot A} = \frac{q}{(h/L) \cdot A} \tag{5-1}$$

Since the area, A, and the length, L, are difficult to determine in field conditions; they were replaced with a factor, F, which is more applicable to such boundary conditions:

$$k = \frac{q}{h \cdot F} \tag{5-2}$$

The F factor retains the same dimensions as the area divided by the sample length in Equation 5-1, however it is dependent on the shape of the object at the interface with the soil. Several equations for F have been published for various piezometers and

observation-wells that are commonly used today. The goal of the research is to validate the F factor for the specific probe to be used with the device (Figure 5-1). Both theoretical and experimental approaches were examined in this process.

The procedure for establishing a final F factor began with evaluating three widely accepted theories related to the probe. The first is based on charts published by Hvorslev in 1951. The second is an equation used for the Packer test that is easily applied to a porous probe, and the third involves a computer assisted finite element analysis. Confirmation of the theories depended on results from field tests. A correlation study was conducted between the FPTD and the double ring infiltrometer. The intent was not to obtain an accurate correlation value, but to gain confidence in the device.

Hvorslev's Charts

In 1951, M.J. Hvorslev published "Time Lag and Soil Permeability in Groundwater Observations" in which he discusses flow through intakes and well points. Hvorslev presents a chart summarizing permeability formulas for various types of wells and intakes (Figure 5-2). No single case could correctly model the probe but by using a method of subtraction the equation for the probe can be derived. To arrive at a probe with an impermeable base, case four needs to be subtracted from case eight:

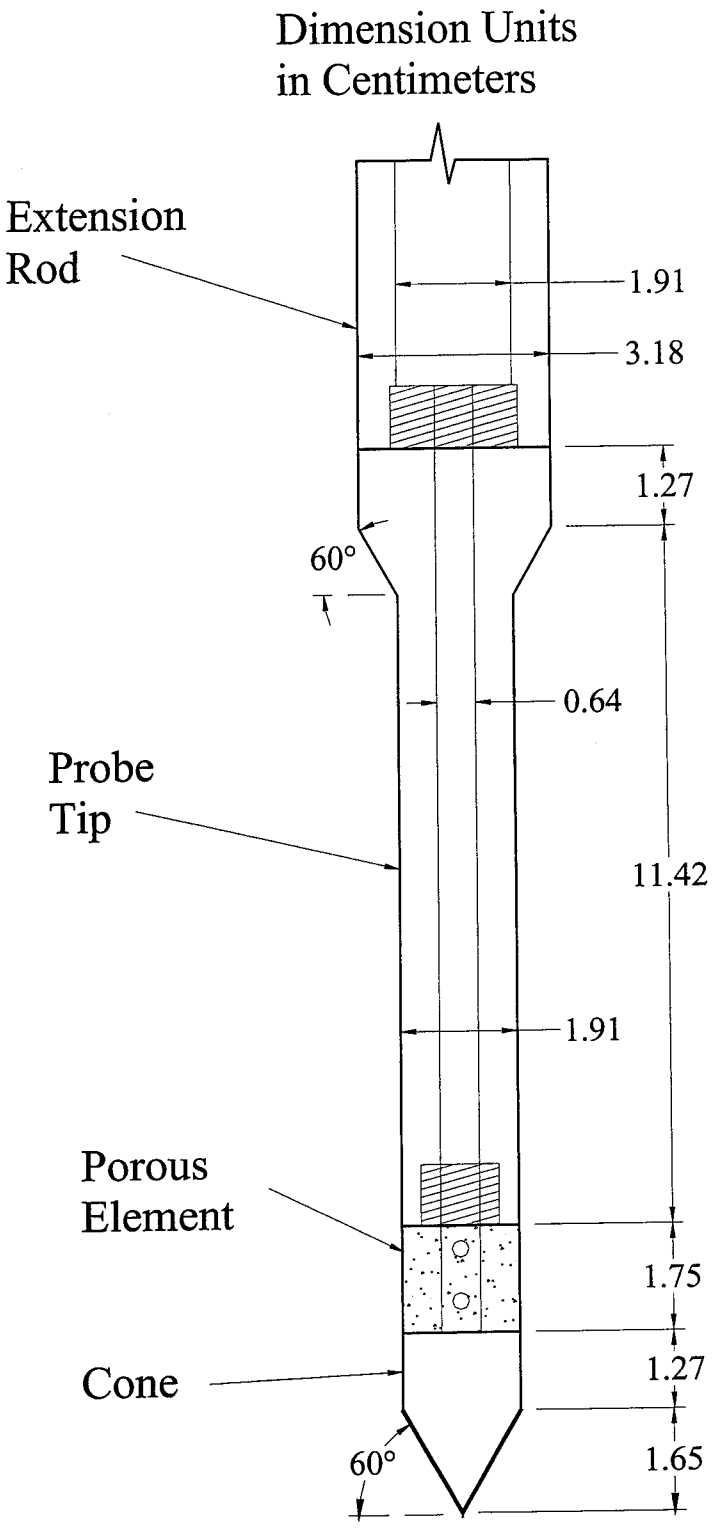

Figure 5-1: FPTD probe.

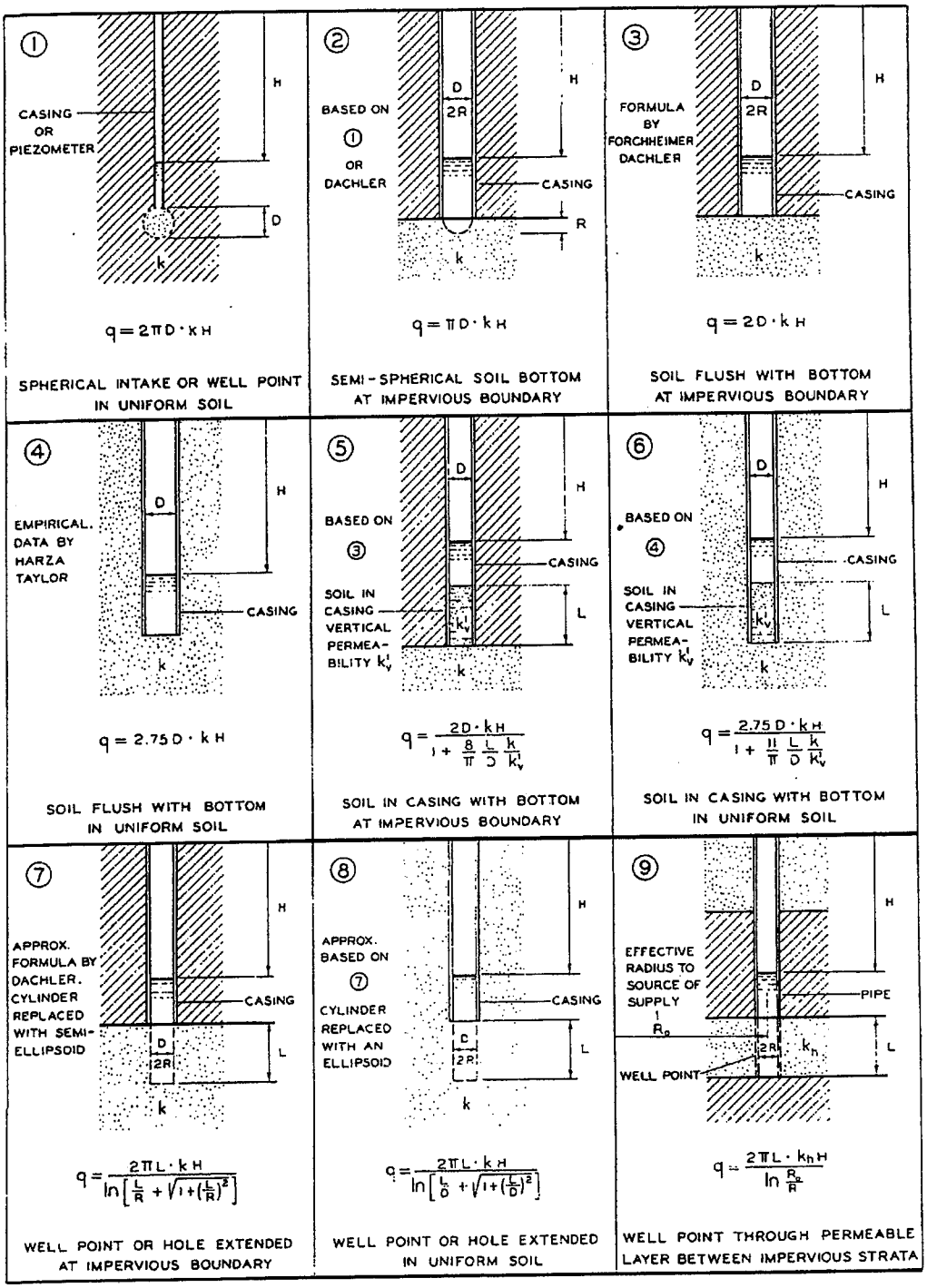

Figure 5-2: Hvorslev's charts.

$$q = \frac{2\pi L \cdot kH}{\ln\left[\frac{L}{D} + \sqrt{1+\left(\frac{L}{D}\right)^2}\right]} - 2.75D \cdot kH \qquad (5\text{-}3)$$

Thus, the F factor for the probe is equal to:

$$F = \frac{2\pi L}{\ln\left[\frac{L}{D} + \sqrt{1+\left(\frac{L}{D}\right)^2}\right]} - 2.75D \qquad (5\text{-}4)$$

where L and D are the length and the diameter of the porous element, respectively. For the dimensions of the porous element, where D equals 1.905 cm and L equals 1.746 cm, the F factor is calculated below:

$$F = \frac{2\pi \cdot (1.746)}{\ln\left[\frac{1.746}{1.905} + \sqrt{1+\left(\frac{1.746}{1.905}\right)^2}\right]} - 2.75 \cdot (1.905) = 8.12\,\text{cm} \qquad (5\text{-}5)$$

Packer/Lugeon Equations

The benefit of adopting the Packer/Lugeon equation from the packer test (Equation 2-5 and 2-6) is that the concept from both tests are similar, thus the idealized flow pattern is expected to be the same. Both allow water to exit from the sides giving significant weight to the flow in the horizontal direction while restricting the flow in the vertical direction with an impermeable base.

To justify the validity of the Packer/Lugeon equation for FPTD results, a mathematical derivation of the equations is presented. The following is based on an

analysis presented by M.E. Harr and in combination with the fundamental laws of flow through porous media; along with the following assumptions:

1. Semi-infinite porous medium
2. Homogeneous material
3. Uniform and continuous flow region
4. Steady state / spherical flow.

To begin, the following parameters must be defined:

R = Radius of influence (i.e., the effective radius of the flow region under study).

$\phi(R)$ = The potential at a distance R from the center of the sphere.

2r = Diameter of the test hole.

$L_o = 2L$ = Length of the test section.

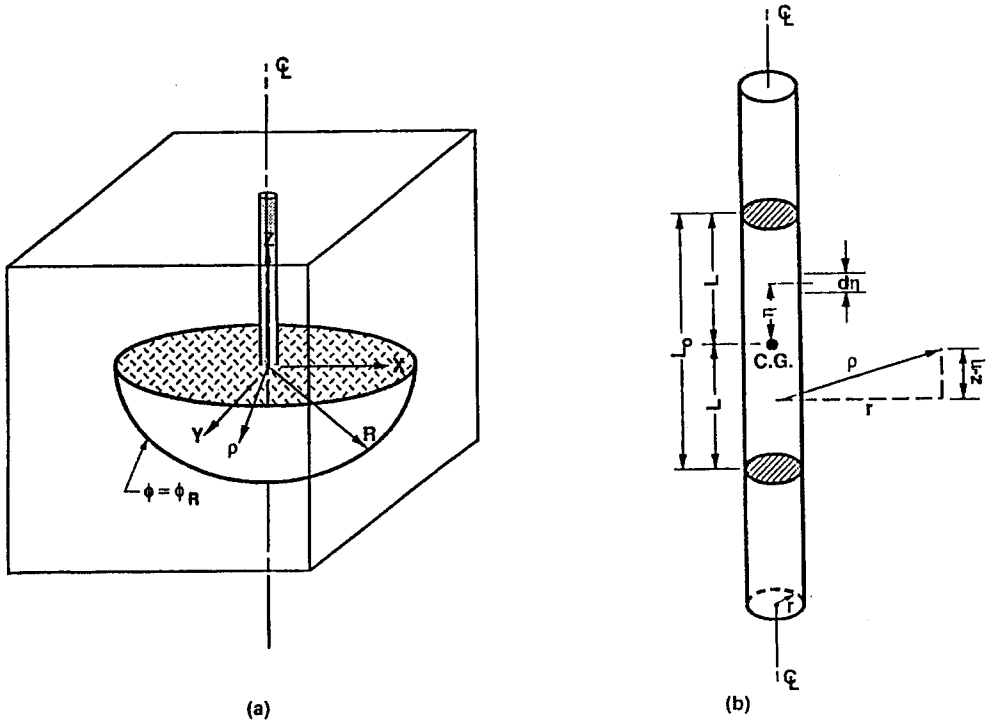

Figure 5-3: Geometric configuration of (a) the flow region, and (b) the test section.

The discharge, q, at any radial distance ρ from the source at the center of the sphere is

$$q = 4\pi\rho^2 \upsilon_p = 4\pi\rho^2 \frac{\partial\phi}{\partial\rho} \tag{5-6}$$

$$\frac{\partial\phi}{\partial\rho} = \frac{q}{4\pi\rho^2} \tag{5-7}$$

where $4\pi\rho^2$ = surface area of sphere

υ_ρ = radial velocity.

By integrating equation 5-7, we get the potential, ϕ:

$$\phi = -\frac{q}{4\pi\rho} + C \tag{5-8}$$

To determine the constant of integration, C, the boundary conditions at the hole must be defined:

$$\rho = r, \text{ and } \phi = \phi_o \tag{5-9}$$

Therefore, the constant, C, resolves to:

$$C = \phi_o + \frac{q}{4\pi r} \tag{5-10}$$

Thus by applying Equation 5-10 into 5-09, the potential, ϕ becomes:

$$\phi = \frac{q}{4\pi}\left(\frac{1}{r} - \frac{1}{\rho}\right) + \phi_o \tag{5-11}$$

where $r \leq \rho \leq R$.

The discharge, q, is assumed to be constant along the test section with the discharge per unit length expressed as:

$$\frac{dq}{d\eta} = \frac{q}{2L} \Rightarrow dq = \frac{q}{2L} d\eta \tag{5-12}$$

Assuming Equation 5-8 to represent the potential at any point in the flow region,

$$d\phi = \frac{dq}{4\pi\rho} \tag{5-13}$$

ρ can be expressed using cylindrical coordinates shown in Figure 5-3,

$$\rho = \sqrt{r\ + (z-\eta)^2} \tag{5-14}$$

Combine Equations 5-12, 5-13, and 5-14 to obtain

$$d\phi = \left(\frac{q}{2L}\right)\cdot d\eta\left(\frac{1}{4\pi\rho}\right) \Rightarrow \left[\frac{q}{8\pi L\left(\sqrt{r^2+(z-\eta)^2}\right)}\right]\cdot d\eta \tag{5-15}$$

By integrating Equation 5-5 and setting the limits of integration from $-\frac{L_o}{2}$ to $+\frac{L_o}{2}$,

$$\phi(r,z) = \frac{q}{8\pi L}\cdot\int_{-L}^{+L}\frac{d\eta}{\sqrt{r^2+(z-\eta)^2}} \tag{5-16}$$

The next step is to multiply Equation 5-16 by $\frac{1/r}{1/r}$:

$$\phi(r,z) = \frac{q}{8\pi L}\cdot\int_{-L}^{+L}\frac{(1/r)\cdot d\eta}{(1/r)\cdot\sqrt{r^2+(z-\eta)^2}}$$

$$= \frac{q\cdot(1/r)}{8\pi L}\cdot\int_{-L}^{+L}\frac{d\eta}{\sqrt{\frac{r^2}{r^2}+\frac{(z-\eta)^2}{r^2}}}$$

$$= \frac{q\cdot(1/r)}{8\pi L}\cdot\int_{-L}^{+L}\frac{d\eta}{\sqrt{1+\left(\frac{z-\eta}{r}\right)^2}} \tag{5-17}$$

By substituting $\frac{z-\eta}{r}$ for x, and taking the derivative of both sides as $dx = -\frac{d\eta}{r}$,

$$\phi(r,z) = \frac{q \cdot (1/r)}{8\pi L} \cdot \int_{\frac{z+L}{r}}^{\frac{z-L}{r}} \frac{-r \cdot dx}{\sqrt{1+x^2}}$$

$$= -\frac{q}{8\pi L} \cdot \int_{\frac{z+L}{r}}^{\frac{z-L}{r}} \frac{dx}{\sqrt{1+x^2}} \qquad (5\text{-}18)$$

Recall that

$$\frac{d \sinh^{-1}(x)}{dx} = \frac{1}{\sqrt{x^2+1}} \qquad (5\text{-}19)$$

By completing the integration in Equation 5-18 and substituting in Equation 5-19,

$$\phi(r,z) = \frac{-q}{8\pi L}\left[\sinh^{-1}(x)\right]_{\frac{z+L}{r}}^{\frac{z-L}{r}}$$

$$= \frac{q}{8\pi L}\left[\sinh^{-1}\left(\frac{z+L}{r}\right) - \sinh^{-1}\left(\frac{z-L}{r}\right)\right] \qquad (5\text{-}20)$$

Harr concludes that the equipotential surfaces given by Equation 5-20 form ellipsoids. By assuming $z = 0$ and substituting $L_o = 2L$, Equation 5-20 becomes

$$\phi(r) = \frac{q}{2\pi L_o}\sinh^{-1}\left(\frac{L_o}{2r}\right) \approx \frac{q}{2\pi L_o}\ln\left(\frac{L_o}{r}\right) \qquad (5\text{-}21)$$

If $\frac{L_o}{2r} >> 1$, then $\sinh^{-1}\left(\frac{L_o}{2r}\right)$ is approximately equal to $\ln\left(\frac{L_o}{r}\right)$. A final substitution is made with $kh = \phi$ into Equation 5.21 and solved with respect to the permeability, K:

$$k = \frac{q}{2\pi L_o h}\sinh^{-1}\left(\frac{L_o}{2r}\right), \text{ for } r \le L_o < 10r \qquad (5\text{-}22)$$

and

$$k = \frac{q}{2\pi L_o h}\ln\left(\frac{L_o}{r}\right), \text{ for } L_o \ge 10r \qquad (5\text{-}23)$$

where k = coefficient of permeability

h = applied pressure head

L_o = length of the test section

q = discharge

r = radius of the test section.

Equations 5-22 and 5-23 are known as the Packer/Lugeon equations commonly used by the U.S. Bureau of Reclamation for the insitu determination of the permeability from the packer test. For the dimensions of the porous element, L_o = 1.746 cm and r = 0.953 cm, Equation 5-22 applies, thus the F factor is calculated as

$$F = \frac{2\pi L_o}{\sinh^{-1}\left(L_o/2r\right)} = \frac{2\pi \cdot 1.746}{\sinh^{-1}\left(1.746/2 \cdot 0.953\right)} = 13.36\,\text{cm} \qquad (5\text{-}24)$$

Finite Element Modeling

Finite element modeling (FEM) provides a computer powered mathematical verification and analysis of the factors that govern the relationship between the flow rate and the applied head through a porous probe. It is a powerful tool providing insight into several previous unknowns. The effect of the shape of the probe and anisotropic conditions are no longer mysteries. It also gives a visual image of the expected flow field as well as the physical size of the bulb of influence around the probe.

The software used to model the probe is version 7.11 of PLAXIS. It is a powerful software designed to perform soil and rock analyses. Once a model of the probe is created, the variables can be altered to produce a range of solutions.

Plaxis Flow Theory

The basis of the Plaxis flow theory stems from Darcy's law:

$$q_x = -k_x \frac{\partial \phi}{\partial x} \tag{5-25}$$

$$q_y = -k_y \frac{\partial \phi}{\partial y} \tag{5-26}$$

Equation 5-25 and 5-26 express the relationship between the discharge, q, permeability, k, and the hydraulic gradient. The head, ϕ, is defined as

$$\phi = y - \frac{p}{\gamma_w} \tag{5-27}$$

where y is the vertical position, p is the stress in the pore fluid and γ_w is the unit weight of the fluid. Using the above relationships, Plaxis reiterates the computation process for each element in the mesh (Figure 5-4) until the results satisfy steady state conditions as defined by the following continuity condition:

$$\frac{\partial q_x}{\partial x} + \frac{\partial q_y}{\partial y} = 0 \tag{5-28}$$

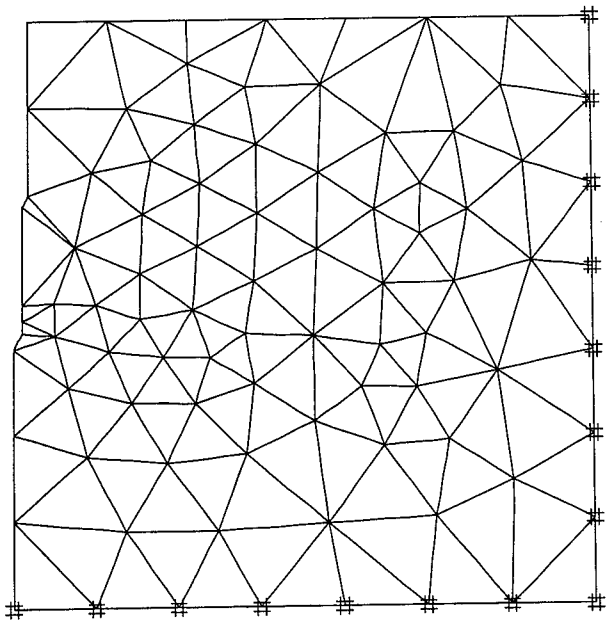

Figure 5-4: Generated mesh from Plaxis.

Modeling the Probe and Boundary Conditions

Before a model is created, several initial settings must be specified. The program allows the user to define the cross section as axisymmetrical or plane strain. An axisymmetric model is used for circular structures with a uniform radial cross section. Final results are displayed per unit radian about the vertical axis. A plane strain model is used for structures with a uniform cross section where results are presented per unit length perpendicular to the cross section. Since the probe has a uniform cross section about the central axis, an axisymmetrical representation of the probe using a 15-node element mesh is best suited for the analyses. Figure 5-5 is the model created within the Plaxis program.

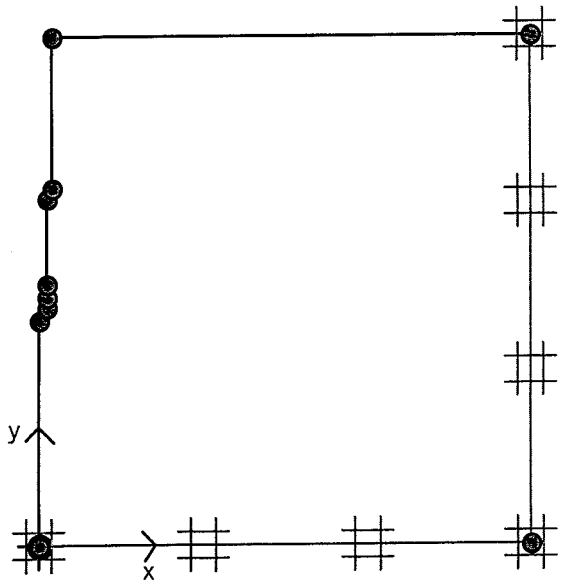

Figure 5-5: Modeling the probe within Plaxis.

Upon first glance of Figure 5-5, it is difficult to visualize the location of the probe. The centerline of the probe is located on the y-axis with the dimensions radially extending in the positive x direction. Figure 5-6 has the same features as Figure 5-5, however the probe is drawn in for visual assistance.

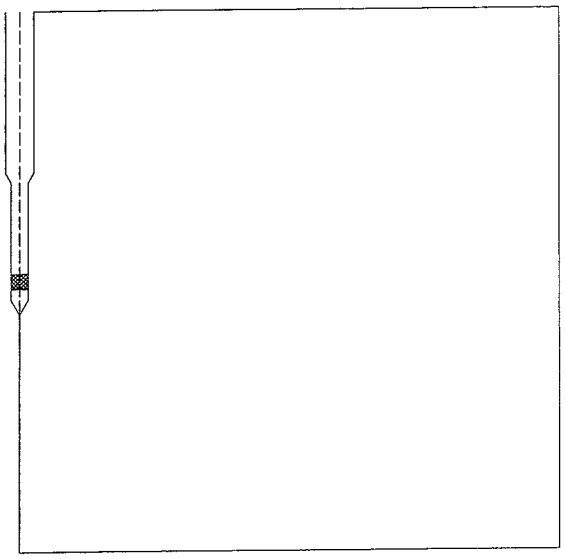

Figure 5-6: Location of the probe within the PLAXIS model.

In the model, the surrounding soil extends two feet from the centerline; a size assumed to enclose the zone of influence. The depth of the soil layer is also two feet with the placement of the porous stone at midpoint. Graphical proof will be presented later that a soil mass with these dimensions does provide adequate coverage. Once the layout of the model was finalized, the next step was to assign material properties to the soil. Table 5-1 outlines each material property with the corresponding value used in the model. Most of the parameters have no effect on the permeability and therefore were identified appropriately.

Table 5-1: Material property as used in the Plaxis model.

General		
Materials Set	Identification:	no influence
	Material Model:	no influence
	Material Type:	Drained
General Properties	γ_{dry}:	no influence
	γ_{wet}:	no influence
Permeability	k_x:	user defined
	k_y:	user defined
Parameter		
Stiffness	E_{ref}:	no influence
	ν (nu):	no influence
Alternatives	G_{ref}:	no influence
	E_{oed}:	no influence
Strength	c_{ref}:	no influence
	ϕ(phi):	no influence
	ψ(psi):	no influence
Interface		
Strength		no influence
Real Interface Thickness	δ-inter:	no influence
Permeability		Drain

With the material properties identified, the final step before the program can perform the analysis is to define the boundary conditions. Referring to Figure 5-7, the

thick lines along the edge of the soil mass represents a closed flow boundary. Only at the interface between the porous element and the soil mass is where a head of water is applied.

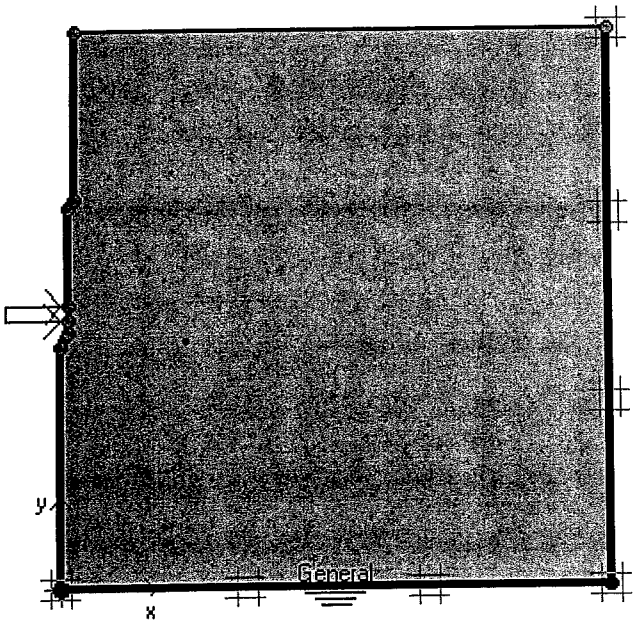

Figure 5-7: Boundary conditions.

Finite Element Analysis and Results

With a completed model, Plaxis computed the flow rate through the porous stone under corresponding permeability and applied head conditions. By altering the initial information, a wide range of results was accumulated. Once reduced, these provided insight into several unknowns. The program was utilized to analyze the F factor across a wide range of applied heads as well as across a spectrum of permeability values (under isotropic and anisotropic conditions). It also provided a visual image of the flow field and the bulb of influence surrounding the probe.

The F factor was back calculated from the following relationship:

$$F = \frac{q}{k \cdot h} \tag{5-29}$$

where F is the F factor (cm), q is the flow rate (cm^3/sec), k is the permeability (cm/sec), and h is the applied head (cm). Plaxis requires the input of the permeability and the applied head values prior to solving for the flow rate. The first F factor analysis, using Equation 5-29, was performed assuming isotropic conditions. A total of fifty data points were collected (Table 5-2). Based on initial conclusions, the F factor is independent of the flow, head, and the permeability and appears to be only a function of the probe dimensions. Figure 5-8 graphs the F factor versus the applied head.

Table 5-2: Flow rate results from Plaxis.

k (cm/sec)	Applied Head (in) 100	90	80	70	60	50	40	30	20	10
x 10^0	-	-	-	-	-	-	-	-	-	-
x 10^-1	-	-	-	-	-	9296.4	7437.1	5577.8	3718.6	1859.3
x 10^-2	1859.3	1673.4	1487.4	1301.5	1115.6	929.6	743.7	557.8	371.9	185.9
x 10^-3	185.9	167.3	148.7	130.1	111.6	93.0	74.4	55.8	37.2	18.6
x 10^-4	18.6	16.7	14.9	13.0	11.2	9.3	7.4	5.6	3.7	1.9
x 10^-5	1.9	1.7	1.5	1.3	1.1	0.9	0.7	0.6	0.4	0.2
x 10^-6	0.19	0.17	0.15	0.13	0.11	-	-	-	-	-

*Flow values reported in cm/min

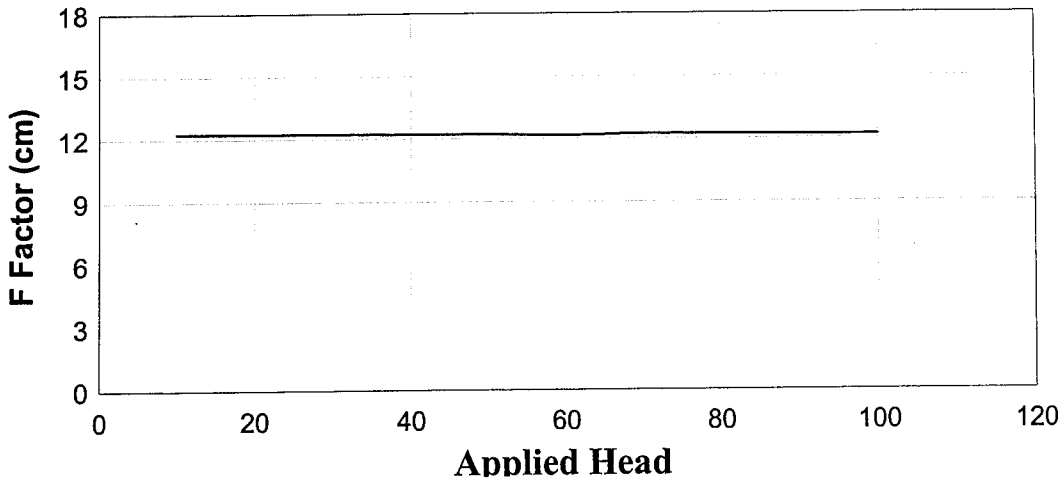

Figure 5-8: Relationship between the F factor and the applied head.

Based on Figure 5-8, the F factor remained constant at 12.2 cm under isotropic conditions, however it varied proportionally with the ratio of horizontal permeability to vertical permeability (Figure 5-9). The F factor was back calculated from a variation of Equation 5-29:

$$F = \frac{q}{h \cdot \sqrt{k_x \cdot k_y}} \tag{5-30}$$

where k_x is the horizontal permeability (cm/sec), k_y is the vertical permeability (cm/sec), and all other variables can be referenced to Equation 5-29. A final F factor analysis reveals that the F factor is dependent on the dimensions of the probe and the ratio of horizontal to vertical permeability. Well-mixed and compacted base and sub-base materials have been found to have horizontal to vertical permeability ratios varying near isotropic levels between 0.9 to 1.1.

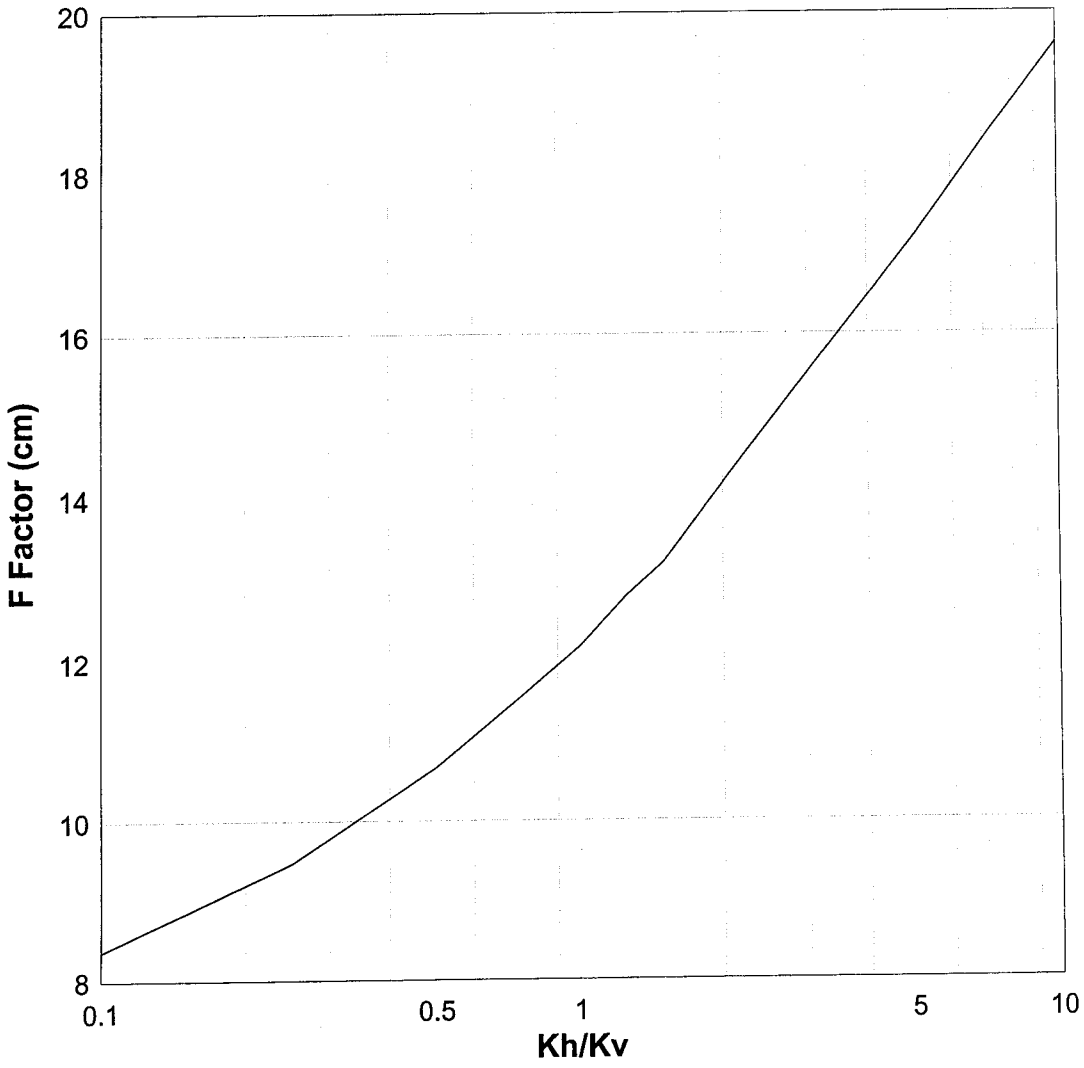

Figure 5-9: Relationship between the F factor and the anisotropic ratio.

Based on an F factor of 12.2 cm, a graph (Figure 5-10) of the flow rate versus the permeability at various values of constant head was created. This graph provides a quick reference for determining the permeability at the test location.

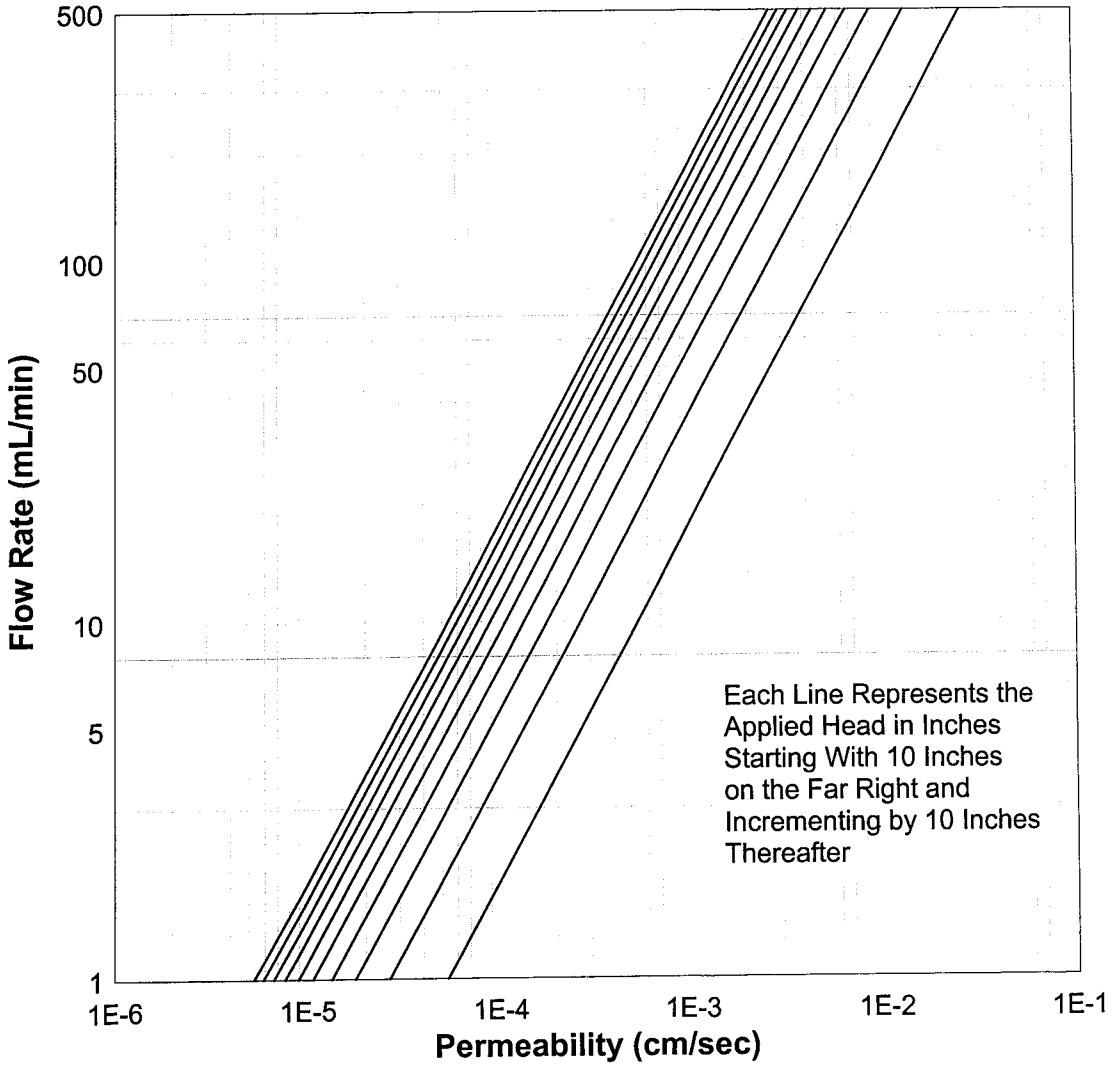

Figure 5-10: Plaxis field graph for quick reference.

Proposed F Factor

The three theories presented have all defined the F factor based on the shape of the porous element. However the difference among them is in their assumptions on the flow field. Figure 5-11 plots each method acting under an arbitrarily chosen head of 36 inches or 91.4 cm. The data are not from actual field results but are presented to

graphically portray the differences. Hvorslev's method assumes that the zone of influence around the

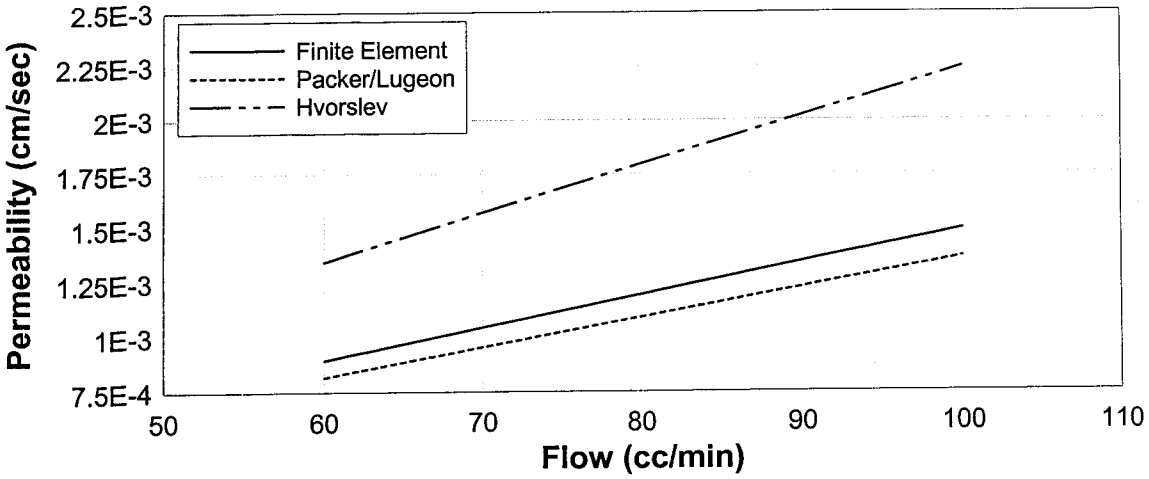

Figure 5-11: Differences among the theories acting under an equivalent driving head.

probe is shaped like a cylinder and does not migrate directly below the probe. The Packer/Lugeon equation is equivalent to Case 8 of Hvorslev's chart. This method does not account for an impermeable base since it assumes that flow field is shaped like a bulb and would migrate below the probe regardless. The finite element solution is similar to the results of the Packer/Lugeon method since both assume a zone of influence with similar attributes. The difference between these two methods is that the finite element solution accounts for the presence of the probe.

Consideration of the probe is important since it functions as a flow boundary and therefore alters the flow pattern. Thus, it is proposed that the F factor applied to any future calculation of the permeability be based on the finite element solution of 12.2 cm.

CHAPTER 6
VALIDATING THE F FACTOR

The F factor from the finite element analysis will be used to identify the relationship between the exit flow rate and the applied head with the permeability of the surrounding soil. The analysis relies on mathematical theoretical solutions based on the governing laws of flow through porous media. Before the solution is applied to any field investigations, a validation process is necessary. Primarily, this process will be performed with intent to create confidence with the finite element solution.

To verify the proposed F factor, tests were required in material where the permeability was approximately known. The testing scheme called for a double ring infiltrometer test (Figure 6.01) at a location with uniform soil followed by a test using the FPTD. The double ring infiltrometer test was chosen because it is a field method standardized by ASTM (designated as ASTM D 3385) and it is inexpensive and a relatively simple test to perform.

After the double ring test was completed, the rings were removed to allow access for the experimental device. The probe was then inserted directly through the center of the test area. This method eliminated any influence of variability between the results of the double ring test and the permeability device.

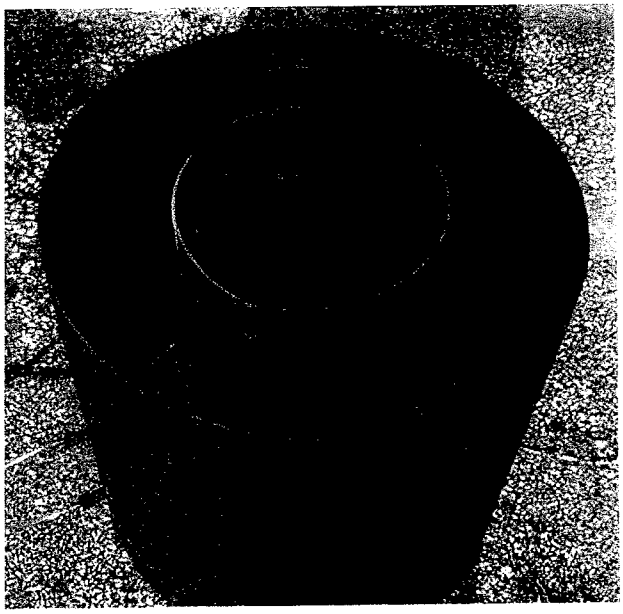

Figure 6-1: Double ring infiltrometer.

It is known that the flow pattern of water migrating from the center ring of the infiltrometer test and from the porous element of the probe into the soil is not equivalent and therefore results will not precisely match. However, results are comparable since the intent is not to correlate but to use the double ring results for guidance and verification. If the results from a double ring test designated a soil as permeable with a permeability of approximately 10^{-3}, then it would be expected that results using a porous probe would be similar. A large number of methods to determine the permeability already exist. If all were performed on the same soil mass then it would be highly expected that a variety of values would result, but that a generalized conclusion of the permeability could be obtained.

Fifteen comparative tests were performed at several site locations. Four tests were performed at the State Materials Office (SMO), one test on SR 9A in Jacksonville, FL (SR9A), three at a parking field on Bledsoe Drive on the University of Florida

campus (BD), three at an Alachua County park on Willinston Road (WP), three at Flavet Field on the University of Florida campus (FF), and one test on US 90 west of US 301 in north Florida (US90). Since the double ring test does not account for the applied head of water in the calculation, it was necessary to use the same head for both methods. The data from this study are summarized in Table 6.01 and indicate that the device does produce results that reflect the actual permeability of the soil when using an F factor of 12.2 cm. The difference between results from each method did not exceed 80 percent with lows approaching 10 percent. Figure 6.02 plots the results from Table 6.01. Upon first glance, it is obvious that the FPTD consistently under predicts when compared to the double ring infiltrometer test. Specific details from each test are provided in Appendix C.

Table 6-1: Comparison of results between the double ring infiltrometer test and the FPTD.

Test ID	K_{DR} ($\times 10^{-3}$)	K_{FPTD} ($\times 10^{-3}$)	K_{FPTD}/K_{DR}	% Diff
SMO - 1	5.33	2.94	0.55	44.9
SMO - 2	3.89	4.82	1.24	23.8
SMO - 3	7.50	2.83	0.38	62.3
SMO - 4	4.72	4.25	0.90	10.1
SR9A	0.76	0.85	1.11	11.3
BD-1	1.39	0.33	0.23	76.5
BD-2	5.67	3.09	0.54	45.5
BD-3	2.32	0.93	0.40	59.9
WP-1	5.94	1.32	0.22	77.8
WP-2	2.14	1.19	0.56	44.5
WP-3	2.86	1.13	0.39	60.6
FF-1	3.00	0.59	0.20	80.2
FF-2	1.00	0.70	0.70	30.2
FF-3	1.03	0.59	0.57	43.0
US90	0.80	0.91	1.14	13.8

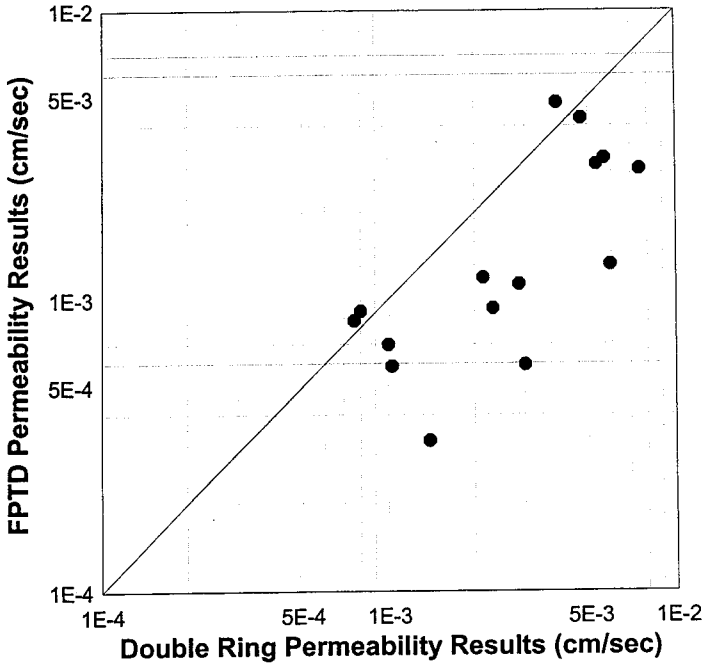

Figure 6-2: Comparison of results between the FPTD and the double ring test.

The grain size data accumulated during the double ring study provided the opportunity to estimate the permeability of the soil using the D_{10} relationship. This relationship is discussed in Chapter 2 and states that the C factor varies from 0.4 to 1.2 with 1.0 being the average. The permeability was calculated by using the minimum, maximum and average of this range. Results are shown in Table 6-2. When compared with results from the device, the back calculated C factor averages 0.11. This value is below the expected range of results but it does conclude that the device is conservative. It should be stated, however, that the D_{10} correlation is not intended to provide reliable permeability results. It is only used for comparative purposes and quick estimations.

Table 6-2: D_{10} correlation results.

Test ID	D_{10} (mm)	Permeability (cm/sec) C=1.0	C=0.4	C=1.2	K_{rpid} (cm/sec)	Back Calculated C
SMO-1	0.14	1.96E-02	7.84E-03	2.35E-02	2.94E-03	0.15
SMO-2	0.14	1.96E-02	7.84E-03	2.35E-02	4.82E-03	0.25
SMO-3	0.14	1.96E-02	7.84E-03	2.35E-02	2.83E-03	0.14
SMO-4	0.14	1.96E-02	7.84E-03	2.35E-02	4.25E-03	0.22
BD-1	0.14	1.96E-02	7.84E-03	2.35E-02	3.30E-04	0.02
BD-2	0.14	1.96E-02	7.84E-03	2.35E-02	3.09E-03	0.16
BD-3	0.14	1.96E-02	7.84E-03	2.35E-02	9.30E-04	0.05
FF-1	0.11	1.21E-02	4.84E-03	1.45E-02	5.90E-04	0.05
FF-2	0.11	1.21E-02	4.84E-03	1.45E-02	7.00E-04	0.06
FF-3	0.13	1.69E-02	6.76E-03	2.03E-02	5.90E-04	0.03
WP-1	0.09	8.10E-03	3.24E-03	9.72E-03	1.32E-03	0.16
WP-2	0.09	8.10E-03	3.24E-03	9.72E-03	1.19E-03	0.15
WP-3	0.09	8.10E-03	3.24E-03	9.72E-03	1.13E-03	0.14
SR90A-1	0.13	1.69E-02	6.76E-03	2.03E-02	8.50E-04	0.05
US90-1	0.14	1.96E-02	7.84E-03	2.35E-02	9.10E-04	0.05

CHAPTER 7
CONCLUSIONS

The main objective of this research was to enhance the Field Permeability Testing Device to become a safer and easier device to operate. The device was designed to measure the permeability of base and sub-base layers beneath pavements using a porous probe. In this research, several methods that correlate the use of a probe to the permeability are presented. The methods are then verified by comparing results from the double ring infiltrometer test and the FPTD.

Summary of Enhancements and Modifications

Several improvements were made to the FPTD to eliminate shortcomings associated with safety and efficiency issues. Prior to restructuring, the operator controls were located on the left side of the device. This configuration places the operator between the device and the next vehicle lane when tests were performed on existing roadways. In response, the control box was detached from the device giving the operator the freedom to place it in the tow vehicle or at any other suitable location. The control box is connected to the FPTD through two 30-foot long cables.

After safety issues were addressed, the next step was to improve the efficiency and operating time of the device. In the original system, the coring device was positioned at the front of the trailer with the center ram at the center. When tests were performed over existing pavements, the operator was required to raise and level the trailer before coring through the pavement. After the road was cored, the trailer was lowered and

repositioned to align the center ram over the hole. Once again, the trailer would need to be raised and leveled before attaching the probe to the ram and performing a test. This process could take almost one hour to complete before any data were collected.

To reduce the setup time, a rotating plate was designed and constructed on which both the center ram and coring device stand rest. Under the new system, the trailer would be raised and leveled only one time per test. Once the pavement has been cored, the plate is rotated 90 degrees to align the probe over the hole. This new feature has reduced the setup time from one hour to twenty minutes.

Time saving modifications were also made to the hydraulic leveling system. The four hydraulic leveling jacks were removed and replaced with larger hydraulic jacks that did not require any change to their orientation after traveling. The new jacks are simply raised and lowered through the controls and eliminate any need to use the tongue jack during testing.

Other enhancements were made to the components used during testing. New pressure transducers were installed on the Mariotte tank and the falling head tube. A laptop computer with data acquisition capabilities was then connected with the existing flow meter and the new pressure transducers. Data are now automatically recorded during a constant or falling head test. Other minor changes have been made and are discussed in Chapter 4.

Correlating the Use of a Probe with the Permeability

Three methods that describe the relationship between the flow through a porous probe and the permeability were presented in Chapter 5. The first method discussed is based on Hvorslev's charts, the second method uses the Packer/Lugeon equations, and

the third comes from a finite element computer analysis using Plaxis. All are based on the governing laws of flow through porous media including Darcy's law. The finite element solution was chosen as the benchmark method for future calculations since it was the only method to account for the shape of the probe. The other methods were based on the same theories but only considered the shape of the porous element. The shape of the entire probe is important since it acts like a boundary affecting the flow pattern, thus affecting the permeability.

The finite element solution suggests that an F factor of 12.2 cm be used assuming isotropic conditions. Therefore, the permeability can be calculated from field results using the following formula:

$$k = \frac{q}{12.2 \cdot h} \tag{7-1}$$

Where k is the permeability of the soil in cm/sec, q is the exit flow rate in cm^3/sec, and h is the applied head in cm.

Verifying Results from the Device

A comparison study was performed to ensure that the device does correctly measure the permeability. Results from the FPTD were compared to results from the ASTM standardized double ring infiltrometer test. The goal was not to produce a precise correlation but to gain confidence that the device does function properly.

Fifteen tests were performed. The test sequence began with a double ring test at a location with consistent soil. After the test was completed, the rings were removed and the probe was inserted through the center of the test area. Using this approach eliminated any influence of variability.

Final results were welcoming. The maximum difference between the methods did not exceed 80 percent. This range is reasonable considering that greater differences are not unusual amongst other methods. The permeability has been known to differ by as much as two to three times among results using a single field method in the same soil type.

Concluding Comments

If results from the device are only compared with each other then it can produce an accurate assessment of roadbed conditions. Each test result is more valuable as more data become available. The permeability under pavements in poor condition could be compared with results under those that perform better. Therefore, the device is best suited for permeability surveys. A database would prove useful in this case.

APPENDIX A
FIELD PERMEABILITY DATA

Appendix A is a compilation of all field-testing performed with the device during the project duration.

Field Permeability Data

Fifty-six tests have been performed over the course of the project duration. The research schedule was subdivided into three phases. The first phase included preliminary testing of the device. Results were inspected to ensure that Darcy's relationship was not being violated and that the device was functioning properly. Ten tests were performed during this phase and two device errors were discovered. It was found that the pressure gauge was not obtaining static readings due its placement within the system. This problem was quickly solved by relocating the pressure gage to the Mariotte tank. In addition, the device was lacking a method of de-airing the water lines. In response, a bleed valve was installed on the probe extension rod ensuring that any trapped air would be removed.

The second phase included a validation study. Results from the device were compared with results from the ASTM standardized double ring test. Fifteen tests were completed during this phase. The goal was not to produce a precise correlation but to gain confidence that the device is measuring the permeability of the soil. A detailed discussion of the results from this phase is presented in Chapter 6.

The third phase includes data accumulation from various locations around the state. Four tests were performed at the I-75 weigh station in Ocala, FL. Eight tests were performed on a damaged segment of I-10 near Monticello, FL. Another field survey was performed on I-4 in Lakeland, FL where 19 tests were completed.

Phase One

An unused concrete slab was selected as the testing location within the State Materials Office facility. The slab, which once supported a warehouse, is eight inches thick on the south end and four inches thick on the north end. Ten constant head tests were performed. Sieve analysis tests revealed A-3 material as the underlying soil.

Field Permeablilty Testing Device

Test ID: 1

Phase I : Preliminary Testing

Date : 5/21/99

Location : State Materials Office

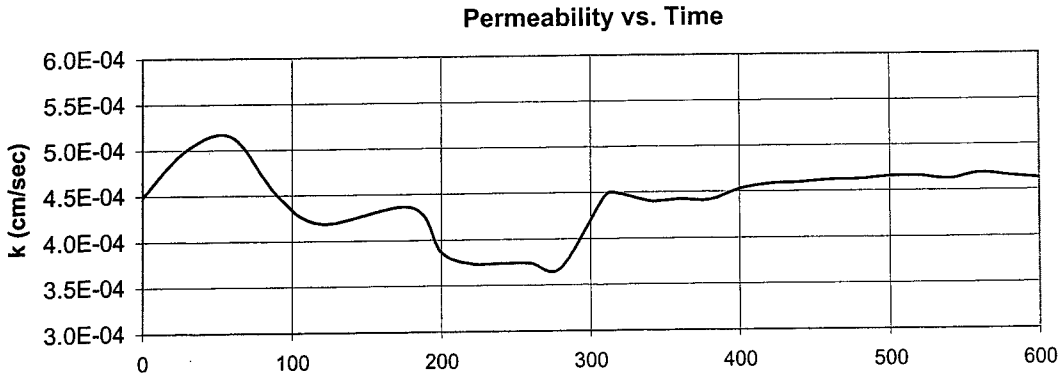

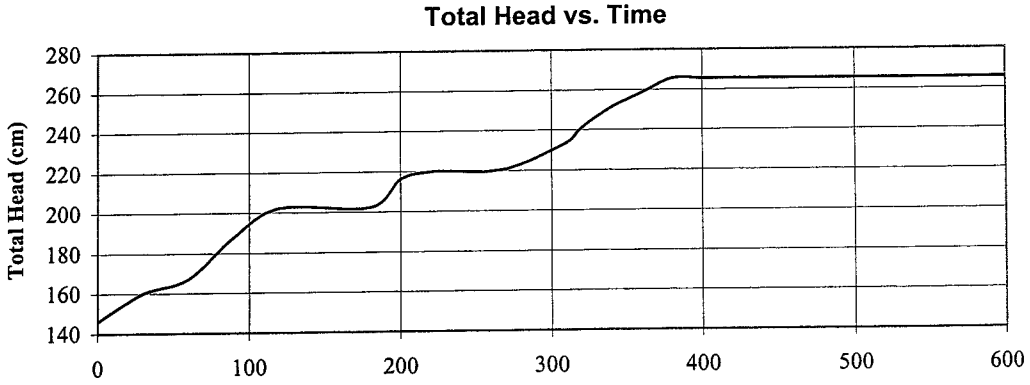

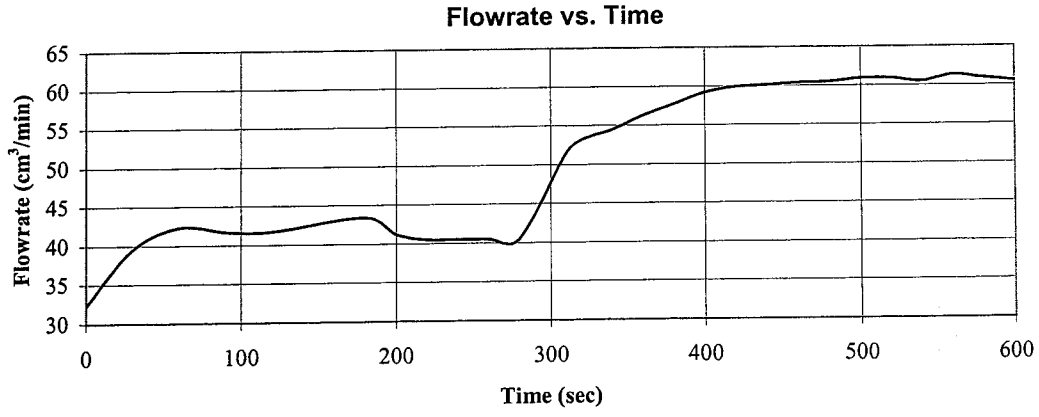

Field Permeablilty Testing Device

Test ID: 2

Phase I: Preliminary Testing

Date : 5/25/99

Location : State Materials Office

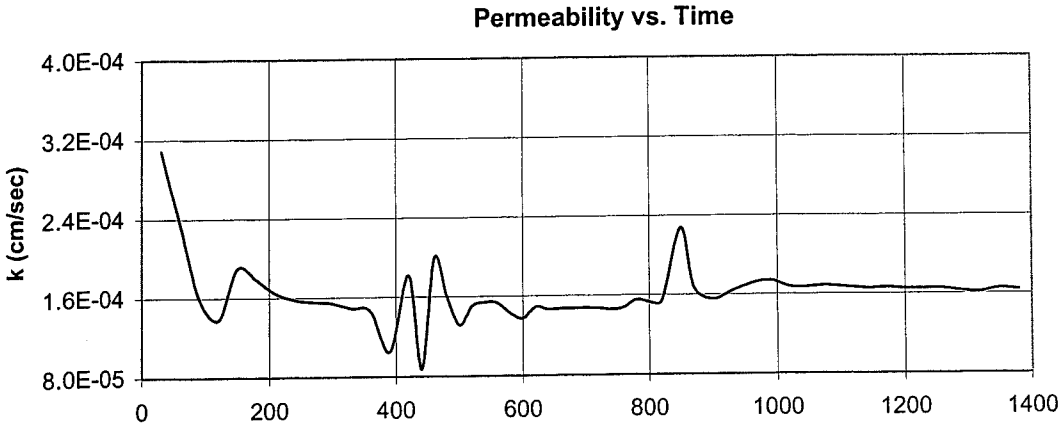

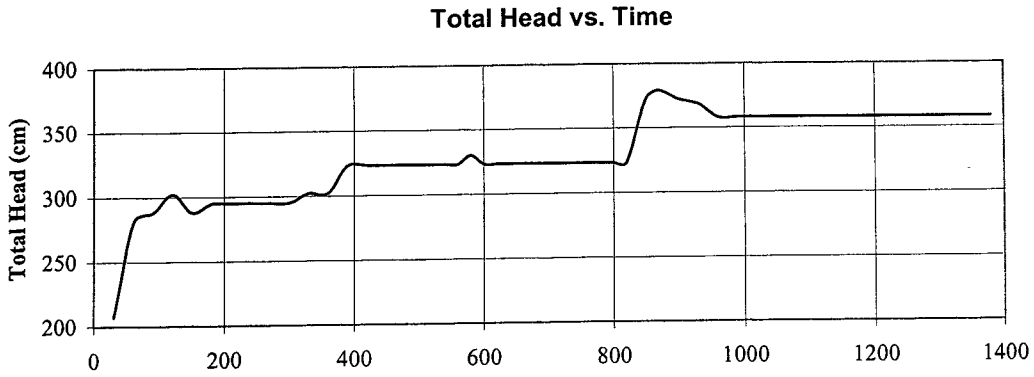

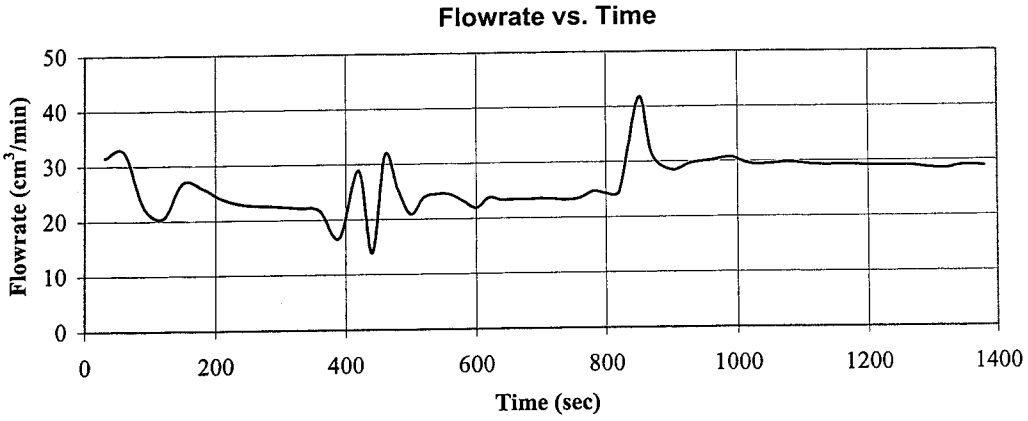

Field Permeablilty Testing Device

Test ID: 3

Phase I: Preliminary Testing

Date : 5/21/99

Location : State Materials Office

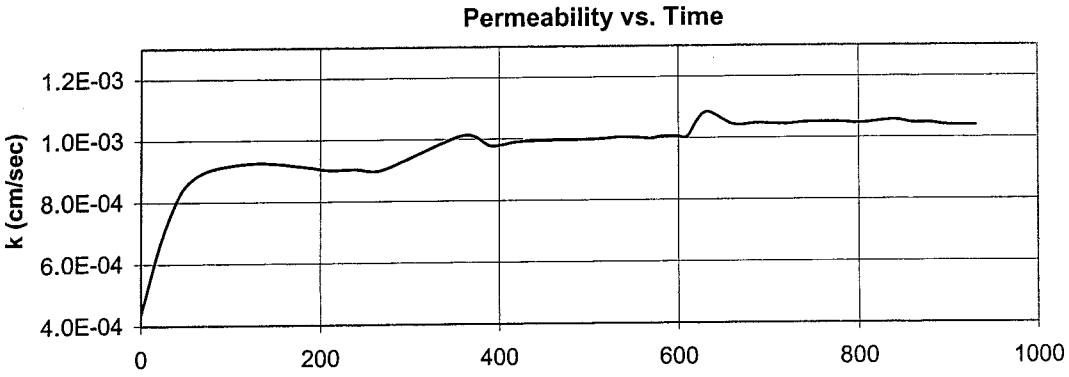

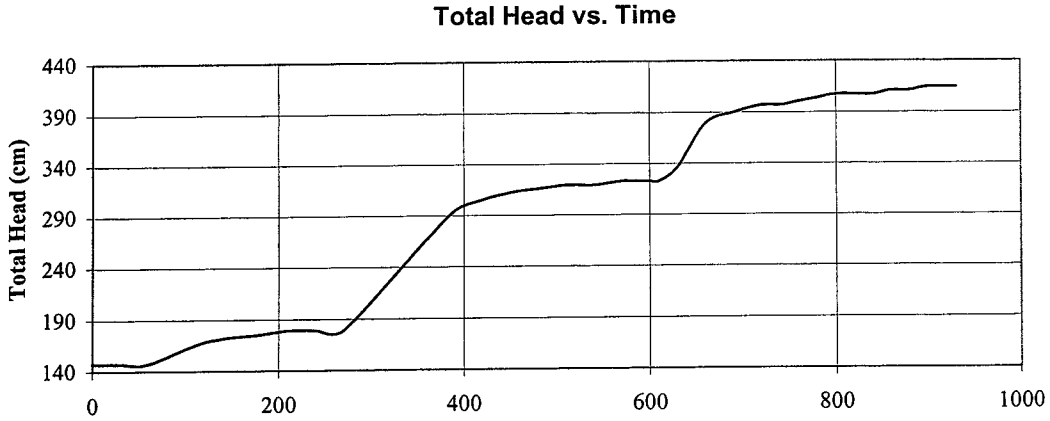

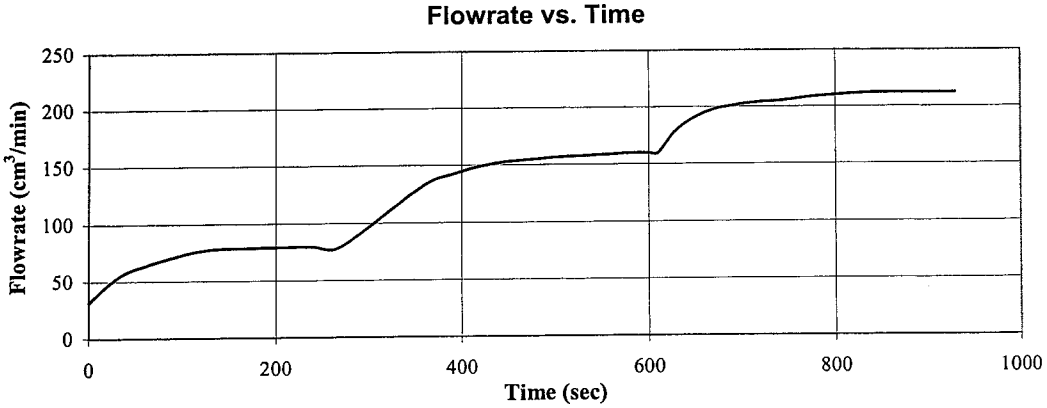

Field Permeablilty Testing Device

Test ID: 4

Phase I: Preliminary Testing

Date : 5/25/99

Location : State Materials Office

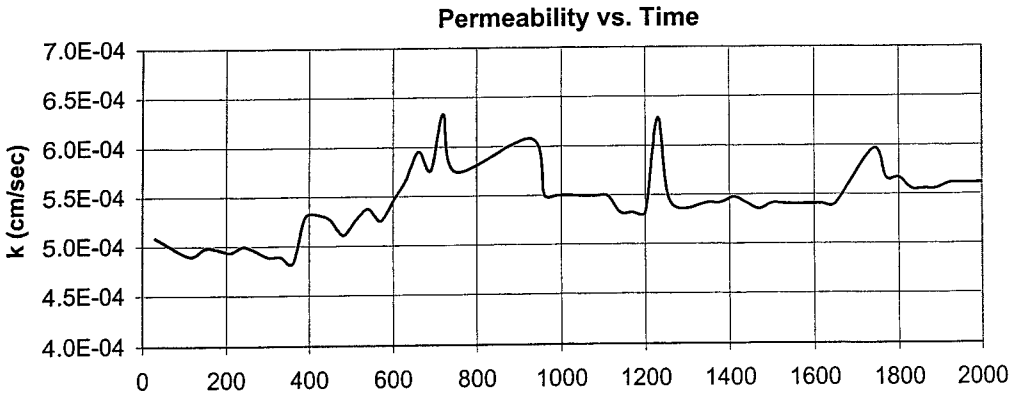

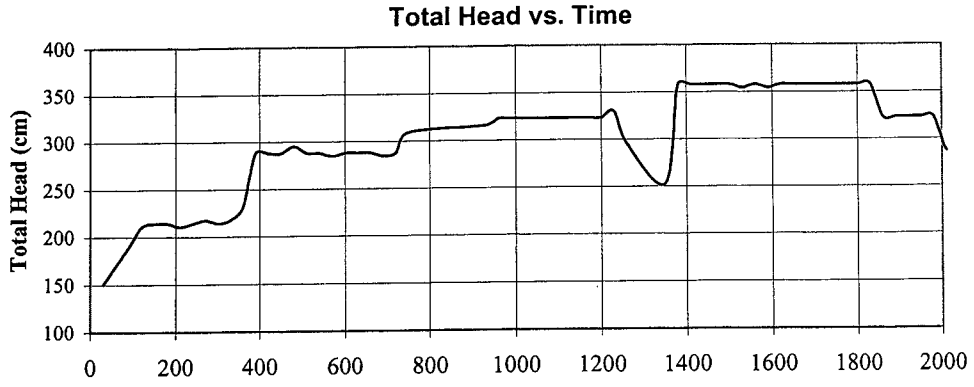

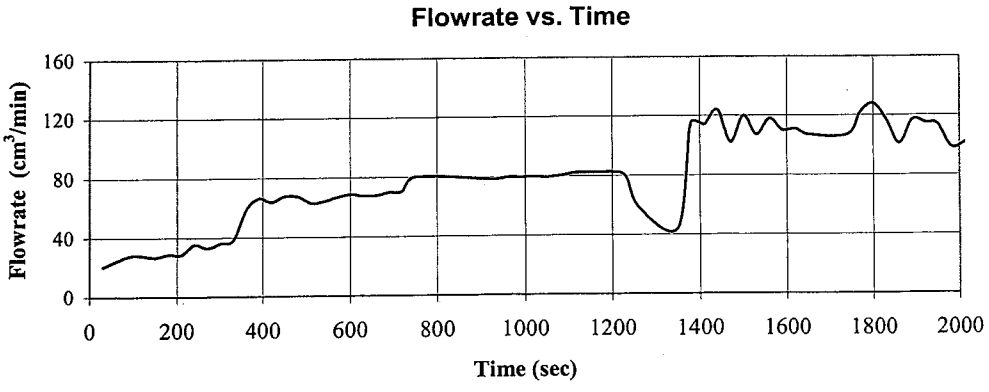

Field Permeablilty Testing Device

Test ID: 5

Phase I: Preliminary Testing

Date : 6/3/99

Location : State Materials Office

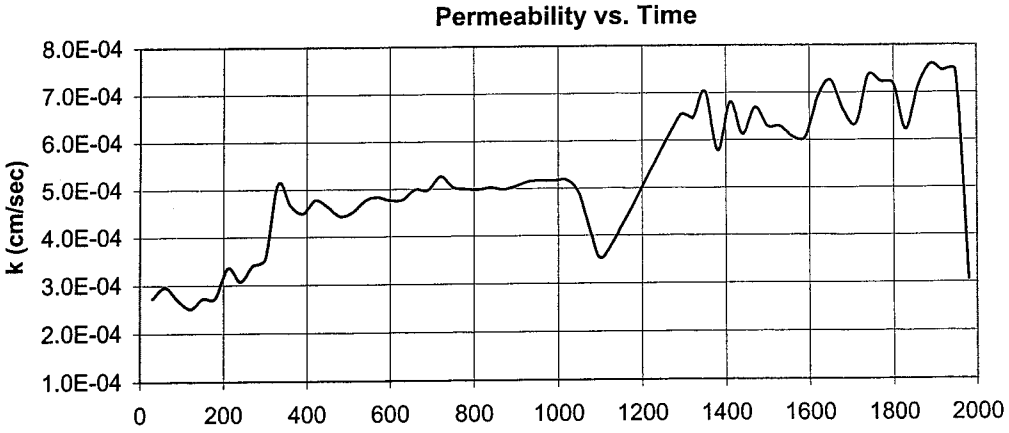

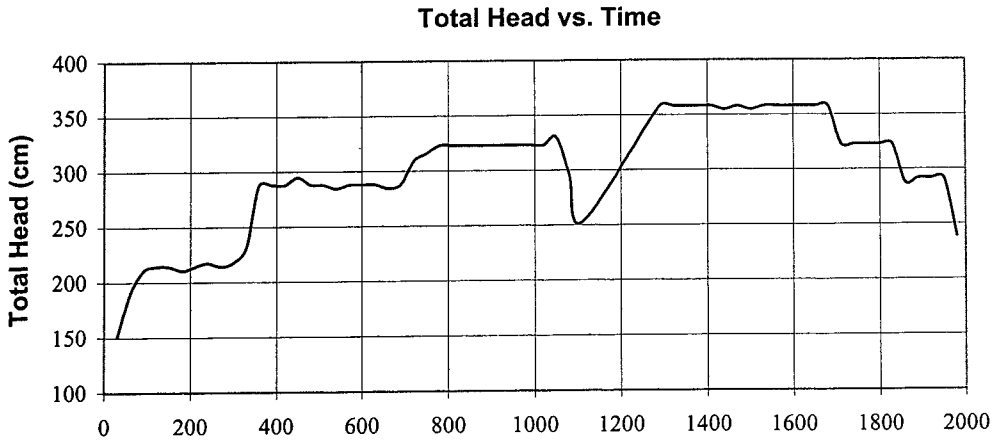

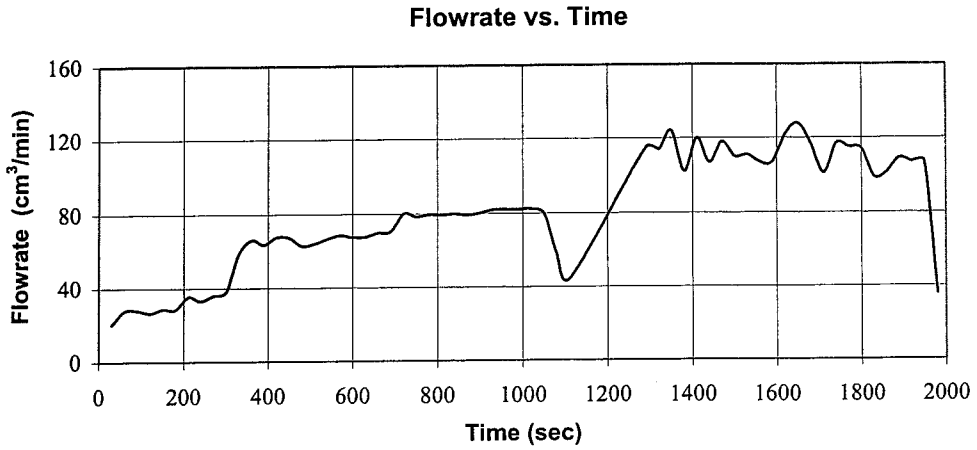

Field Permeablilty Testing Device

Test ID: 6

Phase I: Preliminary Testing

Date : 6/3/99

Location : State Materials Office

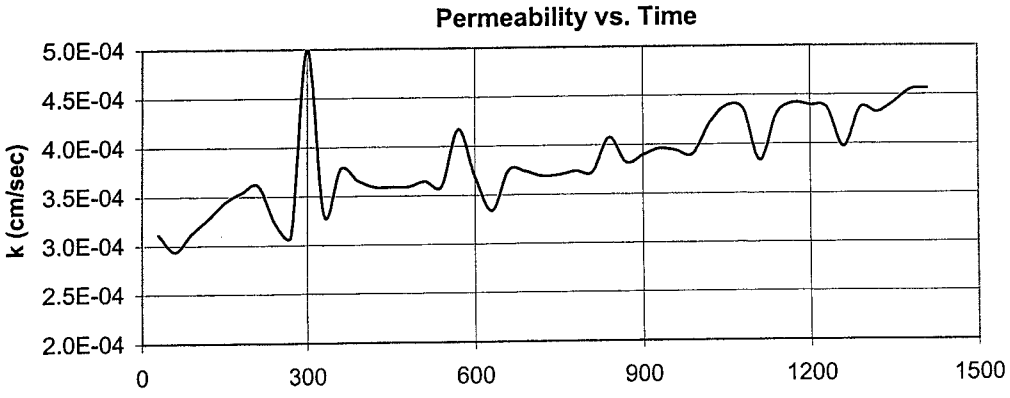

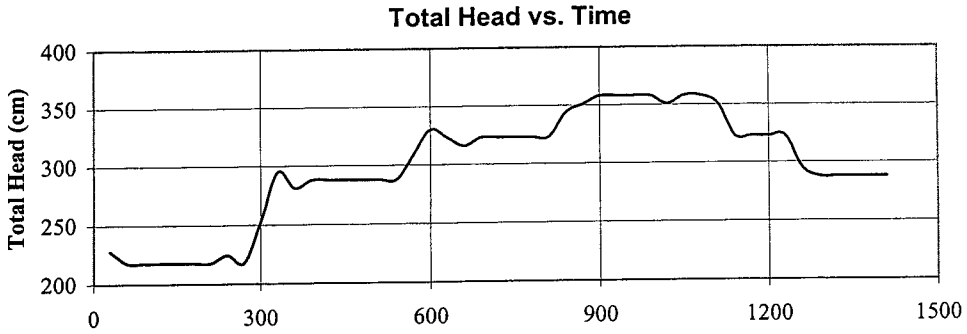

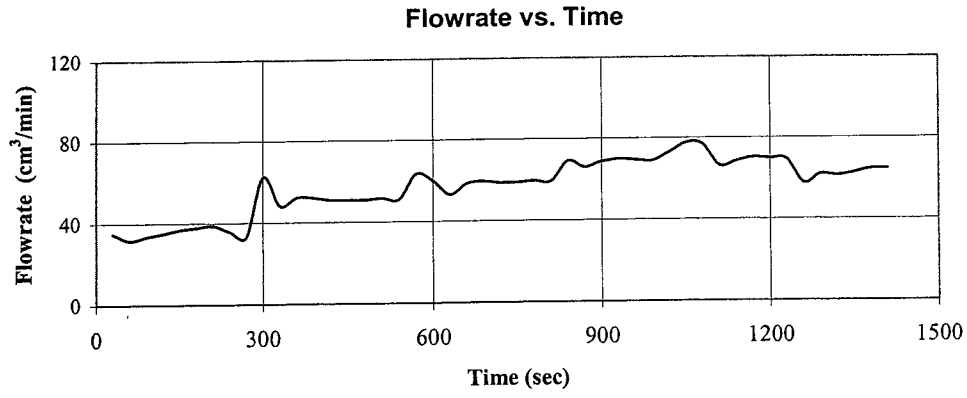

Field Permeablilty Testing Device

Phase I: Preliminary Testing
Location : State Materials Office

Test ID: 7
Date : 6/8/99

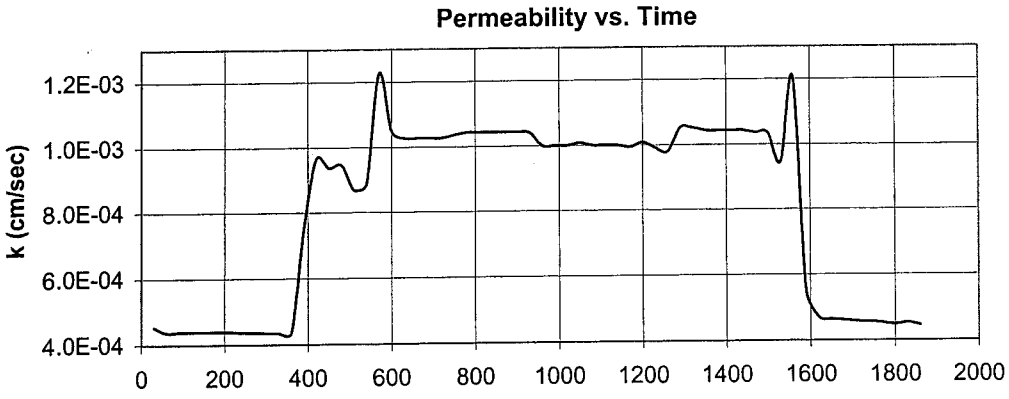

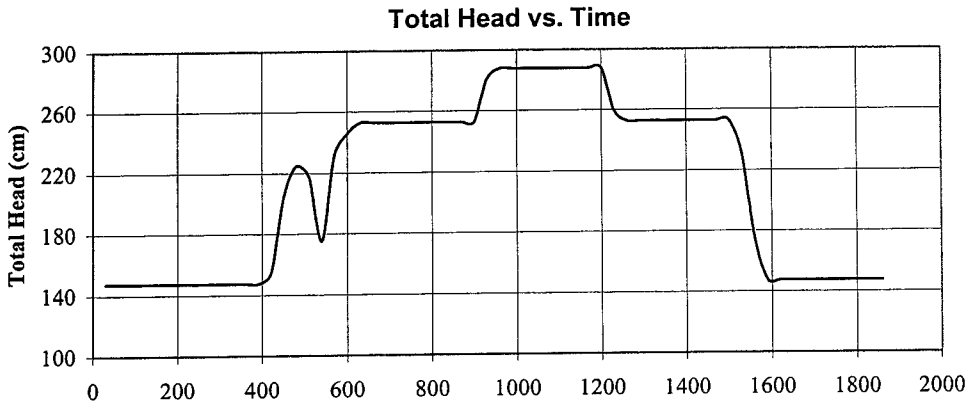

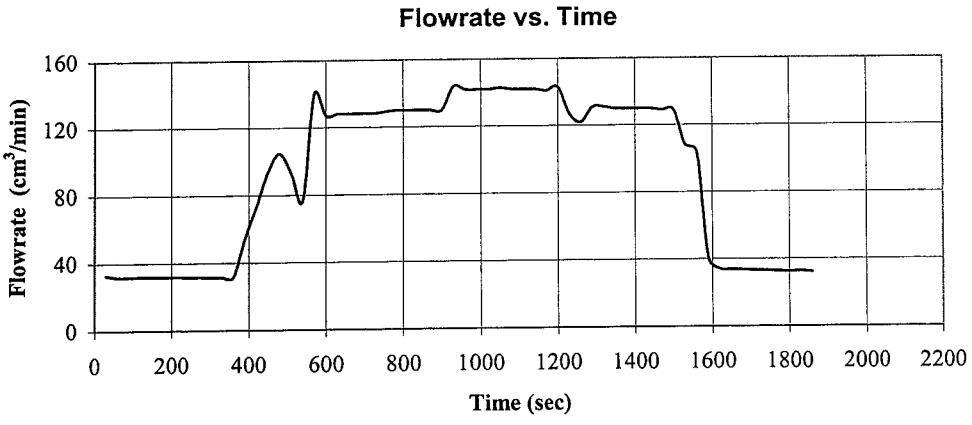

Field Permeablilty Testing Device

Phase I: Preliminary Testing
Location : State Materials Office

Test ID: 8
Date : 6/10/99

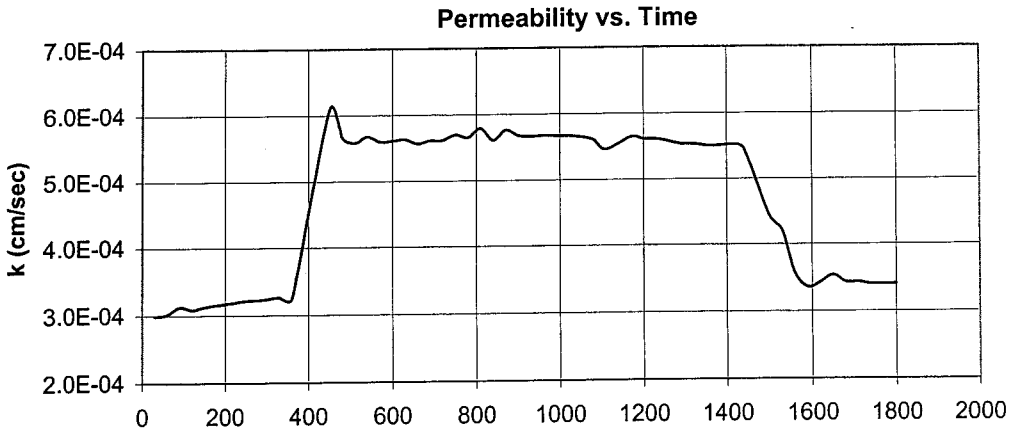

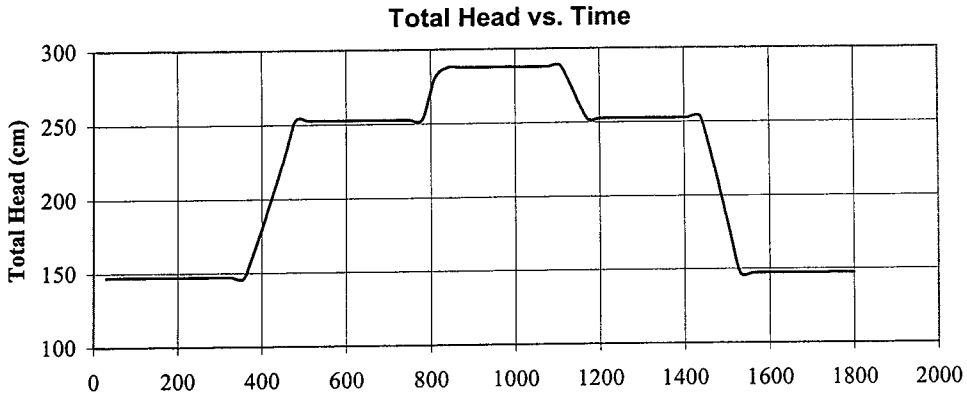

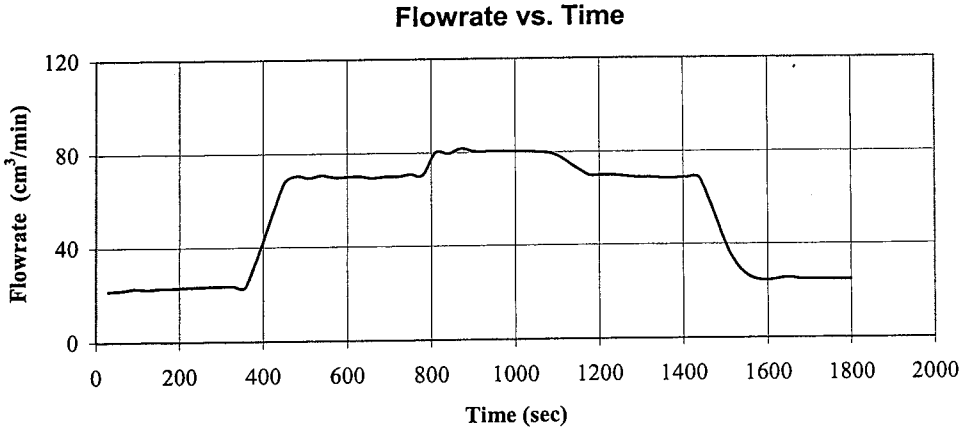

Field Permeablilty Testing Device

Test ID: 9

Phase I: Preliminary Testing

Date : 6/10/99

Location : State Materials Office

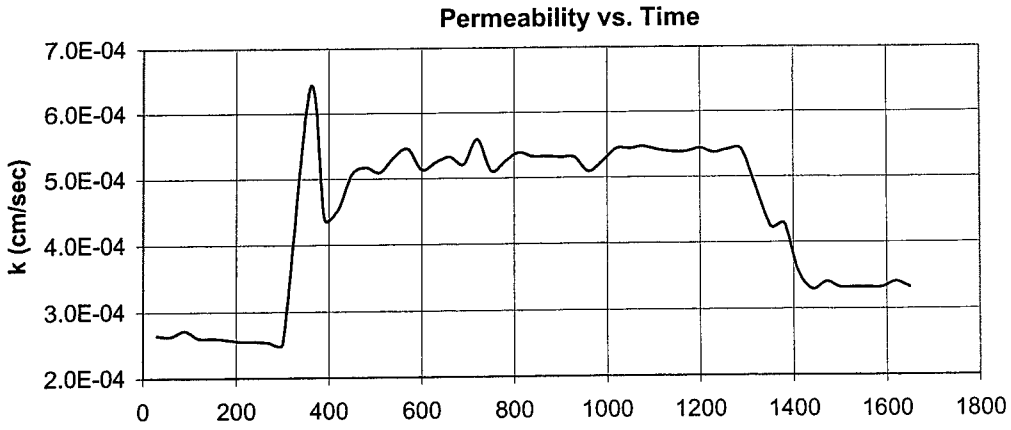

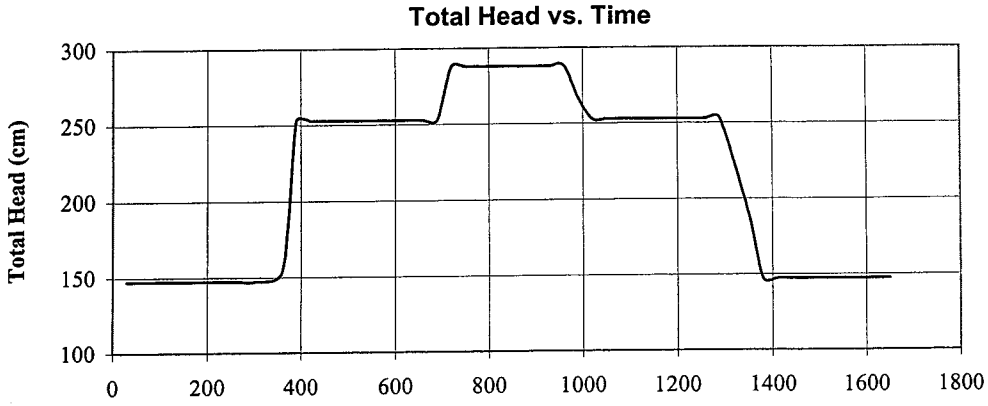

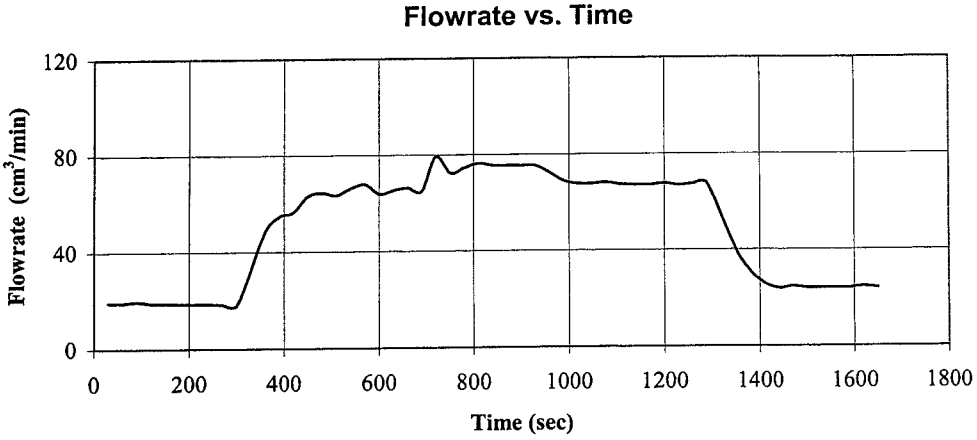

Field Permeablilty Testing Device

Test ID: 10

Phase I: Preliminary Testing

Date : 6/11/99

Location : State Materials Office

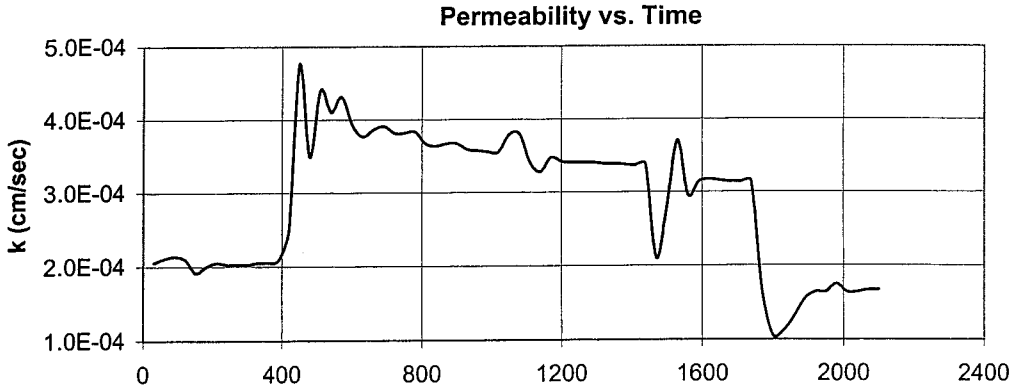

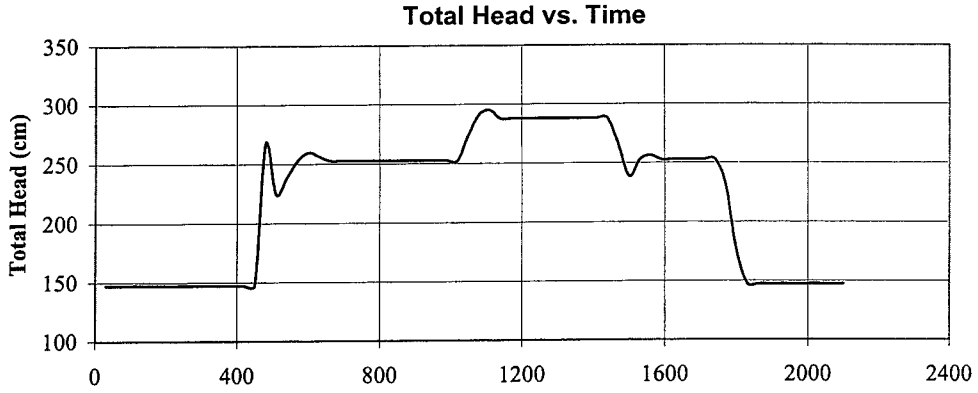

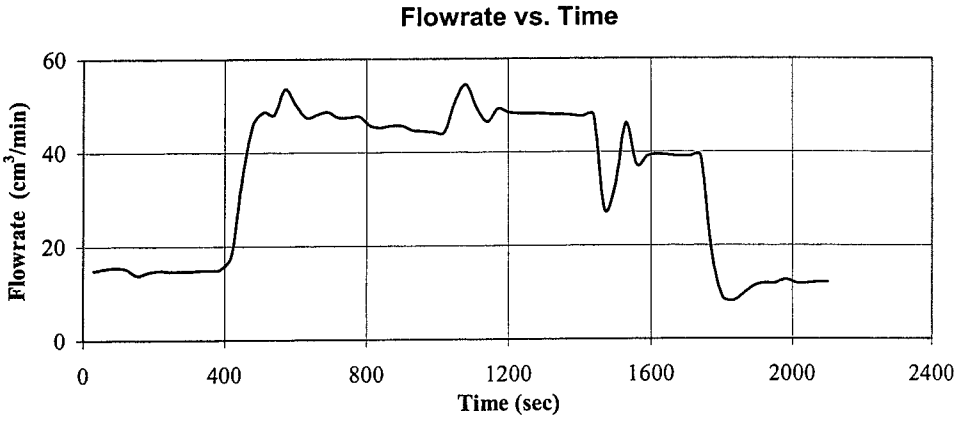

Field Permeablilty Testing Device

Test ID:

Phase I: Preliminary Testing **Date : 5/21/99**

Location : State Materials Office

Sieve Analysis

Test Location: 2

Sieve No.	Diameter (mm)	M_{sv} (g)	$M_{sv,s}$ (g)	M_s (g)	% Soil Retained	%Soil Passing
4	4.75	509.93	509.93	0.00	0.00	100
10	2.00	438.80	439.23	0.43	0.09	99.91
20	0.85	533.67	536.43	2.76	0.55	99.36
40	0.425	463.16	528.26	65.10	13.04	86.32
60	0.25	444.09	579.94	135.85	27.21	59.12
100	0.15	521.63	762.07	240.44	48.15	10.97
200	0.075	333.19	372.80	39.61	7.93	3.04
Pan	-	352.50	367.66	15.16	3.04	0.00
			Sum =	499.35		

Test Location: 4

Sieve No.	Diameter (mm)	M_{sv} (g)	$M_{sv,s}$ (g)	M_s (g)	% Soil Retained	%Soil Passing
4	4.75	509.93	512.9	2.97	0.59	99.4
10	2.00	438.71	440.21	1.50	0.30	99.10
20	0.85	533.92	536.95	3.03	0.60	98.50
40	0.425	463.24	526.77	63.53	12.68	85.82
60	0.25	444.05	576.59	132.54	26.45	59.37
100	0.15	521.61	763.88	242.27	48.34	11.03
200	0.075	333.17	374.64	41.47	8.28	2.75
Pan	-	352.44	366.26	13.82	2.76	0.00
			Sum =	501.13		

Field Permeablilty Testing Device

Test ID:

Phase I: Preliminary Testing

Date : 5/21/99

Location : State Materials Office

Results:

Test Location	D_{10}	D_{30}	D_{60}	C_u	C_z
2	0.14	0.19	0.25	1.79	1.03
4	0.14	0.19	0.25	1.79	1.03

Test Location	% Gravel	% Coarse Sand	% Medium Sanc	% Fine Sand	% Fines
2	0	0.09	13.59	83.28	3.04
4	0	0.89	13.29	83.06	2.76

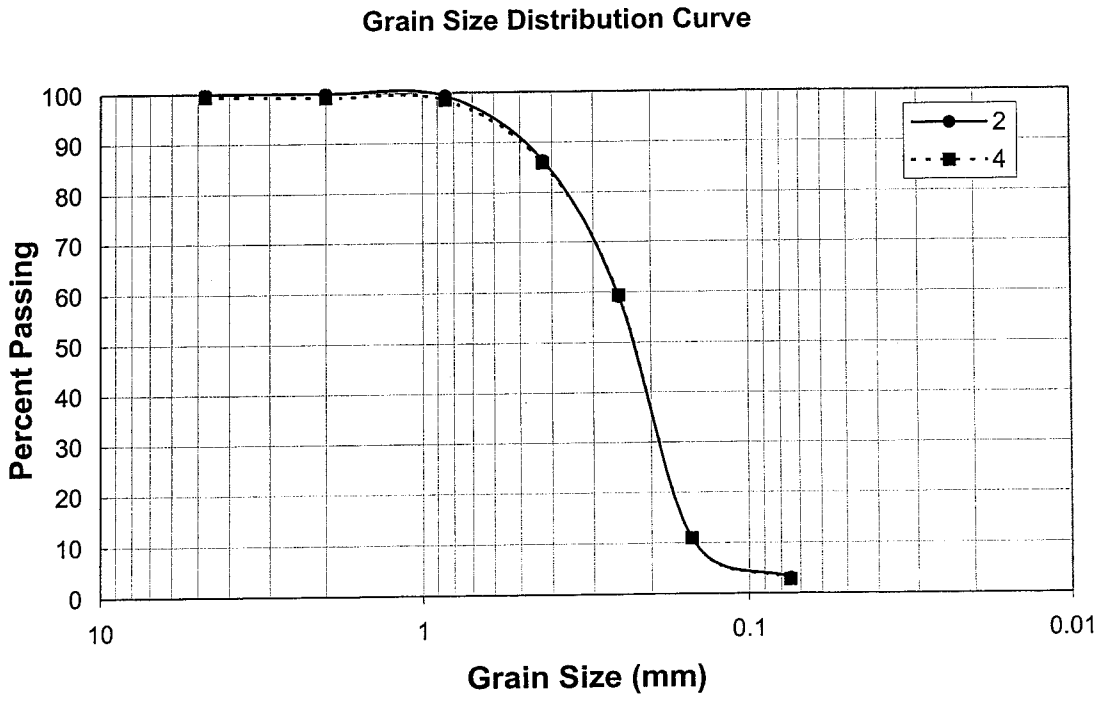

Phase Two

Fifteen standard tests including the double ring infiltrometer were performed at various locations in A-3 material. Four were performed at the State Materials Office, three on a field alongside Bledsoe Drive at the University of Florida, three on Flavet Field also at the University of Florida, three at an Alachua County park located on US 441 and Willinston Road, one test on State Road 9A in Jacksonville, FL, and one test on US 90 west of US 301. The test sequence began with a double ring test at a location with consistent soil. After the test was completed, the rings were removed and the probe was inserted through the center of the test area. The procedure for the double ring infiltrometer test is outlined in ASTM D 3385.

Summary of Results

Test ID	k_{DR} ($\times 10^{-3}$)	k_{FPTD} ($\times 10^{-3}$)	k_{FPTD}/k_{DR}	% Diff.
SMO - 1	5.33	2.94	0.55	44.9
SMO - 2	3.89	4.82	1.24	23.8
SMO - 3	7.50	2.83	0.38	62.3
SMO - 4	4.72	4.25	0.90	10.1
BD-1	1.39	0.33	0.23	76.5
BD-2	5.67	3.09	0.54	45.5
BD-3	2.32	0.93	0.40	59.9
FF-1	3.00	0.59	0.20	80.2
FF-2	1.00	0.70	0.70	30.2
FF-3	1.03	0.59	0.57	43.0
WP-1	5.94	1.32	0.22	77.8
WP-2	2.14	1.19	0.56	44.5
WP-3	2.86	1.13	0.39	60.6
SR9A - 1	0.76	0.85	1.11	11.3
US90-1	0.80	0.91	1.14	13.8

Field Permeablilty Testing Device

Test ID: SMO-1

Phase II: Validation Study

Date : 7/22/99

Location : State Materials Office

Sleeve Diameter (in):	0.775
Sleeve Length (in):	0.685
Shape Factor (cm):	8.21
Depth of Probe (in):	8
Elevation (in):	-
Elevation Head (in):	18

Time (min)	Gauge Pressure Reading (psi)	Flowmeter Reading (cc/min)	Total Head (cm)	Insitu Permeability (cm/sec)
0.5	0.00	176	45.7	7.82E-03
5.0	0.00	160	45.7	7.11E-03
10.0	0.00	146	45.7	6.48E-03
15.0	0.00	138	45.7	6.13E-03
20.0	0.00	134	45.7	5.95E-03
30.0	0.00	125	45.7	5.55E-03
40.0	0.00	121	45.7	5.37E-03
50.0	0.00	119	45.7	5.29E-03
60.0	0.00	115	45.7	5.11E-03
80.0	0.00	114	45.7	5.06E-03
90.0	0.00	110	45.7	4.89E-03
110.0	0.00	110	45.7	4.89E-03
120.0	0.00	108	45.7	4.80E-03

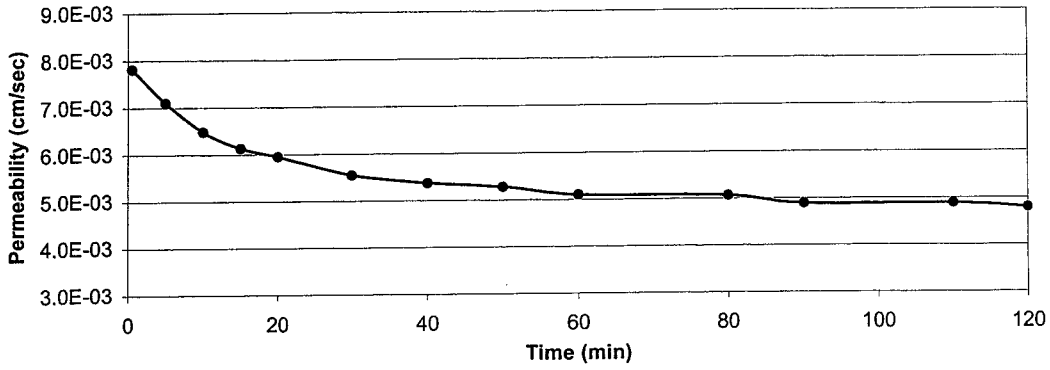

ASTM D 3385 - Infiltration Rate of Soils in Field Using Double-Ring Infiltrometer

Project Identification: SMO-1

Project Location: DOT State Materials Office

Liquid Used: Water pH: 7.0

Tested By: Michael Garau

Depth to water table: unknown (ft)

Penetration of rings: Inner: 5.5 (in) Outer: 5.5 (in)

Constants	Area (cm^2)	Depth of Liquid (cm)	Liquid Containers No.	Vol./ΔH (cm^2/cm)
Inner Ring:	729.7			
Annular Space:	2189.0			

Liquid Level Maintained Using: ☐ Flow Valve ☐ Float Valve ☐ Mariotte Tube ☒ Other: Refilling

Trial No.		Date	Time hr:min	Elapsed Time Δ/(total) min	Flow Readings: Inner Ring Reading cm	Inner Ring Flow cm^3	Annular Space Reading cm	Annular Space Flow cm^3	Liquid Temp. °C	Incr. Infiltration Rate: Inner cm/h	Annular cm/h	Ground Temp. = ____ °F / °C @ depth of ____ (in) Remarks: Weather Conditions, etc.
1	S	7/6/99	10:15	15	-	3000	-	11900	25	16.4	21.7	
	E	7/6/99	10:30	15	-		-		25			
2	S	7/6/99	10:30	15	-	3500	-	9500	25	19.2	17.4	
	E	7/6/99	10:45	30	-		-		25			
3	S	7/6/99	10:45	15	-	3500	-	11000	25	19.2	20.1	
	E	7/6/99	11:00	45	-		-		25			
4	S	7/6/99	11:00	15	-	3500	-	12000	25	19.2	21.9	
	E	7/6/99	11:15	60	-		-		25			
5	S	7/6/99	11:15	15	-	3500	-	10000	25	19.2	18.3	
	E	7/6/99	11:30	75	-		-		25			
6	S											
	E											
7	S											
	E											
8	S											
	E											
9	S											
	E											
10	S											
	E											

Ring Dimensions: Inner Ring: 30.48 cm (12 in) diameter, 60.96 cm (24 in) height
Outer Ring: 60.96 cm (24 in) diameter, 60.96 cm (24 in) height

Field Permeablilty Testing Device

Test ID: SMO-2

Phase II: Validation Study

Date : 7/23/99

Location : State Materials Office

Sleeve Diameter (in):	0.775
Sleeve Length (in):	0.685
Shape Factor (cm):	8.21
Depth of Probe (in):	8
Elevation (in):	-
Elevation Head (in):	18

Time (min)	Gauge Pressure Reading (psi)	Flowmeter Reading (cc/min)	Total Head (cm)	Insitu Permeability (cm/sec)
0.0	0.00	173	45.7	7.68E-03
5.0	0.00	177	45.7	7.86E-03
7.0	0.00	178	45.7	7.91E-03
9.0	0.00	182	45.7	8.08E-03
12.0	0.00	182	45.7	8.08E-03
14.0	0.00	184	45.7	8.17E-03
20.0	0.00	189	45.7	8.39E-03
40.0	0.00	192	45.7	8.53E-03
65.0	0.00	192	45.7	8.53E-03
100.0	0.00	190	45.7	8.44E-03
160.0	0.00	180	45.7	7.99E-03
210.0	0.00	177	45.7	7.86E-03

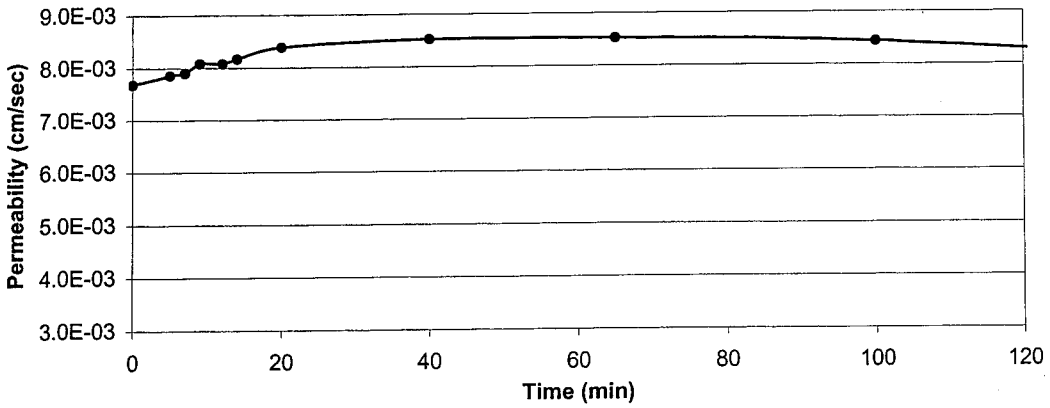

ASTM D 3385 - Infiltration Rate of Soils in Field using Double Ring Infiltrometer

Project Identification: SMO-2

Project Location: DOT State Materials Office

Liquid Used: Water pH: 7.0

Tested By: Michael Garau

Depth to water table: unknown (ft)

Penetration of rings: Inner: 5.5 (in) Outer: 5.5 (in)

Constants	Area (cm^2)	Depth of Liquid (cm)	Liquid Containers No.	Liquid Containers Vol./ΔH (cm^2/cm)
Inner Ring:	729.7	45.7	-	-
Annular Space:	2189.0	45.7	-	-

Liquid Level Maintained Using: ☐ Flow Valve ☐ Float Valve ☐ Mariotte Tube ☒ Other: Refilling

Trial No.		Date	Time hr:min	Elapsed Time Δ/(total) min	Flow Readings: Inner Ring Reading cm	Inner Ring Flow cm^3	Annular Space Reading cm	Annular Space Flow cm^3	Liquid Temp. °C	Incr. Infiltration Rate: Inner cm/h	Annular cm/h	Ground Temp. = 20 °C @ depth of 8 (in) Remarks: Weather Conditions, etc.
1	S	7/799	10:15	15	-	2100	-	10300	25	11.5	18.8	
	E	7/799	10:30	15	-		-		25			Cloudy
2	S	7/799	10:30	15	-	2500	-	9900	25	13.7	18.1	
	E	7/799	10:45	30	-		-		25			
3	S	7/799	10:45	15	-	2500	-	10700	25	13.7	19.6	
	E	7/7/99	11:00	45	-		-		25			
4	S	7/799	11:00	15	-	2100	-	10000	25	11.5	18.3	
	E	7/799	11:15	60	-		-		25			
5	S	7/799	11:15	15	-	2600	-	11000	25	14.3	20.1	
	E	7/799	11:30	75	-		-		25			
6	S	7/799	11:30	15	-	2800	-	12700	25	15.3	23.2	
	E	7/799	11:45	90	-		-		25			
7	S	7/799	11:45	15	-	2400	-	9700	25	13.2	17.7	
	E	7/799	12:00	105	-		-		25			
8	S											
	E											
9	S											
	E											
10	S											
	E											

Ring Dimensions: Inner Ring: 30.48 cm (12 in) diameter, 60.96 cm (24 in) height
Outer Ring: 60.96 cm (24 in) diameter, 60.96 cm (24 in) height

Field Permeablilty Testing Device

Test ID: SMO-3

Phase II: Validation Study

Date : 7/22/99

Location : State Materials Office

Sleeve Diameter (in):	0.775
Sleeve Length (in):	0.685
Shape Factor (cm):	8.21
Depth of Probe (in):	8
Elevation (in):	-
Elevation Head (in):	18

Time (min)	Gauge Pressure Reading (psi)	Flowmeter Reading (cc/min)	Total Head (cm)	Insitu Permeabilit y (cm/sec)
0.0	0.00	132	45.7	5.86E-03
5.0	0.00	125	45.7	5.55E-03
9.0	0.00	121	45.7	5.37E-03
11.0	0.00	119	45.7	5.29E-03
20.0	0.00	115	45.7	5.11E-03
45.0	0.00	108	45.7	4.80E-03
55.0	0.00	104	45.7	4.62E-03
75.0	0.00	110	45.7	4.89E-03
80.0	0.00	108	45.7	4.80E-03
90.0	0.00	104	45.7	4.62E-03
120.0	0.00	104	45.7	4.62E-03

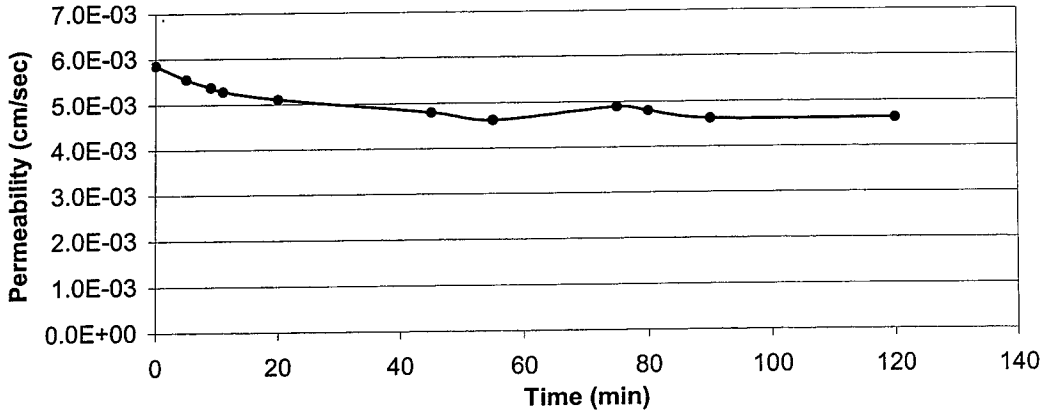

ASTM D 3385 - Infiltration Rate of Soils in Field using Double Ring Infiltrometer

Project Identification: SMO-3

Project Location: DOT State Materials Office

Liquid Used: Water pH: 7.0

Tested By: Michael Garau

Depth to water table: unknown (ft)

Penetration of rings: Inner: 5.5 (in) Outer: 5.5 (in)

Constants	Area (cm^2)	Depth of Liquid (cm)	Liquid Containers No.	Liquid Containers Vol./ΔH (cm^2/cm)
Inner Ring:	729.7	45.7	-	-
Annular Space:	2189.0	45.7	-	-

Liquid Level Maintained Using: ☐ Flow Valve ☐ Float Valve ☐ Mariotte Tube ☒ Other: Refilling

Trial No.		Date	Time hr:min	Elapsed Time Δ/(total) min	Flow Readings Inner Ring Reading cm	Flow Readings Inner Ring Flow cm^3	Flow Readings Annular Space Reading cm	Flow Readings Annular Space Flow cm^3	Liquid Temp. °C	Incr. Infiltration Rate Inner cm/h	Incr. Infiltration Rate Annular cm/h	Ground Temp. = 20 °C @ depth of 8 (in) Remarks: Weather Conditions, etc.
1	S	7/8/99	11:15	15	-	4900	-	17000	25	26.9	31.1	
	E	7/8/99	11:30	15	-		-		25			Cloudy
2	S	7/8/99	11:30	15	-	3600	-	15000	25	19.7	27.4	
	E	7/8/99	11:45	30	-		-		25			
3	S	7/8/99	11:45	15	-	4800	-	16000	25	26.3	29.2	
	E	7/8/99	12:00	45	-		-		25			
4	S	7/8/99	12:00	15	-	4900	-	16000	25	26.9	29.2	
	E	7/8/99	12:15	60	-		-		25			
5	S	7/8/99	12:15	15	-	5100	-	17000	25	28.0	31.1	
	E	7/8/99	12:30	75	-		-		25			
6	S											
	E											
7	S											
	E											
8	S											
	E											
9	S											
	E											
10	S											
	E											

Ring Dimensions: Inner Ring: 30.48 cm (12 in) diameter, 60.96 cm (24 in) height
Outer Ring: 60.96 cm (24 in) diameter, 60.96 cm (24 in) height

Field Permeablilty Testing Device

Test ID: SMO-4

Phase II: Validation Study

Date : 7/26/99

Location : State Materials Office

Sleeve Diameter (in):	0.775
Sleeve Length (in):	0.685
Shape Factor (cm):	8.21
Depth of Probe (in):	8
Elevation (in):	-
Elevation Head (in):	18

Time (min)	Gauge Pressure Reading (psi)	Flowmeter Reading (cc/min)	Total Head (cm)	Insitu Permeability (cm/sec)
1.0	0.00	150	45.7	6.66E-03
5.0	0.00	150	45.7	6.66E-03
15.0	0.00	150	45.7	6.66E-03
28.0	0.00	152	45.7	6.75E-03
35.0	0.00	152	45.7	6.75E-03
40.0	0.00	154	45.7	6.84E-03
58.0	0.00	154	45.7	6.84E-03
71.0	0.00	156	45.7	6.93E-03
115.0	0.00	156	45.7	6.93E-03
120.0	0.00	156	45.7	6.93E-03

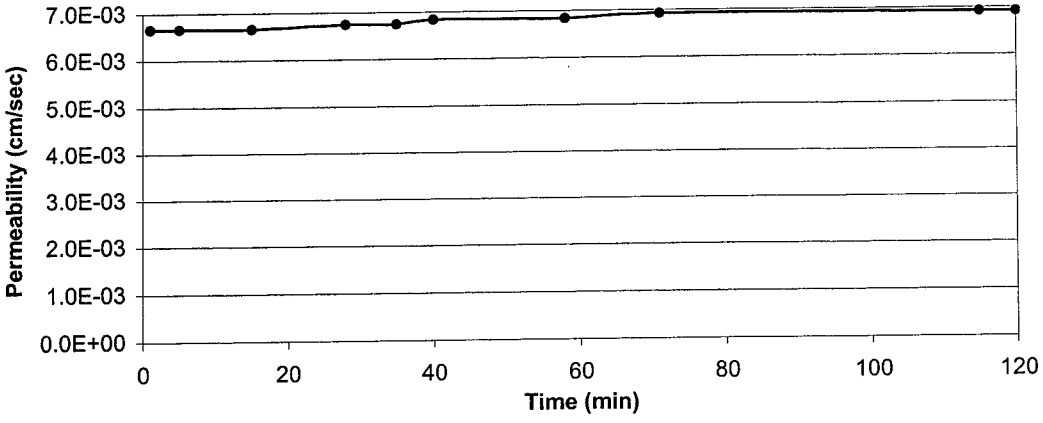

ASTM D 3385 - Infiltration Rate of Soils in Field using Double Ring Infiltrometer

Project Identification: SMO-4

Project Location: DOT State Materials Office

Liquid Used: Water pH: 7.0

Tested By: Michael Garau

Depth to water table: unknown (ft)

Penetration of rings: Inner: 5.5 (in) Outer: 5.5 (in)

Constants	Area (cm^2)	Depth of Liquid (cm)	Liquid Containers No.	Liquid Containers Vol./ΔH (cm^2/cm)
Inner Ring:	729.7	45.7	-	-
Annular Space:	2189.0	45.7	-	-

Liquid Level Maintained Using: ☐ Flow Valve ☐ Float Valve ☐ Mariotte Tube ☒ Other: Refilling

Ground Temp. = 20 °C @ depth of 8 (in)

Trial No.		Date	Time hr:min	Elapsed Time Δ(total) min	Flow Readings: Inner Ring Reading cm	Flow Readings: Inner Ring Flow cm^3	Flow Readings: Annular Space Reading cm	Flow Readings: Annular Space Flow cm^3	Liquid Temp. °C	Incr. Infiltration Rate: Inner cm/h	Incr. Infiltration Rate: Annular cm/h	Remarks: Weather Conditions, etc.
1	S	7/8/99	2:00	15	-	3000	-	7600	25	16.4	13.9	
	E	7/8/99	2:15	15	-		-		25			Cloudy
2	S	7/8/99	2:15	15	-	3000	-	7900	25	16.4	14.4	
	E	7/8/99	2:30	30	-		-		25			
3	S	7/8/99	2:30	15	-	3000	-	7500	25	16.4	13.7	
	E	7/8/99	2:45	45	-		-		25			
4	S	7/8/99	2:45	15	-	3500	-	8600	25	19.2	15.7	
	E	7/8/99	3:00	60	-		-		25			
5	S	7/8/99	3:00	15	-	3000	-	9000	25	16.4	16.4	
	E	7/8/99	3:15	75	-		-		25			
6	S											
	E											
7	S											
	E											
8	S											
	E											
9	S											
	E											
10	S											
	E											

Ring Dimensions: Inner Ring: 30.48 cm (12 in) diameter, 60.96 cm (24 in) height
Outer Ring: 60.96 cm (24 in) diameter, 60.96 cm (24 in) height

Field Permeablilty Testing Device | **Test ID:** SMO
Phase II: Validation Study | **Date :** 5/21/99
Location : State Materials Office

Sieve Analysis

Test Location: SMO-1, SMO-2

Sieve No.	Diameter (mm)	M_{sv} (g)	$M_{sv,s}$ (g)	M_s (g)	% Soil Retained	%Soil Passing
4	4.75	509.93	509.93	0.00	0.00	100
10	2.00	438.80	439.23	0.43	0.09	99.91
20	0.85	533.67	536.43	2.76	0.55	99.36
40	0.425	463.16	528.26	65.10	13.04	86.32
60	0.25	444.09	579.94	135.85	27.21	59.12
100	0.15	521.63	762.07	240.44	48.15	10.97
200	0.075	333.19	372.80	39.61	7.93	3.04
Pan	-	352.50	367.66	15.16	3.04	0.00
			Sum =	499.35		

Test Location: SMO-3, SMO-4

Sieve No.	Diameter (mm)	M_{sv} (g)	$M_{sv,s}$ (g)	M_s (g)	% Soil Retained	%Soil Passing
4	4.75	509.93	512.9	2.97	0.59	99.4
10	2.00	438.71	440.21	1.50	0.30	99.10
20	0.85	533.92	536.95	3.03	0.60	98.50
40	0.425	463.24	526.77	63.53	12.68	85.82
60	0.25	444.05	576.59	132.54	26.45	59.37
100	0.15	521.61	763.88	242.27	48.34	11.03
200	0.075	333.17	374.64	41.47	8.28	2.75
Pan	-	352.44	366.26	13.82	2.76	0.00
			Sum =	501.13		

Field Permeablilty Testing Device

Phase II: Validation Study
Location : State Materials Office

Test ID: SMO
Date : 5/21/99

Results:

Test Location	D_{10}	D_{30}	D_{60}	C_u	C_z
SMO1, 2	0.14	0.19	0.25	1.79	1.03
SMO3, 4	0.14	0.19	0.25	1.79	1.03

Test Location	% Gravel	% Coarse Sand	% Medium Sand	% Fine Sand	% Fines
SMO1, 2	0	0.09	13.59	83.28	3.04
SMO3, 4	0	0.89	13.29	83.06	2.76

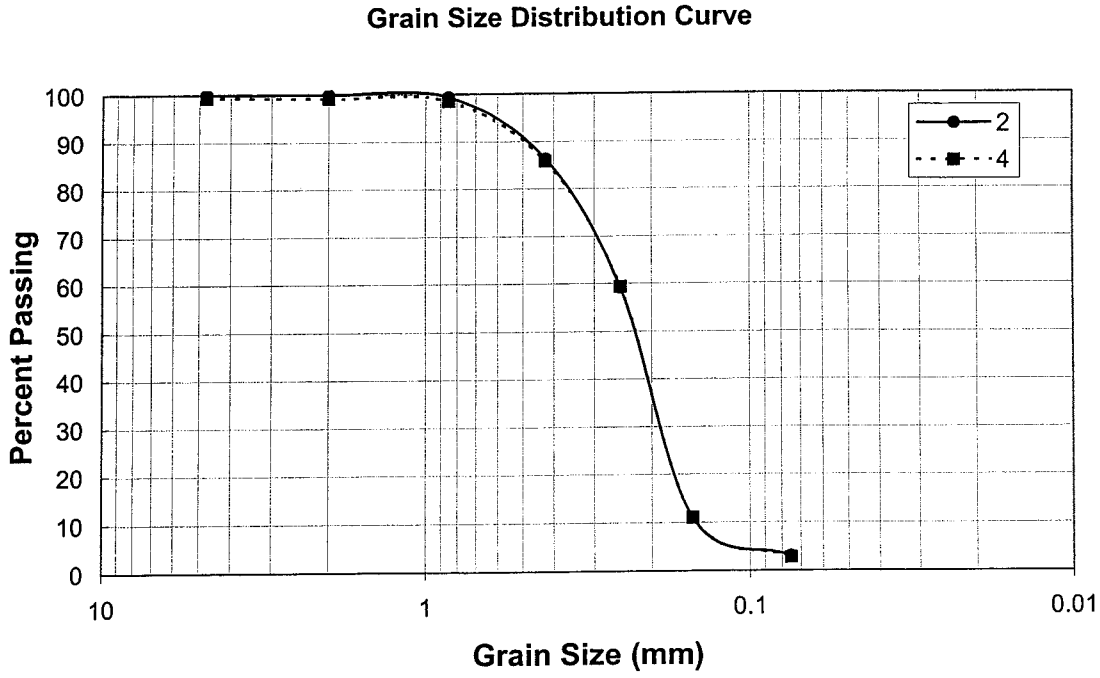

Field Permeablilty Testing Device

Test ID: BD-1

Phase II: Validation Study

Date : 2/1/00

Location : UF Campus Parking Field on Bledsoe Drive

Sleeve Diameter (in):	0.775
Sleeve Length (in):	0.685
Shape Factor (cm):	8.208
Depth of Probe (in):	8.0
Elevation (in):	10.0
Elevation Head (in):	16.5

Time (min)	Gauge Pressure Reading (in H_2O)	Flowmeter Reading (cc/min)	Total Head (cm)	Insitu Permeability (cm/sec)
0.0	0.00	7	41.9	3.39E-04
2.0	0.00	7	41.9	3.39E-04
7.0	0.00	7	41.9	3.39E-04
14.0	0.00	7	41.9	3.39E-04
22.0	0.00	10	41.9	4.85E-04
26.0	0.00	10	41.9	4.85E-04
28.0	0.00	11	41.9	5.33E-04
30.0	0.00	11	41.9	5.33E-04
35.0	0.00	11	41.9	5.33E-04

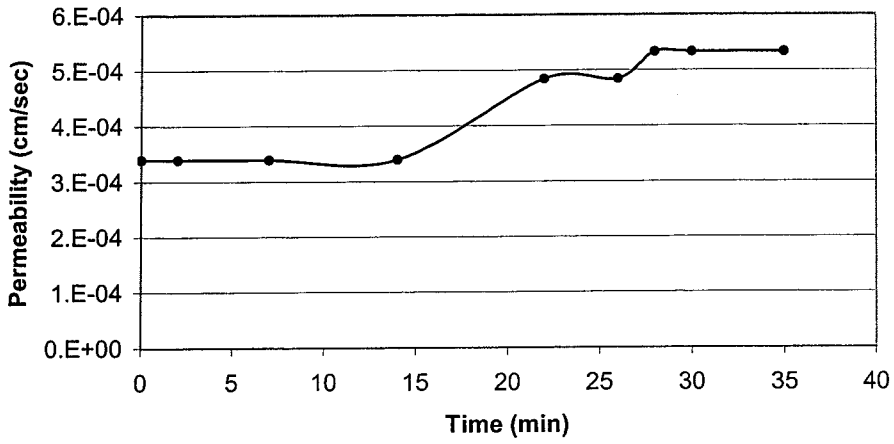

ASTM D 3385 - Infiltration Rate of Soils in Field using Double Ring Infiltrometer

Project Identification: BD-1

Project Location: Parking Field alongside Bledsoe Drive at UF

Liquid Used: Water pH: 7.0

Tested By: Michael Garau

Depth to water table: unknown (ft)

Constants	Area (cm^2)	Depth of Liquid (cm)	Liquid Containers No.	Vol./ΔH (cm^2/cm)
Inner Ring:	729.7			
Annular Space:	2189.0			

Liquid Level Maintained Using: ☐ Flow Valve ☐ Float Valve ☐ Mariotte Tube ☒ Other: Refilling

Penetration of rings: Inner: 3 (in) Outer: 3 (in)

Trial No.		Date	Time hr:min	Elapsed Time Δ/(total) min	Flow Readings: Inner Ring Reading cm	Inner Ring Flow cm^3	Annular Space Reading cm	Annular Space Flow cm^3	Liquid Temp. °C	Incr. Infiltration Rate: Inner cm/h	Incr. Infiltration Rate: Annular cm/h	Ground Temp. = 45 °F @ depth of (in) Remarks: Weather Conditions, etc.
1	S	2/1/00	12:00	15	-	960	-		25	5.3		
	E	2/1/00	12:15	15	-		-		25			Cool and Sunny Conditions
2	S	2/1/00	12:15	15	-	905	-		25	5.0		
	E	2/1/00	12:30	30	-		-		25			
3	S	2/1/00	12:30	15	-	905	-		25	5.0		
	E	2/1/00	12:45	45	-		-		25			
4	S	2/1/00	12:45	15	-	910	-		25	5.0		
	E	2/1/00	1:00	60	-		-		25			
5	S											
	E											
6	S											
	E											
7	S											
	E											
8	S											
	E											
9	S											
	E											
10	S											
	E											

Ring Dimensions: Inner Ring: 30.48 cm (12 in) diameter, 60.96 cm (24 in) height
Outer Ring: 60.96 cm (24 in) diameter, 60.96 cm (24 in) height

Field Permeablilty Testing Device

Test ID: BD-1

Phase II: Validation Study

Date : 2/12/00

Location : UF Campus Parking Field on Bledsoe Drive

Sieve Analysis

Sieve No.	Diameter (mm)	M_{sv} (g)	$M_{sv,s}$ (g)	M_s (g)	% Soil Retained	%Soil Passing
10	2.00	506.01	506.03	0.02	0.00	100.00
20	0.85	411.84	414.75	2.91	0.55	99.45
30	0.60	405.04	421.62	16.58	3.13	96.32
50	0.30	387.48	566.78	179.30	33.86	62.46
70	0.212	441.7	577.7	136.00	25.68	36.77
100	0.15	315	437.1	122.10	23.06	13.71
140	0.106	356.92	401.69	44.77	8.45	5.26
200	0.075	334.30	351.7	17.40	3.29	1.97
Pan	-	371.45	381.9	10.45	1.97	
			Sum =	529.53		

Grain Size Distribution Curve

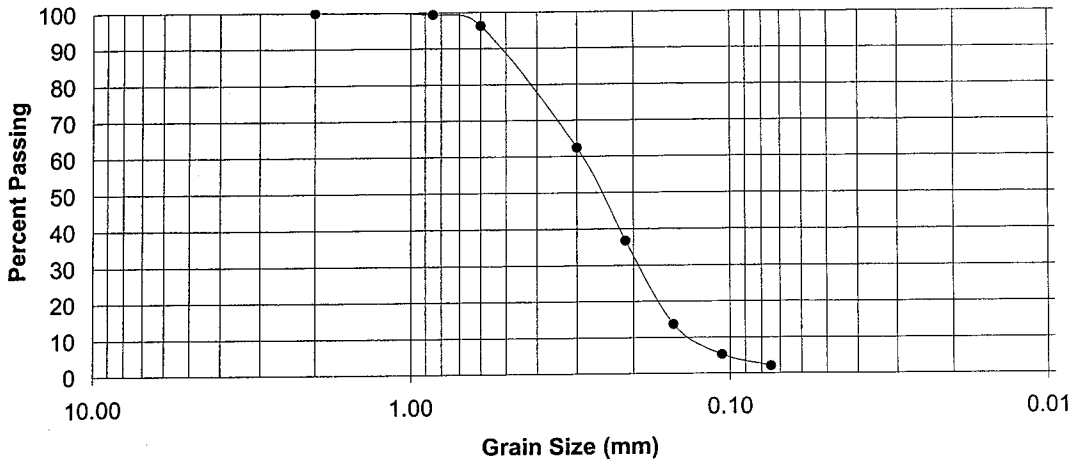

% Gravel :	0.00	D_{10} :	0.14
% Coarse Sand :	0.00	D_{30} :	0.20
% Medium Sand :	22.00	D_{60} :	0.29
% Fine Sand :	76.03	C_u :	2.07
% Fines :	1.97	C_z :	0.99

Field Permeablilty Testing Device

Test ID: BD-2

Phase II: Validation Study

Date : 2/2/00

Location : UF Campus Parking Field on Bledsoe Drive

Sleeve Diameter (in):	0.775
Sleeve Length (in):	0.685
Shape Factor (cm):	8.208
Depth of Probe (in):	8.0
Elevation (in):	10.0
Elevation Head (in):	16.5

Time (min)	Gauge Pressure Reading (in H_2O)	Flowmeter Reading (cc/min)	Total Head (cm)	Insitu Permeability (cm/sec)
0.0	0.00	96	41.9	4.65E-03
5.0	0.00	95	41.9	4.60E-03
10.0	0.00	100	41.9	4.85E-03
18.5	0.00	104	41.9	5.04E-03
30.0	0.00	104	41.9	5.04E-03
35.0	0.00	104	41.9	5.04E-03

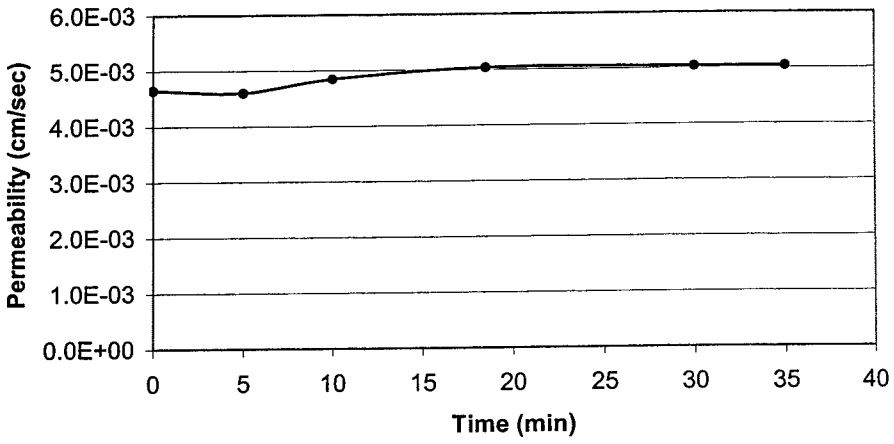

ASTM D 3385 - Infiltration Rate of Soils in Field using Double Ring Infiltrometer

Project Identification: BD-2

Project Location: Parking Field alongside Bledsoe Drive at UF

Liquid Used: Water pH: 7.0

Tested By: Michael Garau

Depth to water table: unknown (ft)

Penetration of rings: Inner: 3 (in) Outer: 3 (in)

Constants	Area (cm^2)	Depth of Liquid (cm)	Liquid Containers No.	Liquid Containers Vol./ΔH (cm^2/cm)
Inner Ring:	729.7			
Annular Space:	2189.0			

Liquid Level Maintained Using: ☐ Flow Valve ☐ Float Valve ☐ Mariotte Tube ☒ Other: Refilling

Trial No.		Date	Time hr:min	Elapsed Time Δ/(total) min	Flow Readings: Inner Ring Reading cm	Inner Ring Flow cm^3	Annular Space Reading cm	Annular Space Flow cm^3	Liquid Temp. °C	Incr. Infiltration Rate: Inner cm/h	Incr. Infiltration Rate: Annular cm/h	Ground Temp. = 45 °F @ depth of ____ (in) Remarks: Weather Conditions, etc.
1	S	2/2/00	12:00	15	-	3390	-		25	18.6		
	E	2/2/00	12:15	15	-		-		25			Cool and Sunny Conditions
2	S	2/2/00	12:15	15	-	3735	-		25	20.5		
	E	2/2/00	12:30	30	-		-		25			
3	S	2/2/00	12:30	15	-	3635	-		25	19.9		
	E	2/2/00	12:45	45	-		-		25			
4	S	2/2/00	12:45	15	-	3720	-		25	20.4		
	E	2/2/00	1:00	60	-		-		25			
5	S	2/2/00	1:00	15	-	3830	-		25	21.0		
	E	2/2/00	1:15	75	-		-		25			
6	S	2/2/00	1:15	15	-	3725	-		25	20.4		
	E	2/2/00	1:30	90	-		-		25			
7	S											
	E											
8	S											
	E											
9	S											
	E											
10	S											
	E											

Ring Dimensions: Inner Ring: 30.48 cm (12 in) diameter, 60.96 cm (24 in) height
Outer Ring: 60.96 cm (24 in) diameter, 60.96 cm (24 in) height

Field Permeablilty Testing Device

Test ID: BD-2
Date : 2/13/00

Phase II: Validation Study
Location : UF Campus Parking Field on Bledsoe Drive

Sieve Analysis

Sieve No.	Diameter (mm)	M_{sv} (g)	$M_{sv,s}$ (g)	M_s (g)	% Soil Retained	%Soil Passing
10	2.00	506.08	506.1	0.02	0.00	100.00
20	0.85	411.90	415.03	3.13	0.59	99.41
30	0.60	405.05	420.74	15.69	2.94	96.47
50	0.30	387.84	568.89	181.05	33.90	62.57
70	0.212	441.73	569.06	127.33	23.84	38.73
100	0.15	315.07	442.89	127.82	23.93	14.80
140	0.106	356.91	409.77	52.86	9.90	4.90
200	0.075	334.29	349.7	15.41	2.89	2.02
Pan	-	371.43	382.2	10.77	2.02	
			Sum =	534.08		

Grain Size Distribution Curve

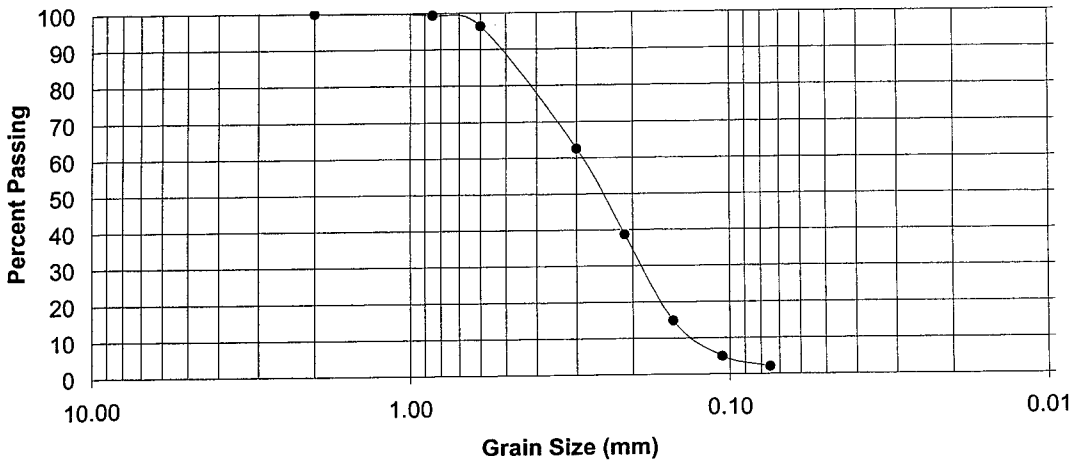

% Gravel :	0.00	D_{10} :	0.14
% Coarse Sand :	0.00	D_{30} :	0.19
% Medium Sand :	21.00	D_{60} :	0.29
% Fine Sand :	76.98	C_u :	2.07
% Fines :	2.02	C_z :	0.89

Field Permeablilty Testing Device

Test ID: BD-3
Date : 2/3/00

Phase II: Validation Study
Location : UF Campus Parking Field on Bledsoe Drive

Sleeve Diameter (in):	0.775
Sleeve Length (in):	0.685
Shape Factor (cm):	8.208
Depth of Probe (in):	8.0
Elevation (in):	13.5
Elevation Head (in):	20.0

Time (min)	Gauge Pressure Reading (in H_2O)	Flowmeter Reading (cc/min)	Total Head (cm)	Insitu Permeability (cm/sec)
0.0	0.00	24	50.8	9.59E-04
5.0	0.00	28	50.8	1.12E-03
10.0	0.00	33	50.8	1.32E-03
15.0	0.00	37	50.8	1.48E-03
20.0	0.00	38	50.8	1.52E-03
25.0	0.00	38	50.8	1.52E-03
30.0	0.00	38	50.8	1.52E-03
35.0	0.00	38	50.8	1.52E-03
40.0	0.00	38	50.8	1.52E-03

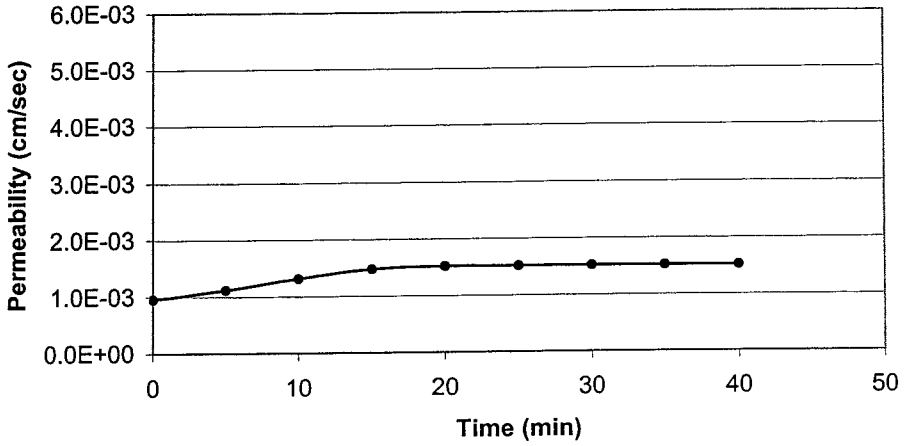

ASTM D 3385 - Infiltration Rate of Soils in Field using Double Ring Infiltrometer

Project Identification: BD-3

Project Location: Parking Field alongside Bledsoe Drive at UF

Liquid Used: Water pH: 7.0

Tested By: Michael Garau

Depth to water table: unknown (ft)

Penetration of rings: Inner: 3 (in) Outer: 3 (in)

Constants	Area (cm^2)	Depth of Liquid (cm)	Liquid Containers No.	Liquid Containers Vol./ΔH (cm^2/cm)
Inner Ring:	729.7			
Annular Space:	2189.0			

Liquid Level Maintained Using: [ ] Flow Valve [ ] Float Valve [ ] Mariotte Tube [x] Other: Refilling

Trial No.		Date	Time	Elapsed Time Δ/(total)	Flow Readings Inner Ring Reading	Flow Readings Inner Ring Flow	Flow Readings Annular Space Reading	Flow Readings Annular Space Flow	Liquid Temp.	Incr. Infiltration Rate Inner	Incr. Infiltration Rate Annular	Ground Temp. = 45 °F @ depth of (in)
			hr:min	min	cm	cm^3	cm	cm^3	°C	cm/h	cm/h	Remarks: Weather Conditions, etc.
1	S	2/3/00	12:00	15	-	1460	-		25	8.0		
	E	2/3/00	12:15	15	-		-		25			Cool and Sunny Conditions
2	S	2/3/00	12:15	15	-	1420	-		25	7.8		
	E	2/3/00	12:30	30	-		-		25			
3	S	2/3/00	12:30	15	-	1480	-		25	8.1		
	E	2/3/00	12:45	45	-		-		25			
4	S	2/3/00	12:45	15	-	1410	-		25	7.7		
	E	2/3/00	1:00	60	-		-		25			
5	S	2/3/00	1:00	15	-	1520	-		25	8.3		
	E	2/3/00	1:15	75	-		-		25			
6	S	2/3/00	1:15	15	-	1530	-		25	8.4		
	E	2/3/00	1:30	90	-		-		25			
7	S											
	E											
8	S											
	E											
9	S											
	E											
10	S											
	E											

Ring Dimensions: Inner Ring: 30.48 cm (12 in) diameter, 60.96 cm (24 in) height
Outer Ring: 60.96 cm (24 in) diameter, 60.96 cm (24 in) height

Field Permeablilty Testing Device

Test ID: BD-3
Date : 2/13/00

Phase II: Validation Study
Location : UF Campus Parking Field on Bledsoe Drive

Sieve Analysis

Sieve No.	Diameter (mm)	M_{sv} (g)	$M_{sv,s}$ (g)	M_s (g)	% Soil Retained	%Soil Passing
10	2.00	505.75	505.76	0.01	0.00	100.00
20	0.85	411.54	414.54	3.00	0.61	99.39
30	0.60	404.73	415.54	10.81	2.21	97.18
50	0.30	387.19	521.34	134.15	27.41	69.77
70	0.212	441.33	567.12	125.79	25.70	44.07
100	0.15	314.83	444.55	129.72	26.50	17.56
140	0.106	356.72	423.87	67.15	13.72	3.85
200	0.075	334.10	343.49	9.39	1.92	1.93
Pan	-	371.24	380.67	9.43	1.93	
			Sum =	489.45		

Grain Size Distribution Curve

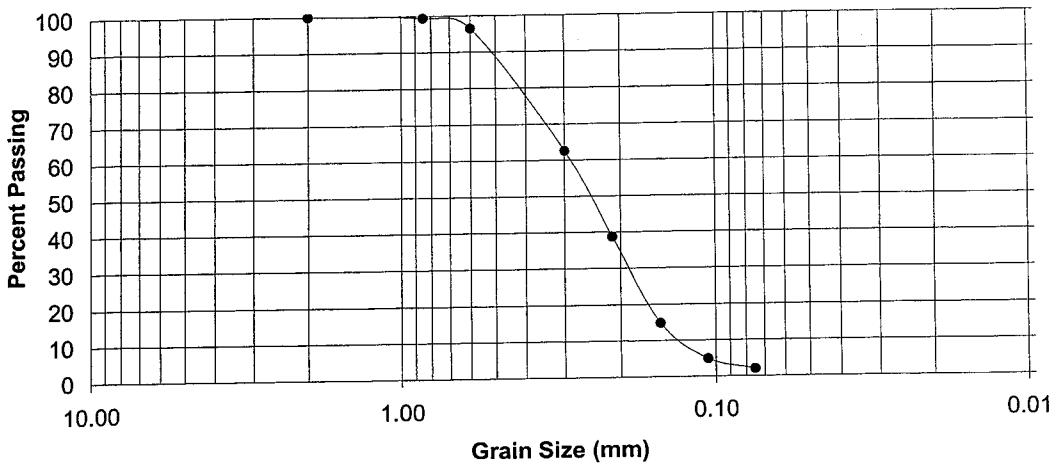

% Gravel :	0.00	D_{10} :	0.14
% Coarse Sand :	0.00	D_{30} :	0.18
% Medium Sand :	22.00	D_{60} :	0.28
% Fine Sand :	76.07	C_u :	2.00
% Fines :	1.93	C_z :	0.83

Field Permeablilty Testing Device

Phase II: Validation Study

Location : Flavet Field on the UF Campus

Test ID: FF-1

Date : 2/18/00

Sleeve Diameter (in):	0.775
Sleeve Length (in):	0.685
Shape Factor (cm):	8.208
Depth of Probe (in):	8.0
Elevation (in):	9.5
Elevation Head (in):	16.0

Time (min)	Gauge Pressure Reading (in H_2O)	Flowmeter Reading (cc/min)	Total Head (cm)	Insitu Permeability (cm/sec)
0.0	0.00	87	40.6	4.35E-03
7.0	0.00	71	40.6	3.55E-03
13.0	0.00	60	40.6	3.00E-03
21.0	0.00	50	40.6	2.50E-03
30.0	0.00	43	40.6	2.15E-03
38.0	0.00	43	40.6	2.15E-03
45.0	0.00	43	40.6	2.15E-03

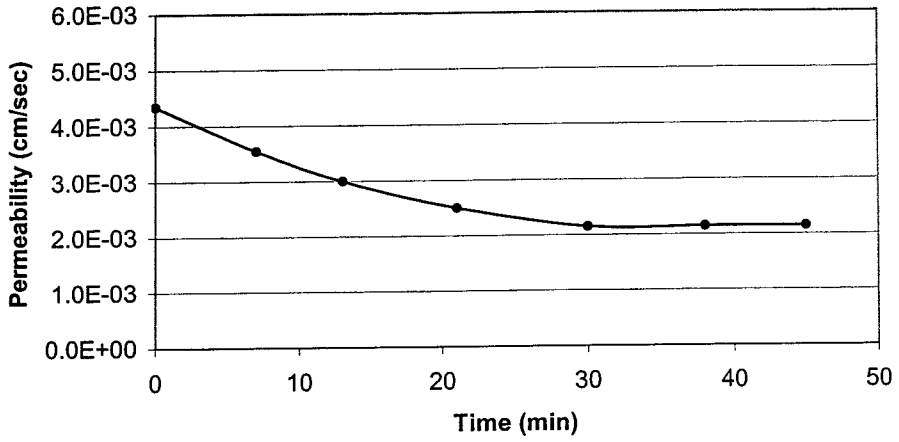

ASTM D 3385 - Infiltration Rate of Soils in Field using Double Ring Infiltrometer

Project Identification: FF-1

Project Location: Flavet Field at UF

Liquid Used: Water pH: 7.0

Tested By: Michael Garau

Depth to water table: unknown (ft)

Penetration of rings: Inner: 3 (in) Outer: 3 (in)

Constants	Area (cm^2)	Depth of Liquid (cm)	Liquid Containers No.	Vol./ΔH (cm^2/cm)
Inner Ring:	729.7			
Annular Space:	2189.0			

Liquid Level Maintained Using: [ ] Flow Valve [ ] Float Valve [ ] Mariotte Tube [x] Other: Refilling

Trial No.		Date	Time hr:min	Elapsed Time Δ/(total) min	Flow Readings: Inner Ring Reading cm	Inner Ring Flow cm^3	Annular Space Reading cm	Annular Space Flow cm^3	Liquid Temp. °C	Incr. Infiltration Rate: Inner cm/h	Annular cm/h	Ground Temp. = 45 °F @ depth of (in) / Remarks: Weather Conditions, etc.
1	S	2/18/00	12:00	15	-	5016.7	-		25	27.5		
	E	2/18/00	12:15	15	-		-		25			Cool and Sunny Conditions
2	S	2/18/00	12:15	15	-	4341.7	-		25	23.8		
	E	2/18/00	12:30	30	-		-		25			
3	S	2/18/00	12:30	15	-	4013.4	-		25	22.0		
	E	2/18/00	12:45	45	-		-		25			
4	S	2/18/00	12:45	15	-	3903.9	-		25	21.4		
	E	2/18/00	1:00	60	-		-		25			
5	S	2/18/00	1:00	15	-	3903.9	-		25	21.4		
	E	2/18/00	1:15	75	-		-		25			
6	S	2/18/00	1:15	15	-	3666.7	-		25	20.1		
	E	2/18/00	1:30	90	-		-		25			
7	S											
	E											
8	S											
	E											
9	S											
	E											
10	S											
	E											

Ring Dimensions: Inner Ring: 30.48 cm (12 in) diameter, 60.96 cm (24 in) height
Outer Ring: 60.96 cm (24 in) diameter, 60.96 cm (24 in) height

Field Permeablilty Testing Device

Phase II: Validation Study

Location : Flavet Field on the UF Campus

Test ID: FF-1

Date : 2/18/00

Sieve Analysis

Sieve No.	Diameter (mm)	M_{sv} (g)	$M_{sv,s}$ (g)	M_s (g)	% Soil Retained	%Soil Passing
10	2.00	471.56	481.33	9.77	1.90	98.10
20	0.85	410.18	422	11.82	2.30	95.80
30	0.60	405.1	421.68	16.58	3.22	92.58
50	0.30	357.04	490.58	133.54	25.95	66.63
70	0.212	441.8	575.5	133.70	25.99	40.64
100	0.15	343.94	451.68	107.74	20.94	19.70
140	0.106	398.5	454.24	55.74	10.83	8.87
200	0.075	337.61	358.1	20.49	3.98	4.89
Pan	-	368.2	393.34	25.14	4.89	

Sum = 514.52

Grain Size Distribution Curve

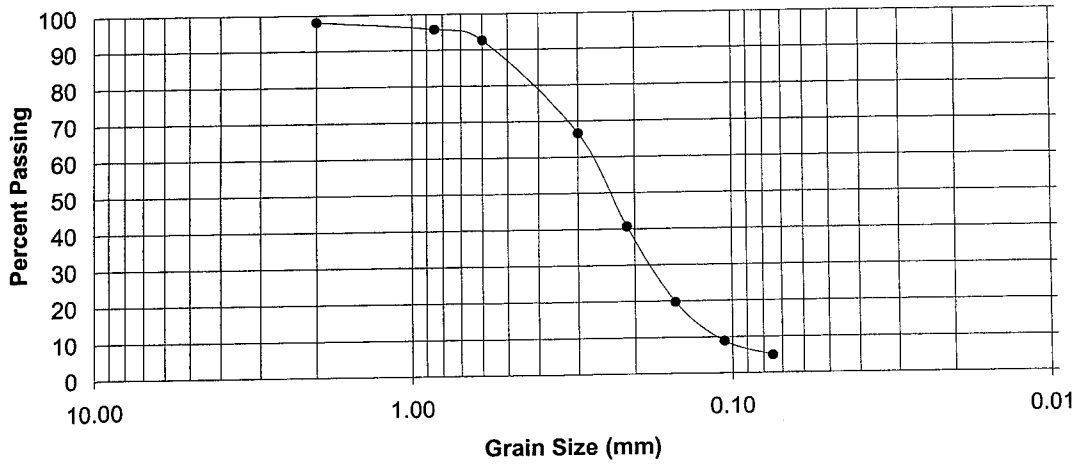

% Gravel :	0.00	D_{10} :	0.11
% Coarse Sand :	1.9	D_{30} :	0.18
% Medium Sand :	18.1	D_{60} :	0.27
% Fine Sand :	75.11	C_u :	2.45
% Fines :	4.89	C_z :	1.09

Field Permeablilty Testing Device

Phase II: Validation Study

Location : Flavet Field on the UF Campus

Test ID: FF-2

Date : 2/19/00

Sleeve Diameter (in):	0.775
Sleeve Length (in):	0.685
Shape Factor (cm):	8.208
Depth of Probe (in):	8.0
Elevation (in):	10.0
Elevation Head (in):	16.5

Time (min)	Gauge Pressure Reading (in H_2O)	Flowmeter Reading (cc/min)	Total Head (cm)	Insitu Permeability (cm/sec)
0.0	0.00	25	41.9	1.21E-03
5.0	0.00	30	41.9	1.45E-03
10.5	0.00	35	41.9	1.70E-03
22.0	0.00	38	41.9	1.84E-03
27.0	0.00	40	41.9	1.94E-03
34.5	0.00	40	41.9	1.94E-03
38.0	0.00	40	41.9	1.94E-03
40.0	0.00	40	41.9	1.94E-03

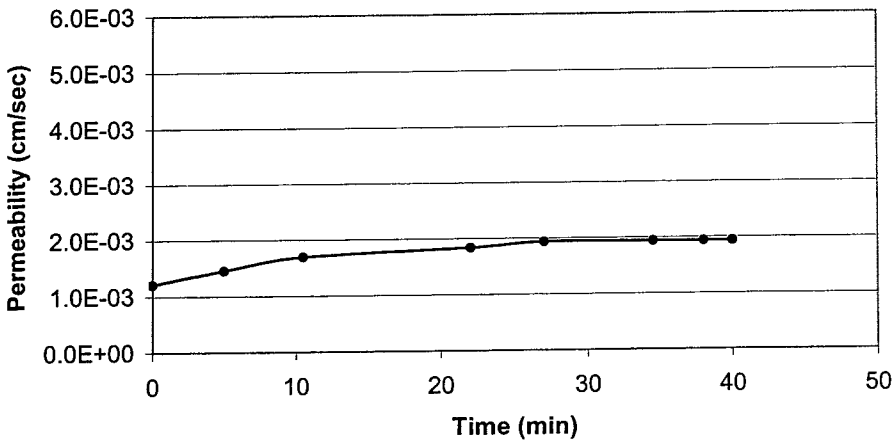

ASTM D 3385 - Infiltration Rate of Soils in Field using Double Ring Infiltrometer

Project Identification: FF-2

Project Location: Flavet Field at UF

Liquid Used: Water pH: 7.0

Tested By: Michael Garau

Depth to water table: unknown (ft)

Constants	Area (cm^2)	Depth of Liquid (cm)	Liquid Containers No.	Vol./ΔH (cm^2/cm)
Inner Ring:	729.7			
Annular Space:	2189.0			

Liquid Level Maintained Using: ☐ Flow Valve ☐ Float Valve ☐ Mariotte Tube

Penetration of rings: Inner: 3 (in) Outer: 3 (in)

☒ Other: Refilling

Ground Temp. = 45 °F @ depth of ____ (in)

Trial No.		Date	Time hr:min	Elapsed Time Δ/(total) min	Flow Readings: Inner Ring Reading cm	Inner Ring Flow cm^3	Annular Space Reading cm	Annular Space Flow cm^3	Liquid Temp. °C	Incr. Infiltration Rate: Inner cm/h	Annular cm/h	Remarks: Weather Conditions, etc.
1	S	2/19/00	12:00	15	-	1714.8	-		25	9.4		
	E	2/19/00	12:15	15	-		-		25			Cool and Sunny Conditions
2	S	2/19/00	12:15	15	-	1532.4	-		25	8.4		
	E	2/19/00	12:30	30	-		-		25			
3	S	2/19/00	12:30	15	-	1441.2	-		25	7.9		
	E	2/19/00	12:45	45	-		-		25			
4	S	2/19/00	12:45	15	-	1441.2	-		25	7.9		
	E	2/19/00	1:00	60	-		-		25			
5	S	2/19/00	1:00	15	-	1404.7	-		25	7.7		
	E	2/19/00	1:15	75	-		-		25			
6	S	2/19/00	1:15	15	-	1404.7	-		25	7.7		
	E	2/19/00	1:30	90	-		-		25			
7	S											
	E											
8	S											
	E											
9	S											
	E											
10	S											
	E											

Ring Dimensions: Inner Ring: 30.48 cm (12 in) diameter, 60.96 cm (24 in) height
Outer Ring: 60.96 cm (24 in) diameter, 60.96 cm (24 in) height

Field Permeablilty Testing Device

Test ID: FF-2
Date : 2/19/00

Phase II: Validation Study
Location : Flavet Field on the UF Campus

Sieve Analysis

Sieve No.	Diameter (mm)	M_{sv} (g)	$M_{sv,s}$ (g)	M_s (g)	% Soil Retained	%Soil Passing
10	2.00	471.58	490.74	19.16	3.77	96.23
20	0.85	410.20	424.36	14.16	2.78	93.45
30	0.60	450.49	464.32	13.83	2.72	90.73
50	0.30	357.06	498.6	141.54	27.82	62.91
70	0.212	441.7	571.35	129.65	25.49	37.42
100	0.15	343.9	445.22	101.32	19.92	17.51
140	0.106	398.45	446.52	48.07	9.45	8.06
200	0.075	337.65	356.74	19.09	3.75	4.30
Pan	-	368.25	390.14	21.89	4.30	
			Sum =	508.71		

Grain Size Distribution Curve

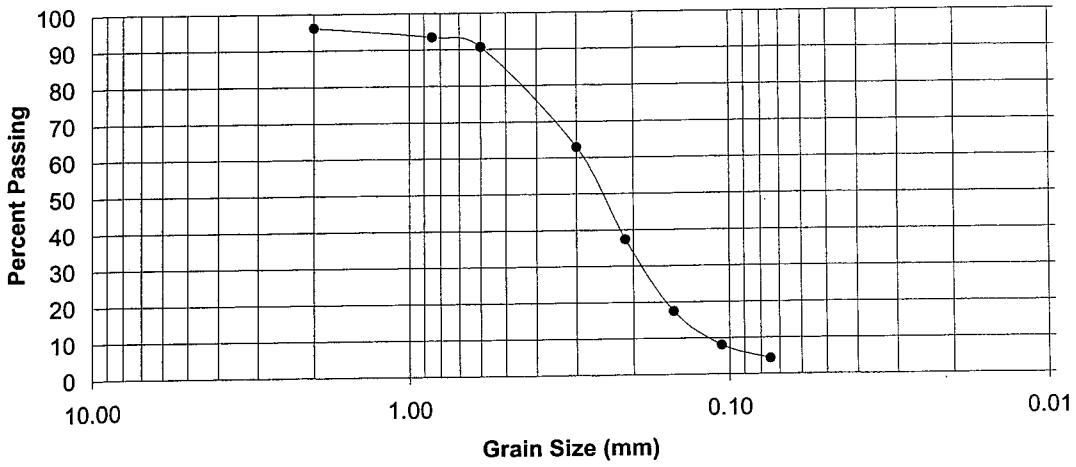

% Gravel :	0.00	D_{10} :	0.11
% Coarse Sand :	3.77	D_{30} :	0.19
% Medium Sand :	20.23	D_{60} :	0.29
% Fine Sand :	71.7	C_u :	2.64
% Fines :	4.3	C_z :	1.13

Field Permeablilty Testing Device

Test ID: FF-3
Date : 2/19/00
Phase II: Validation Study
Location : Flavet Field on the UF Campus

Sleeve Diameter (in):	0.775
Sleeve Length (in):	0.685
Shape Factor (cm):	8.208
Depth of Probe (in):	8.0
Elevation (in):	10.0
Elevation Head (in):	16.5

Time (min)	Gauge Pressure Reading (in H_2O)	Flowmeter Reading (cc/min)	Total Head (cm)	Insitu Permeability (cm/sec)
0.0	0.00	30	41.9	1.45E-03
5.0	0.00	34	41.9	1.65E-03
10.0	0.00	35	41.9	1.70E-03
15.0	0.00	38	41.9	1.84E-03
20.0	0.00	38	41.9	1.84E-03
30.0	0.00	38	41.9	1.84E-03

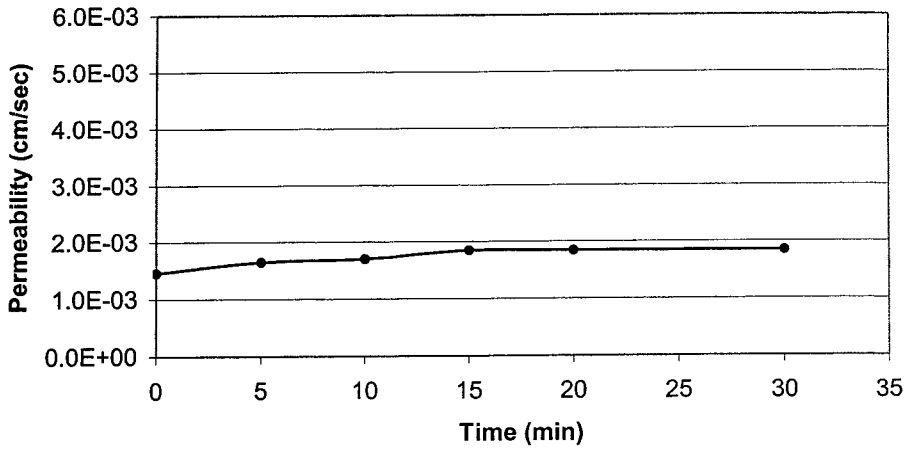

ASTM D 3385 - Infiltration Rate of Soils in Field using Double Ring Infiltrometer

Project Identification: FF-3

Project Location: Flavet Field at UF

Liquid Used: Water pH: 7.0

Tested By: Michael Garau

Depth to water table: unknown (ft) Penetration of rings: Inner: 3 (in) Outer: 3 (in)

Constants	Area (cm^2)	Depth of Liquid (cm)	Liquid Containers No.	Liquid Containers Vol./ΔH (cm^2/cm)
Inner Ring:	729.7			
Annular Space:	2189.0			

Liquid Level Maintained Using: [ ] Flow Valve [ ] Float Valve [ ] Mariotte Tube [x] Other: Refilling

Trial No.		Date	Time hr:min	Elapsed Time Δ/(total) min	Flow Readings: Inner Ring Reading cm	Inner Ring Flow cm^3	Annular Space Reading cm	Annular Space Flow cm^3	Liquid Temp. °C	Incr. Infiltration Rate: Inner cm/h	Incr. Infiltration Rate: Annular cm/h	Remarks: Weather Conditions, etc.
1	S	2/19/00	12:00	15	-	1970.2	-		25	10.8		
	E	2/19/00	12:15	15	-		-		25			Cool and Sunny Conditions
2	S	2/19/00	12:15	15	-	1915.5	-		25	10.5		
	E	2/19/00	12:30	30	-		-		25			
3	S	2/19/00	12:30	15	-	1879.0	-		25	10.3		
	E	2/19/00	12:45	45	-		-		25			
4	S						-					
	E						-					
5	S						-					
	E						-					
6	S						-					
	E						-					
7	S											
	E											
8	S											
	E											
9	S											
	E											
10	S											
	E											

Ground Temp. = 45 °F @ depth of ____ (in)

Ring Dimensions: Inner Ring: 30.48 cm (12 in) diameter, 60.96 cm (24 in) height
Outer Ring: 60.96 cm (24 in) diameter, 60.96 cm (24 in) height

Field Permeablilty Testing Device

Test ID: FF-3
Date : 2/19/00

Phase II: Validation Study
Location : Flavet Field on the UF Campus

Sieve Analysis

Sieve No.	Diameter (mm)	M_{sv} (g)	$M_{sv,s}$ (g)	M_s (g)	% Soil Retained	%Soil Passing
10	2.00	506.16	546.11	39.95	7.48	92.52
20	0.85	412.13	427.37	15.24	2.85	89.67
30	0.60	405.03	425.84	20.81	3.89	85.78
50	0.30	387.55	529.9	142.35	26.64	59.14
70	0.212	441.61	556.14	114.53	21.43	37.71
100	0.15	315.05	422.71	107.66	20.14	17.57
140	0.106	356.9	407.60	50.70	9.49	8.08
200	0.075	334.25	355.52	21.27	3.98	4.10
Pan	-	371.44	393.36	21.92	4.10	
			Sum =	534.43		

Grain Size Distribution Curve

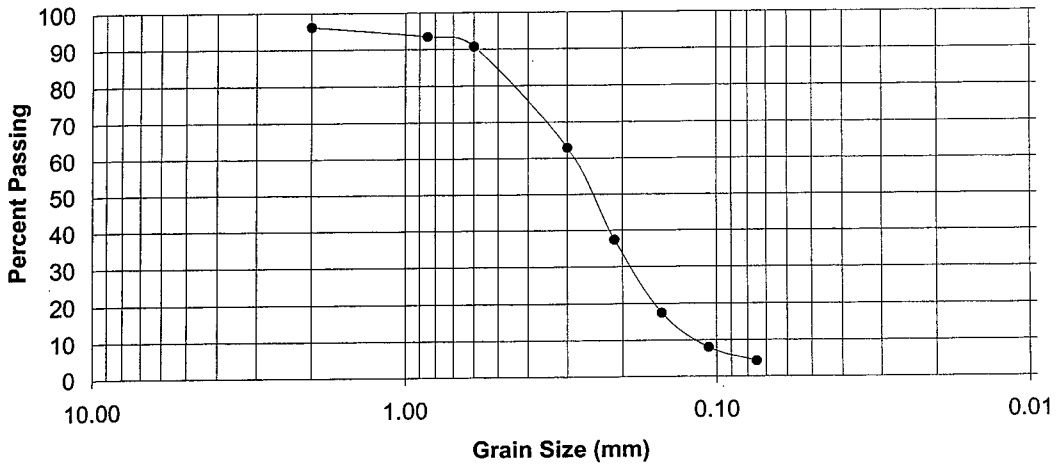

% Gravel :	0.00	D_{10} :	0.13
% Coarse Sand :	7.48	D_{30} :	0.19
% Medium Sand :	16.52	D_{60} :	0.29
% Fine Sand :	71.9	C_u :	2.23
% Fines :	4.1	C_z :	0.96

Field Permeablilty Testing Device

Test ID: WP-1

Phase II: Validation Study

Date : 2/12/00

Location : Alachua County Park on Willinston Rd and 441

Sleeve Diameter (in):	0.775
Sleeve Length (in):	0.685
Shape Factor (cm):	8.208
Depth of Probe (in):	8.0
Elevation (in):	9.5
Elevation Head (in):	16.0

Time (min)	Gauge Pressure Reading (in H_2O)	Flowmeter Reading (cc/min)	Total Head (cm)	Insitu Permeability (cm/sec)
0.0	0.00	87	40.6	4.35E-03
7.0	0.00	71	40.6	3.55E-03
13.0	0.00	60	40.6	3.00E-03
21.0	0.00	50	40.6	2.50E-03
30.0	0.00	43	40.6	2.15E-03
38.0	0.00	43	40.6	2.15E-03
45.0	0.00	43	40.6	2.15E-03

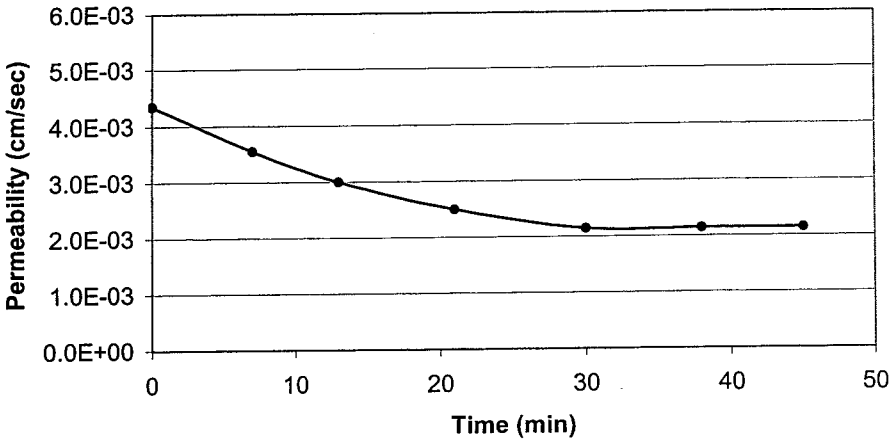

ASTM D 3385 - Infiltration Rate of Soils in Field using Double Ring Infiltrometer

Project Identification: WP-1

Project Location: Alachua County Park on Willinston Rd.

Liquid Used: Water pH: 7.0

Tested By: Michael Garau

Depth to water table: unknown (ft)

Penetration of rings: Inner: 3 (in) Outer: 3 (in)

Constants	Area (cm^2)	Depth of Liquid (cm)	Liquid Containers No.	Vol./ΔH (cm^2/cm)
Inner Ring:	729.7			
Annular Space:	2189.0			

Liquid Level Maintained Using: [ ] Flow Valve [ ] Float Valve [ ] Mariotte Tube [x] Other: Refilling

Trial No.		Date	Time	Elapsed Time Δ/(total)	Flow Readings: Inner Ring Reading	Inner Ring Flow	Annular Space Reading	Annular Space Flow	Liquid Temp.	Incr. Infiltration Rate: Inner	Annular	Ground Temp. = 45 °F @ depth of (in)
			hr:min	min	cm	cm^3	cm	cm^3	°C	cm/h	cm/h	Remarks: Weather Conditions, etc.
1	S	2/12/00	12:00	15	-	5020	-		25	27.5		
	E	2.12/00	12:15	15	-		-		25			Cool and Sunny Conditions
2	S	2/12/00	12:15	15	-	4345	-		25	23.8		
	E	2/12/00	12:30	30	-		-		25			
3	S	2/12/00	12:30	15	-	4005	-		25	22.0		
	E	2/12/00	12:45	45	-		-		25			
4	S	2/12/00	12:45	15	-	3895	-		25	21.4		
	E	2/12/00	1:00	60	-		-		25			
5	S	2/12/00	1:00	15	-	3895	-		25	21.4		
	E	2/12/00	1:15	75	-		-		25			
6	S	2/12/00	1:15	15		3670			25	20.1		
	E	2/12/00	1:30	90					25			
7	S											
	E											
8	S											
	E											
9	S											
	E											
10	S											
	E											

Ring Dimensions: Inner Ring: 30.48 cm (12 in) diameter, 60.96 cm (24 in) height
Outer Ring: 60.96 cm (24 in) diameter, 60.96 cm (24 in) height

Field Permeablilty Testing Device

Test ID: WP-1
Date : 2/12/00

Phase II: Validation Study
Location : Alachua County Park on Willinston Rd and 441

Sieve Analysis

Sieve No.	Diameter (mm)	M_{sv} (g)	$M_{sv,s}$ (g)	M_s (g)	% Soil Retained	%Soil Passing
10	2.00	505.82	507.97	2.15	0.43	99.57
20	0.85	411.66	413.97	2.31	0.46	99.12
30	0.60	404.8	411.78	6.98	1.38	97.74
50	0.30	387.21	483.9	96.69	19.12	78.62
70	0.212	441.4	549.13	107.73	21.30	57.31
100	0.15	314.85	438.1	123.25	24.37	32.94
140	0.106	356.72	444.98	88.26	17.45	15.48
200	0.075	334.12	378.59	44.47	8.79	6.69
Pan	-	371.26	405.08	33.82	6.69	

Sum = 505.66

Grain Size Distribution Curve

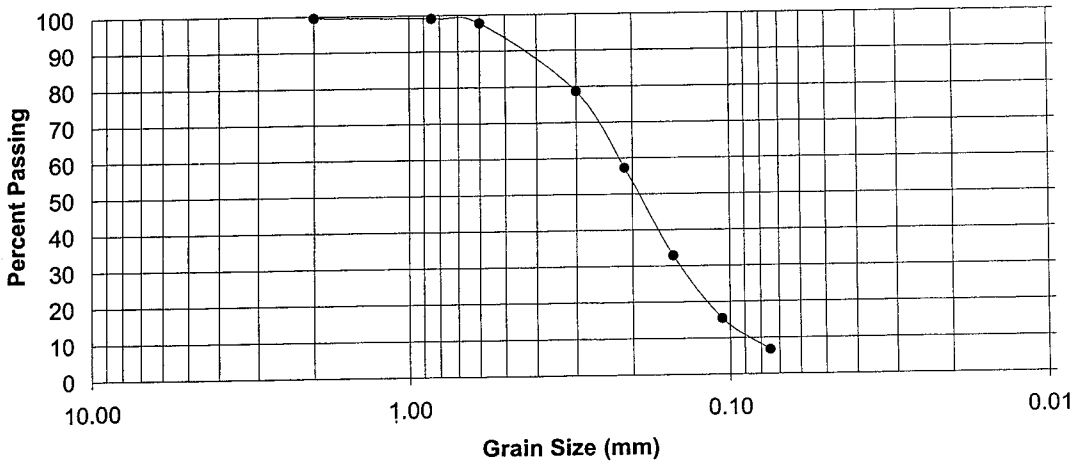

% Gravel :	0.00	D_{10} :	0.09
% Coarse Sand :	0.43	D_{30} :	0.14
% Medium Sand :	10.07	D_{60} :	0.22
% Fine Sand :	82.81	C_u :	2.44
% Fines :	6.69	C_z :	0.99

Field Permeablilty Testing Device

Test ID: WP-2

Phase II: Validation Study

Date : 2/13/00

Location : Alachua County Park on Willinston Rd and 441

Sleeve Diameter (in):	0.775
Sleeve Length (in):	0.685
Shape Factor (cm):	8.208
Depth of Probe (in):	8.0
Elevation (in):	10.0
Elevation Head (in):	16.5

Time (min)	Gauge Pressure Reading (in H_2O)	Flowmeter Reading (cc/min)	Total Head (cm)	Insitu Permeability (cm/sec)
0.0	0.00	25	41.9	1.21E-03
5.0	0.00	30	41.9	1.45E-03
10.5	0.00	35	41.9	1.70E-03
22.0	0.00	38	41.9	1.84E-03
27.0	0.00	40	41.9	1.94E-03
34.5	0.00	40	41.9	1.94E-03
38.0	0.00	40	41.9	1.94E-03
40.0	0.00	40	41.9	1.94E-03

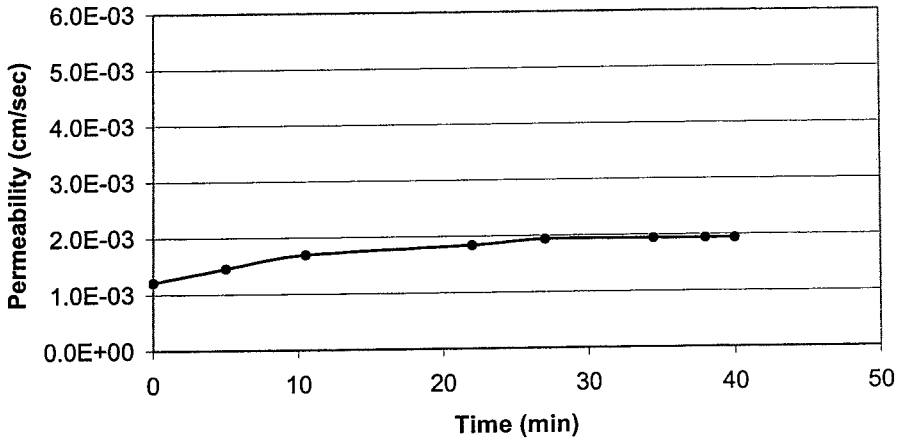

ASTM D 3385 - Infiltration Rate of Soils in Field using Double Ring Infiltrometer

Project Identification: WP-2

Project Location: Alachua County Park on Willinston Rd.

Liquid Used: Water pH: 7.0

Tested By: Michael Garau

Depth to water table: unknown (ft)

Penetration of rings: Inner: 3.5 (in) Outer: 3.5 (in)

Constants	Area (cm^2)	Depth of Liquid (cm)	Liquid Containers No.	Vol./ΔH (cm^2/cm)
Inner Ring:	729.7			
Annular Space:	2189.0			

Liquid Level Maintained Using: [ ] Flow Valve [ ] Float Valve [ ] Mariotte Tube [x] Other: Refilling

Ground Temp. = 45 °F @ depth of ____ (in)

Trial No.		Date	Time hr:min	Elapsed Time Δ/(total) min	Flow Readings: Inner Ring Reading cm	Inner Ring Flow cm^3	Annular Space Reading cm	Annular Space Flow cm^3	Liquid Temp. °C	Incr. Infiltration Rate: Inner cm/h	Incr. Infiltration Rate: Annular cm/h	Remarks: Weather Conditions, etc.
1	S	2/13/00	8:00	15	-	1715	-		25	9.4		
	E	2/13/00	8:15	15	-		-		25			Cool and Sunny Conditions
2	S	2/13/00	8:15	15	-	1540	-		25	8.4		
	E	2/13/00	8:30	30	-		-		25			
3	S	2/13/00	8:30	15	-	1440	-		25	7.9		
	E	2/13/00	8:45	45	-		-		25			
4	S	2/13/00	8:45	15	-	1450	-		25	7.9		
	E	2/13/00	9:00	60	-		-		25			
5	S	2/13/00	9:00	15	-	1405	-		25	7.7		
	E	2/13/00	9:15	75	-		-		25			
6	S	2/13/00	9:15	15	-	1400	-		25	7.7		
	E	2/13/00	9:30	90	-		-		25			
7	S											
	E											
8	S											
	E											
9	S											
	E											
10	S											
	E											

Ring Dimensions: Inner Ring: 30.48 cm (12 in) diameter, 60.96 cm (24 in) height
Outer Ring: 60.96 cm (24 in) diameter, 60.96 cm (24 in) height

Field Permeablilty Testing Device

Test ID: WP-2
Date : 2/13/00
Phase II: Validation Study
Location : Alachua County Park on Willinston Rd and 441

Sieve Analysis

Sieve No.	Diameter (mm)	M_{sv} (g)	$M_{sv,s}$ (g)	M_s (g)	% Soil Retained	%Soil Passing
10	2.00	505.8	518.96	13.16	2.48	97.52
20	0.85	411.57	415.03	3.46	0.65	96.86
30	0.60	404.77	414.05	9.28	1.75	95.11
50	0.30	387.26	495.91	108.65	20.51	74.60
70	0.212	441.35	541.85	100.50	18.97	55.62
100	0.15	314.84	442.89	128.05	24.18	31.45
140	0.106	356.71	444.24	87.53	16.53	14.92
200	0.075	334.09	378.29	44.20	8.35	6.57
Pan	-	371.28	406.1	34.82	6.57	
			Sum =	529.65		

Grain Size Distribution Curve

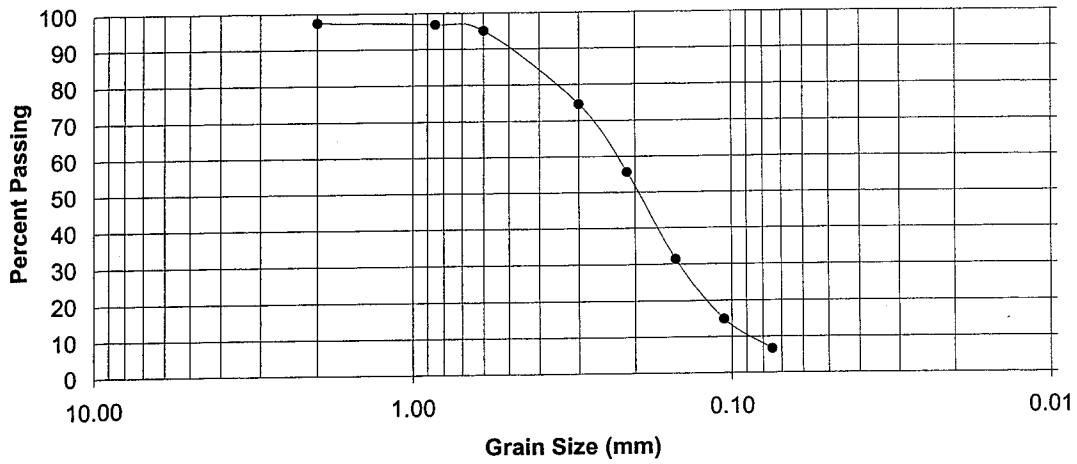

% Gravel :	0.00	D_{10} :	0.09
% Coarse Sand :	2.48	D_{30} :	0.15
% Medium Sand :	13.52	D_{60} :	0.22
% Fine Sand :	77.43	C_u :	2.44
% Fines :	6.57	C_z :	1.14

Field Permeablilty Testing Device

Test ID: WP-3

Phase II: Validation Study

Date : 2/13/00

Location : Alachua County Park on Willinston Rd and 441

Sleeve Diameter (in):	0.775
Sleeve Length (in):	0.685
Shape Factor (cm):	8.208
Depth of Probe (in):	8.0
Elevation (in):	10.0
Elevation Head (in):	16.5

Time (min)	Gauge Pressure Reading (in H_2O)	Flowmeter Reading (cc/min)	Total Head (cm)	Insitu Permeability (cm/sec)
0.0	0.00	30	41.9	1.45E-03
5.0	0.00	34	41.9	1.65E-03
10.0	0.00	35	41.9	1.70E-03
15.0	0.00	38	41.9	1.84E-03
20.0	0.00	38	41.9	1.84E-03
30.0	0.00	38	41.9	1.84E-03

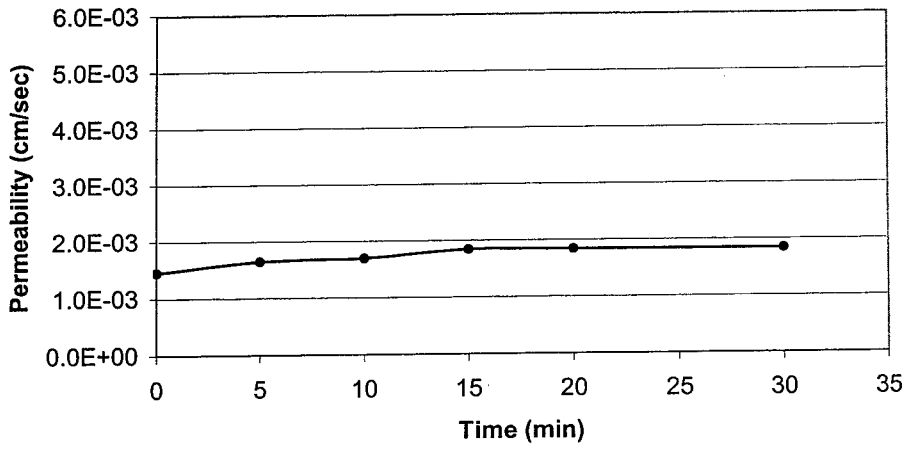

ASTM D 3385 - Infiltration Rate of Soils in Field using Double Ring Infiltrometer

Project Identification: WP-3

Project Location: Alachua County Park on Willinston Rd.

Liquid Used: Water pH: 7.0

Tested By: Michael Garau

Depth to water table: unknown (ft)

Constants	Area (cm^2)	Depth of Liquid (cm)	Liquid Containers No.	Vol./ΔH (cm^2/cm)
Inner Ring:	729.7			
Annular Space:	2189.0			

Liquid Level Maintained Using: ☐ Flow Valve ☐ Float Valve ☐ Mariotte Tube ☒ Other: Refilling

Penetration of rings: Inner: 3.5 (in) Outer: 3.5 (in)

Trial No.		Date	Time hr:min	Elapsed Time Δ/(total) min	Flow Readings: Inner Ring Reading cm	Inner Ring Flow cm^3	Annular Space Reading cm	Annular Space Flow cm^3	Liquid Temp. °C	Incr. Infiltration Rate: Inner cm/h	Annular cm/h	Ground Temp. = 45 °F @ depth of (in) / Remarks: Weather Conditions, etc.
1	S	2/13/00	10:30	15	-	1965	-		25	10.8		
	E	2/13/00	10:45	15	-		-		25			Cool and Sunny Conditions
2	S	2/13/00	10:45	15	-	1910	-		25	10.5		
	E	2/13/00	11:00	30	-		-		25			
3	S	2/13/00	11:00	15	-	1875	-		25	10.3		
	E	2/13/00	11:15	45	-		-		25			
4	S											
	E											
5	S											
	E											
6	S											
	E											
7	S											
	E											
8	S											
	E											
9	S											
	E											
10	S											
	E											

Ring Dimensions: Inner Ring: 30.48 cm (12 in) diameter, 60.96 cm (24 in) height
Outer Ring: 60.96 cm (24 in) diameter, 60.96 cm (24 in) height

Field Permeablilty Testing Device

Test ID: WP-3
Date : 2/13/00

Phase II: Validation Study
Location : Alachua County Park on Willinston Rd and 441

Sieve Analysis

Sieve No.	Diameter (mm)	M_{sv} (g)	$M_{sv,s}$ (g)	M_s (g)	% Soil Retained	%Soil Passing
10	2.00	505.75	508.76	3.01	0.60	99.40
20	0.85	411.54	414.54	3.00	0.60	98.80
30	0.60	404.73	412.75	8.02	1.60	97.20
50	0.30	387.19	485.3	98.11	19.56	77.64
70	0.212	441.33	535.31	93.98	18.74	58.90
100	0.15	314.83	444.55	129.72	25.87	33.03
140	0.106	356.72	443.77	87.05	17.36	15.68
200	0.075	334.10	377.04	42.94	8.56	7.11
Pan	-	371.24	406.92	35.68	7.11	
			Sum =	501.51		

Grain Size Distribution Curve

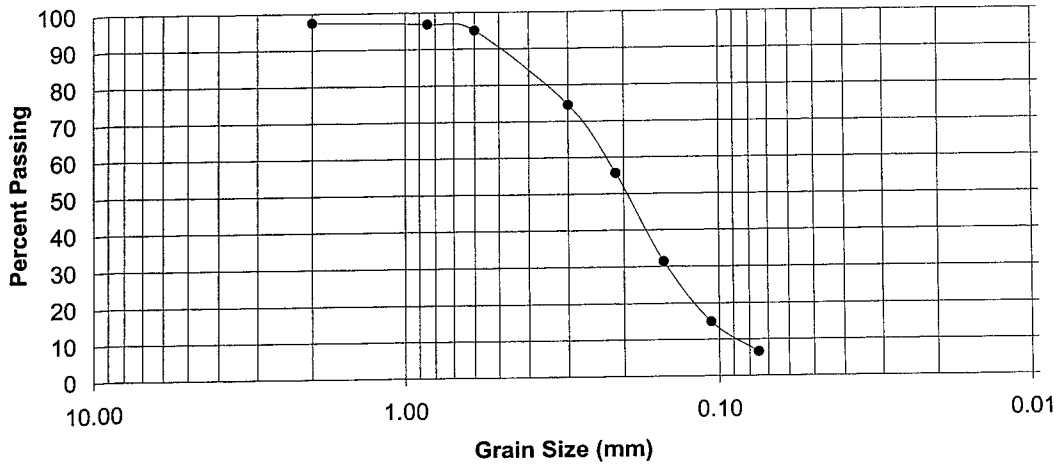

% Gravel :	0.00	D_{10} :	0.09
% Coarse Sand :	0.6	D_{30} :	0.15
% Medium Sand :	14.4	D_{60} :	0.22
% Fine Sand :	77.89	C_u :	2.44
% Fines :	7.11	C_z :	1.14

Field Permeablilty Testing Device

Test ID: SR9A -1

Phase II: Validation Study

Date : 12/2/99

Location : SR-9A between US-1 and Bay Meadows Rd. - Jacksonville

Sleeve Diameter (in):	0.775
Sleeve Length (in):	0.685
Shape Factor (cm):	8.208
Depth of Probe (in):	4.5
Elevation (in):	15.0
Elevation Head (in):	18.0

Time (min)	Gauge Pressure Reading (in H_2O)	Flowmeter Reading (cc/min)	Total Head (cm)	Insitu Permeability (cm/sec)
1.0	0.00	35	45.7	1.55E-03
3.0	0.00	35	45.7	1.55E-03
5.0	0.00	33	45.7	1.47E-03
7.0	0.00	33	45.7	1.47E-03
9.0	0.00	33	45.7	1.47E-03
10.0	0.00	33	45.7	1.47E-03
15.0	0.00	31	45.7	1.38E-03
20.0	0.00	31	45.7	1.38E-03
25.0	0.00	31	45.7	1.38E-03
30.0	0.00	31	45.7	1.38E-03

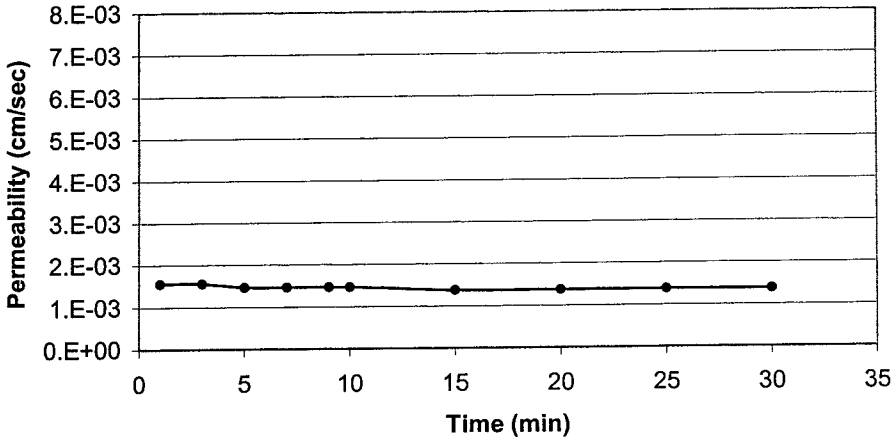

ASTM D 3385 - Infiltration Rate of Soils in Field using Double Ring Infiltrometer

Project Identification: SR9A-1

Project Location: SR-9A - Jacksonville

Liquid Used: Water pH: 7.0

Tested By: Michael Garau

Depth to water table: unknown (ft)

Penetration of rings: Inner: 3.5 (in) Outer: 3.5 (in)

Constants	Area (cm^2)	Depth of Liquid (cm)	Liquid Containers No.	Vol./ΔH (cm^2/cm)
Inner Ring:	729.7			
Annular Space:	2189.0			

Liquid Level Maintained Using: ☐ Flow Valve ☐ Float Valve ☐ Mariotte Tube ☒ Other: Refilling

Trial No.		Date	Time	Elapsed Time Δ/(total)	Flow Readings: Inner Ring Reading	Inner Ring Flow	Annular Space Reading	Annular Space Flow	Liquid Temp.	Incr. Infiltration Rate: Inner	Incr. Infiltration Rate: Annular	Ground Temp. = 45 °F @ depth of (in)
			hr:min	min	cm	cm^3	cm	cm^3	°C	cm/h	cm/h	Remarks: Weather Conditions, etc.
1	S	12/2/99	11:00	15	-	590	-		25	3.2	1.7	
	E	12/2/99	11:15	15	-		-		25			Cool and Sunny Conditions
2	S	12/2/99	11:15	15	-	515	-		25	2.8	2.0	
	E	12/2/99	11:30	30	-		-		25			
3	S	12/2/99	11:30	15	-	455	-		25	2.5	2.0	
	E	12/2/99	11:45	45	-		-		25			
4	S	12/2/99	11:45	15	-	485	-		25	2.7	2.1	
	E	12/2/99	12:00	60	-		-		25			
5	S	12/2/99	12:00	15	-	500	-		25	2.7	1.6	
	E	12/2/99	12:15	75	-		-		25			
6	S	12/2/99	12:15	15	-	500	-		25	2.7	1.8	
	E	12/2/99	12:30	90	-		-		25			
7	S											
	E											
8	S											
	E											
9	S											
	E											
10	S											
	E											

Ring Dimensions: Inner Ring: 30.48 cm (12 in) diameter, 60.96 cm (24 in) height
Outer Ring: 60.96 cm (24 in) diameter, 60.96 cm (24 in) height

Field Permeablilty Testing Device

Test ID: SR9A -1
Phase II: Validation Study **Date :** 12/2/99
Location : SR-9A between US-1 and Bay Meadows Rd. - Jacksonville

Sieve Analysis

Sieve No.	Diameter (mm)	M_{sv} (g)	$M_{sv,s}$ (g)	M_s (g)	% Soil Retained	%Soil Passing
10	2.00	417.41	417.81	0.40	0.08	99.92
20	0.85	401.95	403.72	1.77	0.33	99.59
30	0.60	450.62	452.23	1.61	0.30	99.29
60	0.25	364.65	392.91	28.26	5.31	93.98
100	0.15	315.02	731.31	416.29	78.16	15.83
140	0.106	356.99	425.47	68.48	12.86	2.97
200	0.075	334.77	345.99	11.22	2.11	0.87
Pan	-	375.63	380.24	4.61	0.87	0.00

Grain Size Distribution Curve

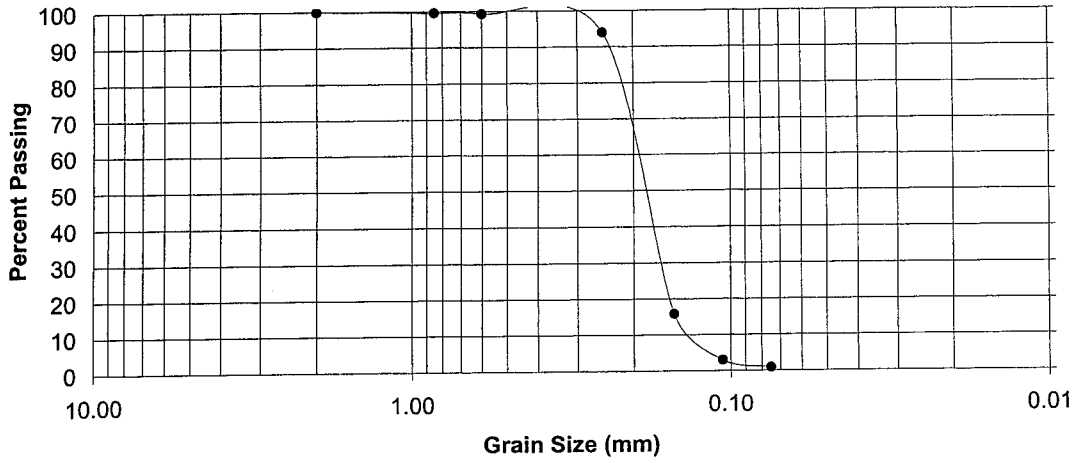

% Gravel :	0.00	D_{10} :	0.13
% Coarse Sand :	0.08	D_{30} :	0.16
% Medium Sand :	0.63	D_{60} :	0.19
% Fine Sand :	99.29	C_u :	1.46
% Fines :	0.87	C_z :	1.04

Field Permeablilty Testing Device

Phase II: Validation Study
Location : US 90 West of US 301

Test ID: US90-1
Date : 10/3/00

Sleeve Diameter (in):	0.775
Sleeve Length (in):	0.685
Shape Factor (cm):	8.208
Depth of Probe (in):	4.5
Elevation (in):	9.0
Elevation Head (in):	12.0

Time (min)	Gauge Pressure Reading (in H_2O)	Flowmeter Reading (cc/min)	Total Head (cm)	Insitu Permeability (cm/sec)
1.0	0.00	18	30.5	1.20E-03
3.0	0.00	17	30.5	1.13E-03
5.0	0.00	17	30.5	1.13E-03
7.0	0.00	16	30.5	1.07E-03
9.0	0.00	16	30.5	1.07E-03
10.0	0.00	16	30.5	1.07E-03
15.0	0.00	14	30.5	9.32E-04
20.0	0.00	13.5	30.5	8.99E-04
25.0	0.00	13.5	30.5	8.99E-04
30.0	0.00	13.5	30.5	8.99E-04

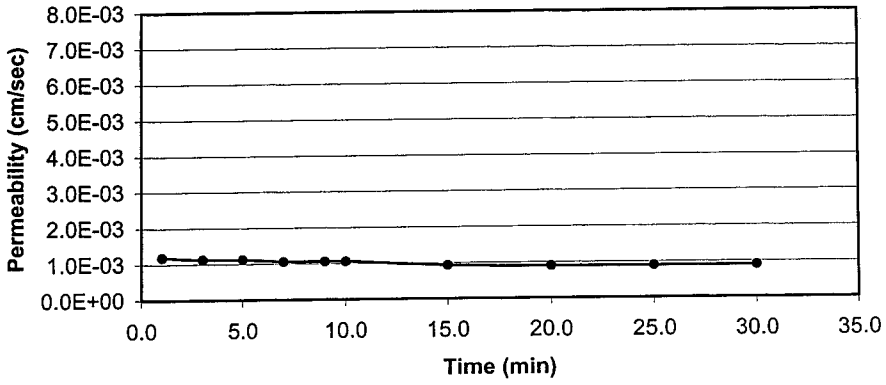

ASTM D 3385 - Infiltration Rate of Soils in Field using Double Ring Infiltrometer

Project Identification: US90-1

Project Location: US 90 West of US 301

Liquid Used: Water pH: 7.0

Tested By: Michael Garau

Depth to water table: unknown (ft) Penetration of rings: Inner: 3 (in) Outer: 3 (in)

Constants	Area (cm^2)	Depth of Liquid (cm)	Liquid Containers No.	Vol./ΔH (cm^2/cm)
Inner Ring:	729.7			
Annular Space:	2189.0			

Liquid Level Maintained Using: ☐ Flow Valve ☐ Float Valve ☐ Mariotte Tube ☒ Other: Refilling

Trial No.		Date	Time	Elapsed Time Δ/(total)	Flow Readings: Inner Ring Reading	Inner Ring Flow	Annular Space Reading	Annular Space Flow	Liquid Temp.	Incr. Infiltration Rate: Inner	Incr. Infiltration Rate: Annular	Ground Temp. = 45 °F @ depth of (in)
			hr:min	min	cm	cm^3	cm	cm^3	°C	cm/h	cm/h	Remarks: Weather Conditions, etc.
1	S	10/3/00	12:00	15	-	474.3	-		25	2.6		
	E	10/3/00	12:15	15	-		-		25			Overcast
2	S	10/3/00	12:15	15	-	492.5	-		25	2.7		
	E	10/3/00	12:30	30	-		-		25			
3	S	10/3/00	12:30	15	-	525.4	-		25	2.9		
	E	10/3/00	12:45	45	-		-		25			
4	S											
	E											
5	S											
	E											
6	S											
	E											
7	S											
	E											
8	S											
	E											
9	S											
	E											
10	S											
	E											

Ring Dimensions: Inner Ring: 30.48 cm (12 in) diameter, 60.96 cm (24 in) height
Outer Ring: 60.96 cm (24 in) diameter, 60.96 cm (24 in) height

Field Permeablilty Testing Device

Phase II: Validation Study

Location : US90 West of US 301

Test ID: US90-1

Date : 10/3/00

Sieve Analysis

Sieve No.	Diameter (mm)	M_{sv} (g)	$M_{sv,s}$ (g)	M_s (g)	% Soil Retained	%Soil Passing
10	2.00	417.41	417.78	0.37	0.07	99.93
20	0.85	401.95	403.75	1.80	0.34	99.59
30	0.60	450.62	452.21	1.59	0.30	99.29
60	0.25	364.65	392.9	28.25	5.33	93.96
100	0.15	315.02	730.96	415.94	78.49	15.47
140	0.106	356.99	425.51	68.52	12.93	2.53
200	0.075	334.77	344.91	10.14	1.91	0.62
Pan	-	375.63	378.92	3.29	0.62	0.00

Grain Size Distribution Curve

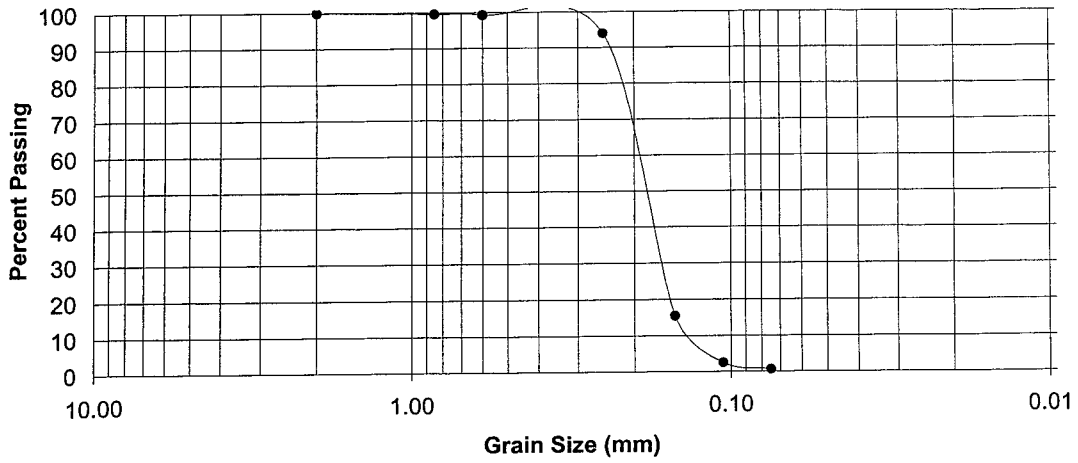

% Gravel :	0.00	D_{10} :	0.14
% Coarse Sand :	0.07	D_{30} :	0.17
% Medium Sand :	0.64	D_{60} :	0.19
% Fine Sand :	98.45	C_u :	1.36
% Fines :	0.84	C_z :	1.09

Phase Three

Phase 3 began with four constant head tests at the I-75 Southbound weigh station in Ocala, FL. The site comprised of 13 inches of concrete supported by a light-tan sandy soil (< 2% fines). Test 1 and 2 were conventional tests. In Test 3 and 4, the probe was inserted using the ADCP testing machine. A 10-lb, 5.5-inch drop was applied in Test 3, while a 10-lb, 11-inch drop was applied during Test 4. A leak was discovered during the first test accounting for the higher flow rate and permeability values. The two methods were compared to evaluate the effect on the permeability when using a dynamic method to insert the probe.

A survey on a 2-mile stretch of I-10 near Monticello, FL was made with eight tests. The section was currently under repair and thus provided the opportunity for the tests. The falling head method was required because of the low permeability. The soil encountered was a poorly mixed silty sand with clay-silt pockets. A similar survey was conducted on I-4 near Lakeland, FL. Nineteen tests were completed using the falling head method on predetermined locations by FDOT District One engineers. The FDOT engineers identified the pavement condition for each location. Results from poor sections were compared with those from well performing pavements. It was concluded that the permeability was consistent throughout the site, thus no correlation could be determined. However, low values of permeability were consistently measured. Samples were not recovered due to time and traffic constraints.

Field Permeablilty Testing Device

Test ID: I75-1

Phase III : Field Testing

Date : 7/27/99

Location : I-75 Southbound Weigh Station - Ocala

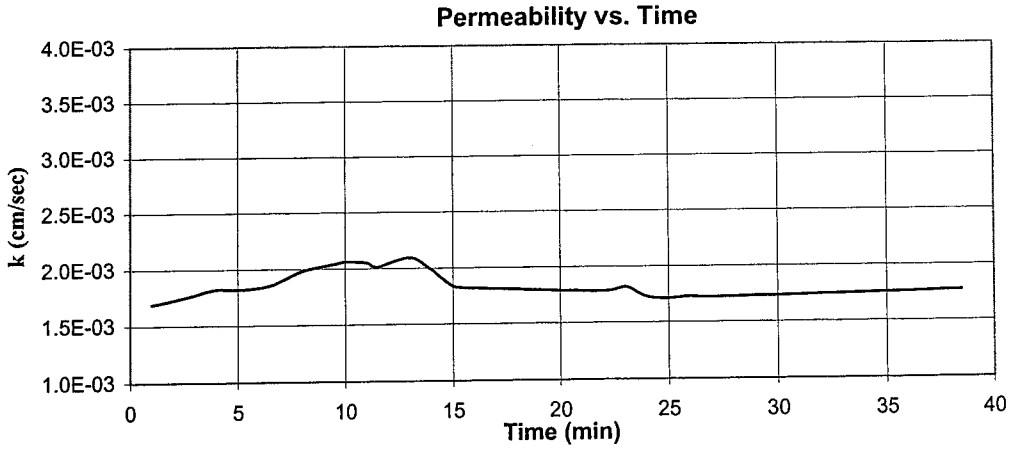

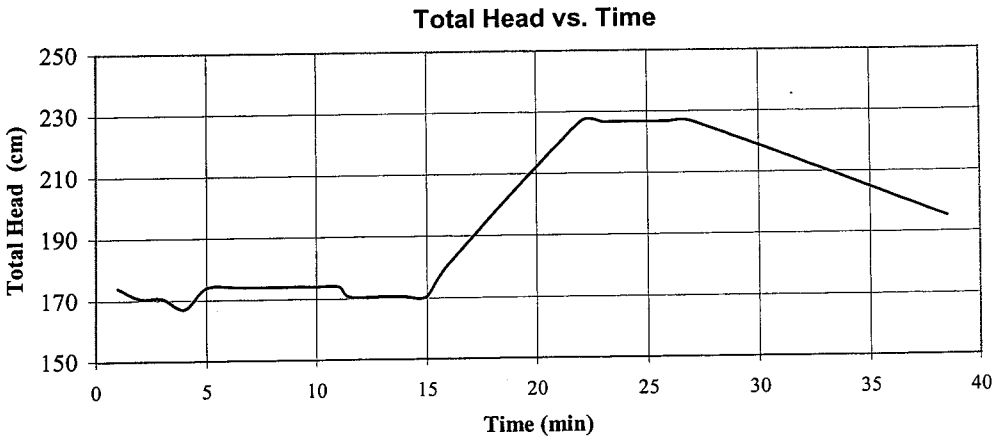

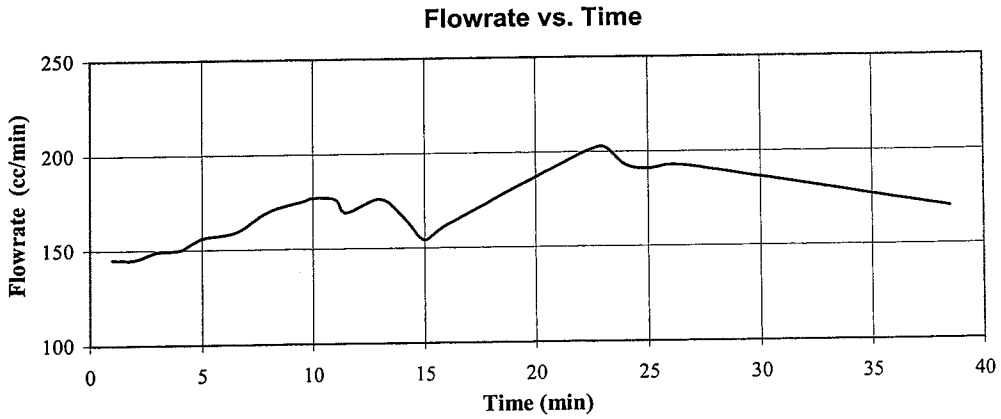

Field Permeablilty Testing Device

Test ID: I75-2

Phase III : Field Testing

Date : 7/27/99

Location : I-75 Southbound Weigh Station - Ocala

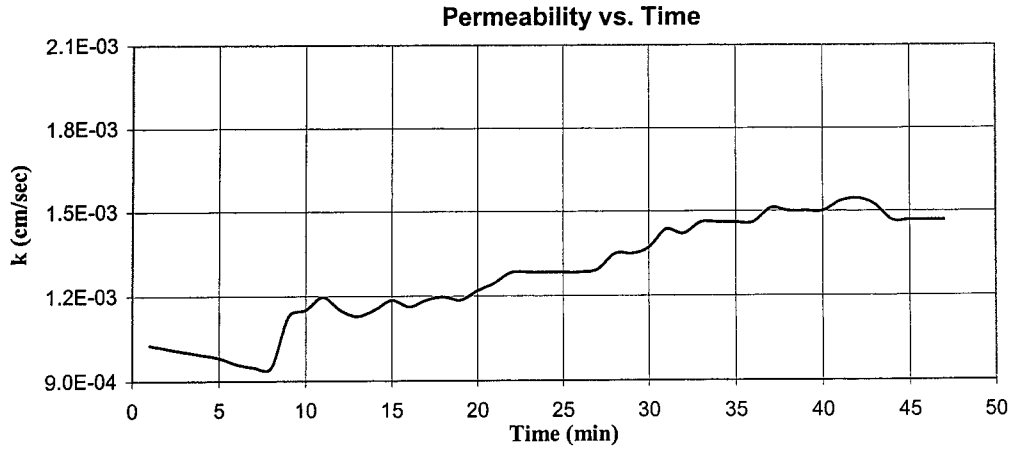

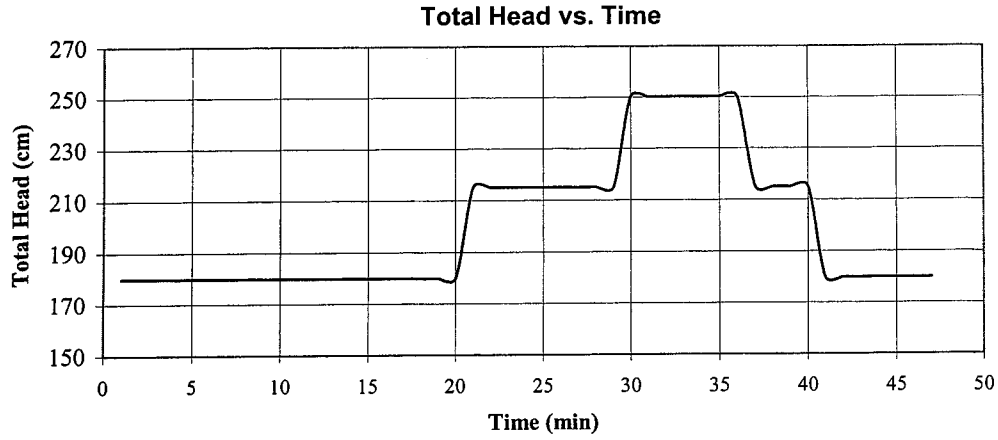

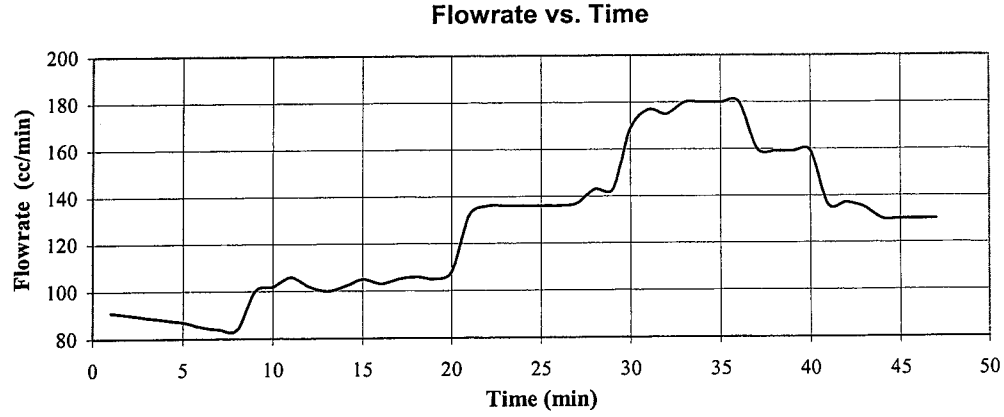

Field Permeablilty Testing Device

Test ID: I75-3

Phase III : Field Testing

Date : 7/27/99

Location : I-75 Southbound Weigh Station - Ocala

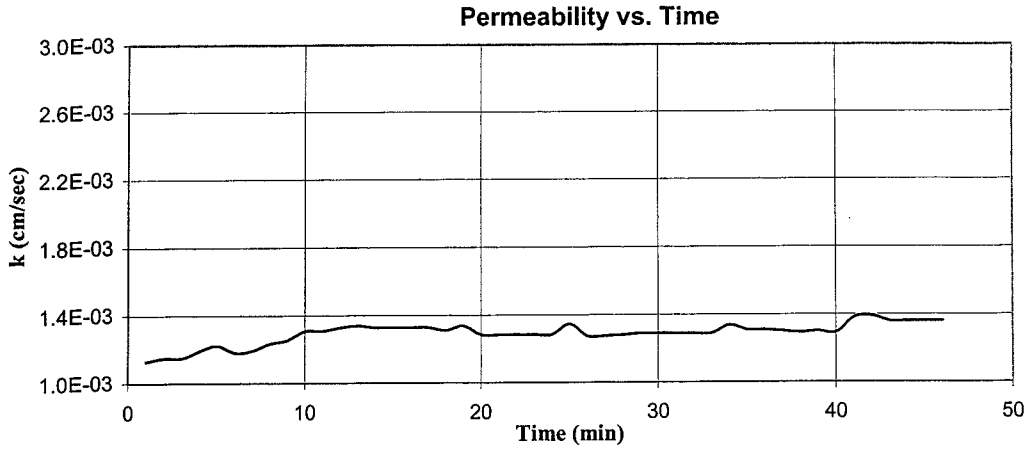

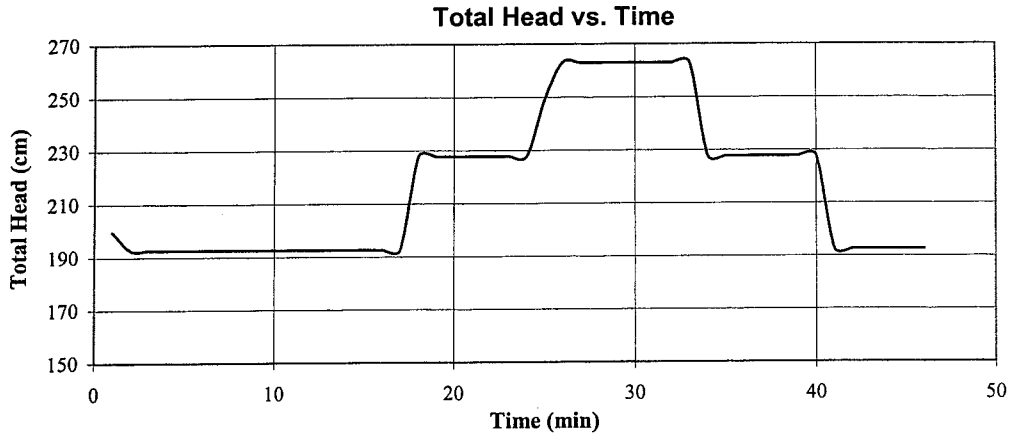

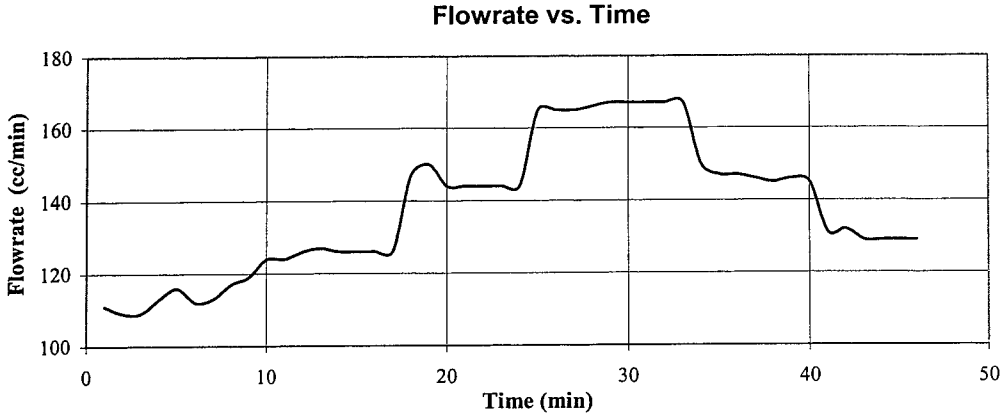

Field Permeablilty Testing Device

Test ID: I75-4

Phase III : Field Testing

Date : 7/27/99

Location : I-75 Southbound Weigh Station - Ocala

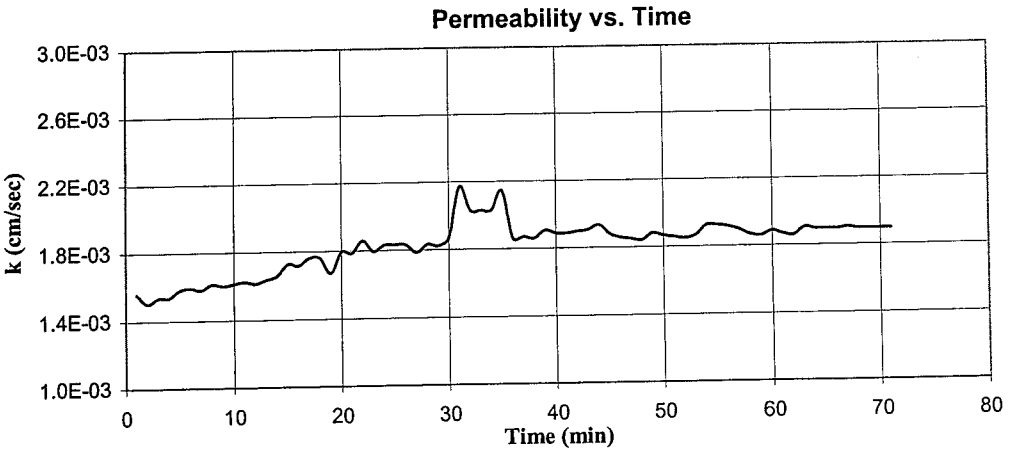

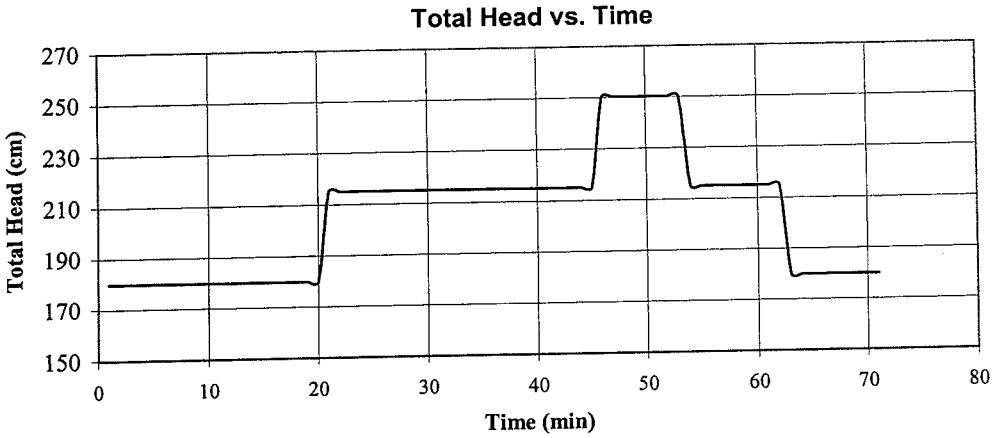

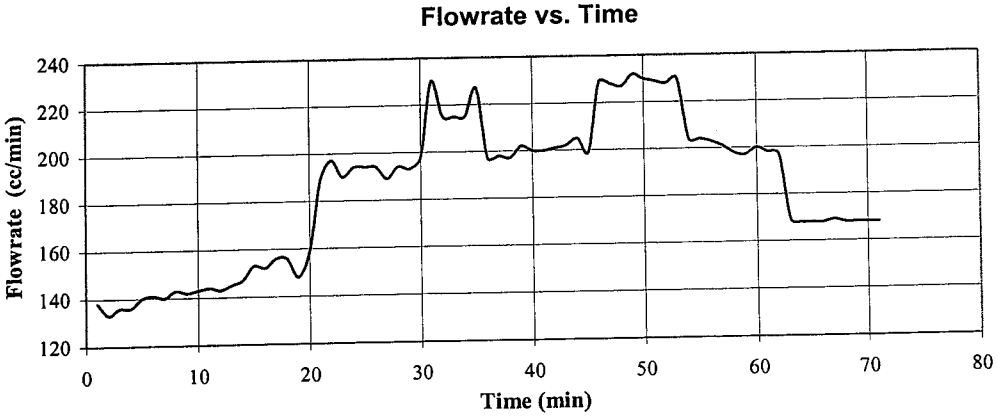

Field Permeablilty Testing Device

Sieve Analysis

Phase III : Field Testing

Date : 7/27/99

Location : I-75 Southbound Weigh Station - Ocala

Sieve No.	Diameter (mm)	M_{sv} (g)	$M_{sv,s}$ (g)	M_s (g)	% Soil Retained	%Soil Passing
4	4.75	509.7	509.7	0.0	0.00	100
10	2.00	466.6	468.8	2.2	0.39	99.61
20	0.85	412.1	435.8	23.7	4.16	95.45
30	0.60	405.2	437.4	32.2	5.66	89.79
50	0.30	387.4	568.8	181.4	31.86	57.93
100	0.15	315.0	576.3	261.3	45.90	12.03
200	0.075	334.7	391.90	57.2	10.05	1.98
Pan	-	375.60	386.9	11.3	1.98	0.00

Sum = 569.3

Results :

D_{10}	D_{30}	D_{60}	C_u	C_z
0.14	0.20	0.31	2.21	0.92

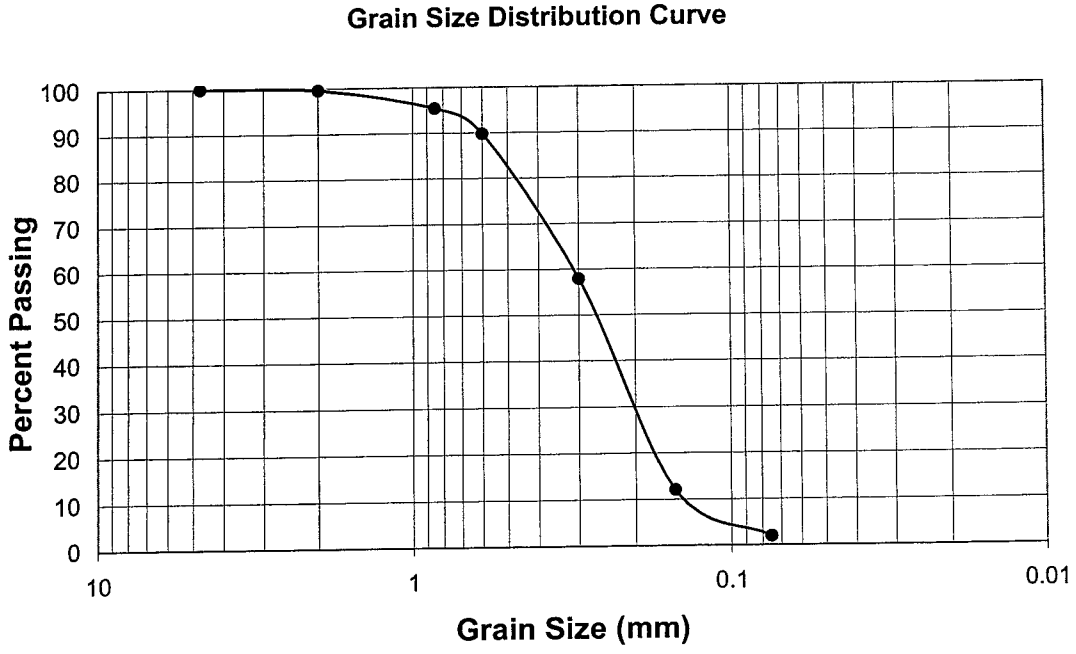

Field Permeablilty Testing Device

Test ID: I10-1
Date : 10/19/99

Phase III : Field Testing
Location : I-10, East Bound Lane - Jefferson County

Site Sketch

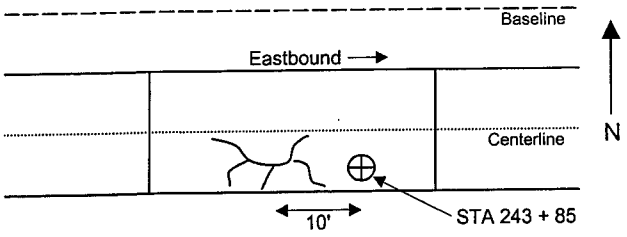

Profile

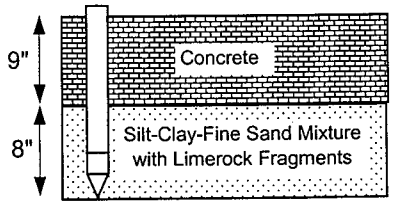

Falling Head Test

Sleeve Diameter (in):	0.775
Sleeve Length (in):	0.685
Shape Factor (cm):	8.208
Depth of Probe into Soil Layer (in):	8.0
Thickness of Concrete (in):	9.0
Standpipe Diameter (in):	0.25
Height of Water Above Concrete (in):	51.5

Time (min)	ΔH (in)	k_f (cm/sec)
8.1	0.75	8.94E-07
15	1.63	1.06E-06
30	3.50	1.15E-06
60	7.38	1.25E-06
90	11.38	1.33E-06

k_f (average): 1.14E-06

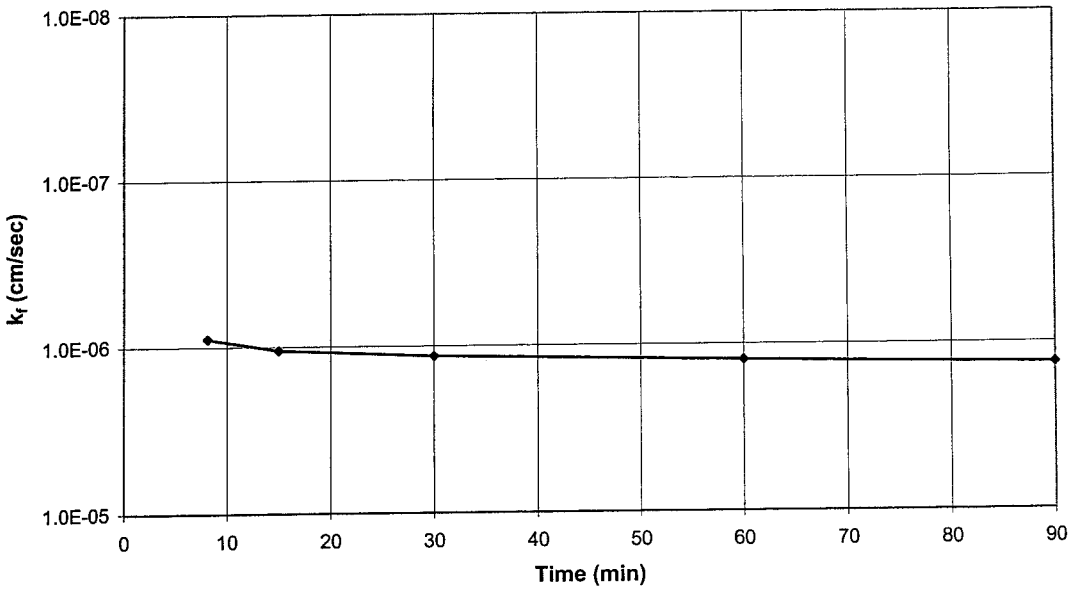

Field Permeablilty Testing Device

Test ID: I10-1
Date : 10/19/99

Phase III : Field Testing
Location : I-10, East Bound Lane - Jefferson County

Sieve Analysis

Sieve No.	Diameter (mm)	M_{sv} (g)	$M_{sv,s}$ (g)	M_s (g)	% Soil Retained	%Soil Passing
4	4.75	509.93	509.93	0.00	0.00	100
10	2.00	438.80	439.23	0.43	0.09	99.91
20	0.85	533.67	536.43	2.76	0.55	99.36
30	0.6	463.16	528.26	65.10	13.04	86.32
60	0.25	444.09	579.94	135.85	27.21	59.12
100	0.15	521.63	762.07	240.44	48.15	10.97
200	0.075	333.19	372.80	39.61	7.93	3.04
Pan	-	352.50	367.66	15.16	3.04	0.00
			Sum =	499.35		

Grain Size Distribution Curve

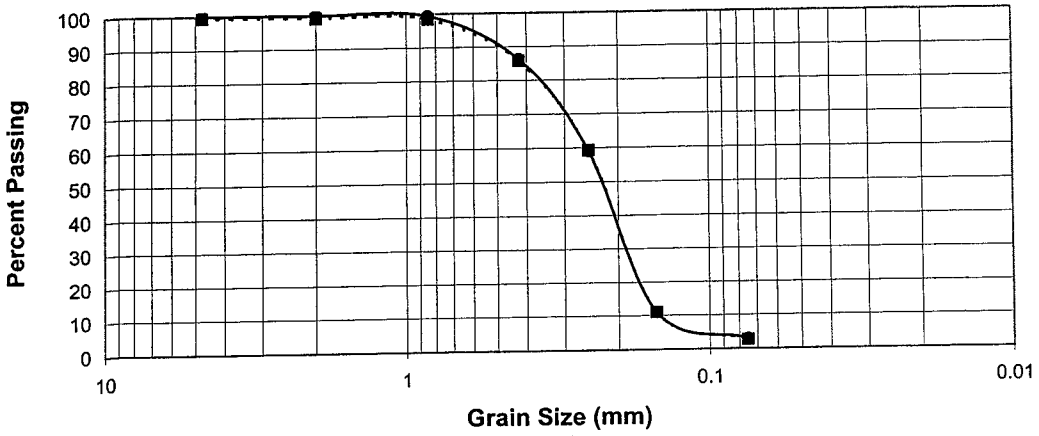

% Gravel :	0.0	D_{10} :	0.26
% Coarse Sand :	0.09	D_{30} :	0.19
% Medium Sand :	13.59	D_{60} :	0.25
% Fine Sand :	83.28	C_u :	0.96
% Fines :	3.04	C_z :	0.56

Field Permeablilty Testing Device

Phase III : Field Testing

Location : I-10, East Bound Lane - Jefferson County

Test ID: I10-2

Date : 10/19/99

Site Sketch

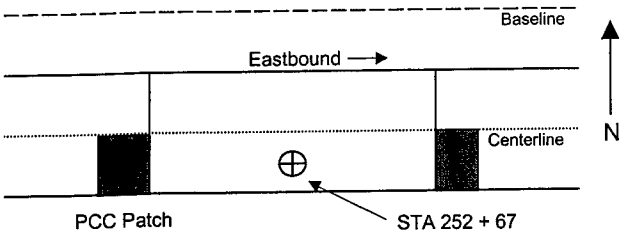

Profile

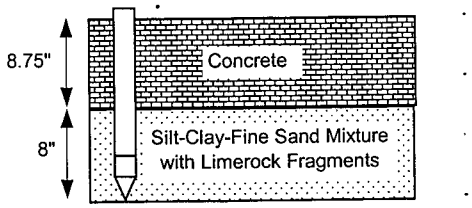

Falling Head Test

Sleeve Diameter (in):	0.775
Sleeve Length (in):	0.685
Shape Factor (cm):	8.208
Depth of Probe into Soil Layer (in):	8.0
Thickness of Concrete (in):	8.75
Standpipe Diameter (in):	0.25
Height of Water Above Concrete (in):	52.75

Time (min)	ΔH (in)	k_f (cm/sec)
7.5	4.25	5.53E-06
15	9.13	6.18E-06
30	18.38	6.75E-06
Re-established Head		
7.5	6.63	8.80E-06
15	12.88	9.00E-06
30	23.38	9.03E-06

k_f (average): 7.55E-06

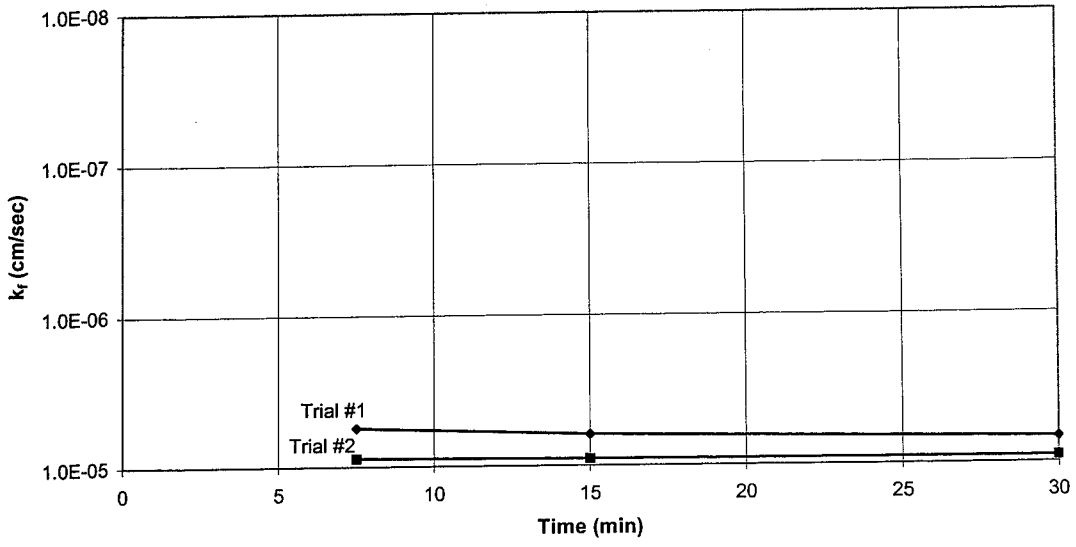

Field Permeablilty Testing Device

Test ID: I10-2
Date : 10/19/99

Phase III : Field Testing
Location : I-10, East Bound Lane - Jefferson County

Sieve Analysis

Sieve No.	Diameter (mm)	M_{sv} (g)	$M_{sv,s}$ (g)	M_s (g)	% Soil Retained	%Soil Passing
4	4.75	509.93	509.93	0.00	0.00	100
10	2.00	438.80	439.23	0.43	0.09	99.91
20	0.85	533.67	536.43	2.76	0.55	99.37
30	0.425	463.16	528.26	65.10	12.90	86.47
60	0.25	444.09	579.94	135.85	26.91	59.56
100	0.15	521.63	762.07	240.44	47.64	11.92
200	0.075	333.19	372.80	39.61	7.85	4.07
Pan	-	352.50	373.05	20.55	4.07	0.00

Sum = 504.74

Grain Size Distribution Curve

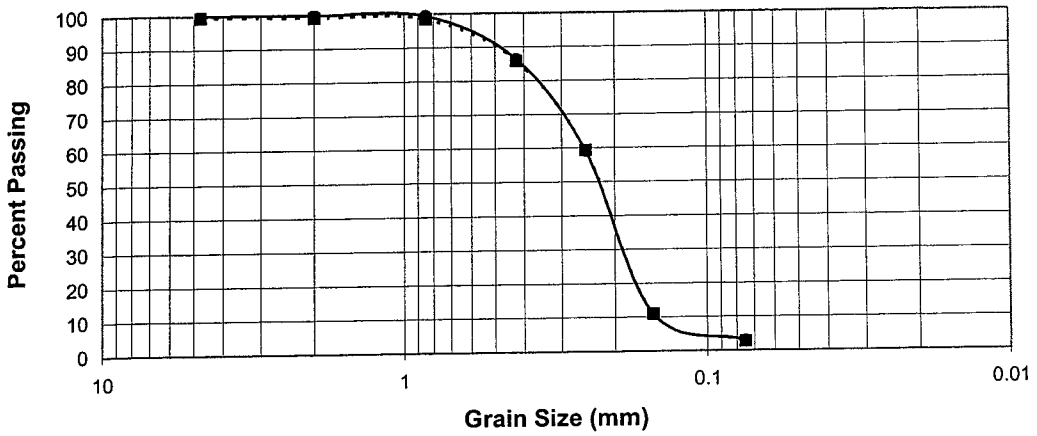

% Gravel :	0.0	D_{10} :	0.15
% Coarse Sand :	0.09	D_{30} :	0.19
% Medium Sand :	13.44	D_{60} :	0.25
% Fine Sand :	82.4	C_u :	1.67
% Fines :	4.07	C_z :	0.96

Field Permeablilty Testing Device

Phase III : Field Testing

Location : I-10, East Bound Lane - Jefferson County

Test ID: I10-3

Date : 10/21/99

Site Sketch

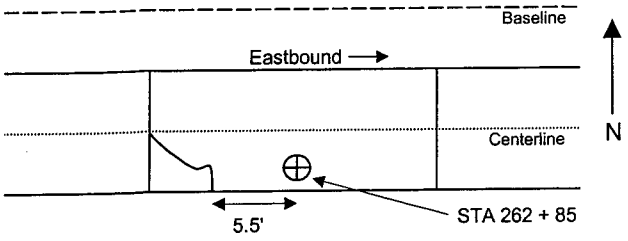

Profile

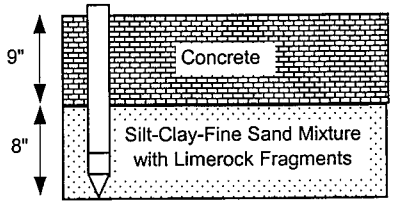

Falling Head Test

Sleeve Diameter (in):	0.775
Sleeve Length (in):	0.685
Shape Factor (cm):	8.208
Depth of Probe into Soil Layer (in):	8.0
Thickness of Concrete (in):	9.0
Standpipe Diameter (in):	0.25
Height of Water Above Concrete (in):	54.38

Time (min)	ΔH (in)	k_f (cm/sec)
7.5	0.63	7.77E-07
15	1.19	7.36E-07
30	2.25	7.02E-07
60	4.38	6.94E-07
90	6.38	6.84E-07

k_f (average): 7.18E-07

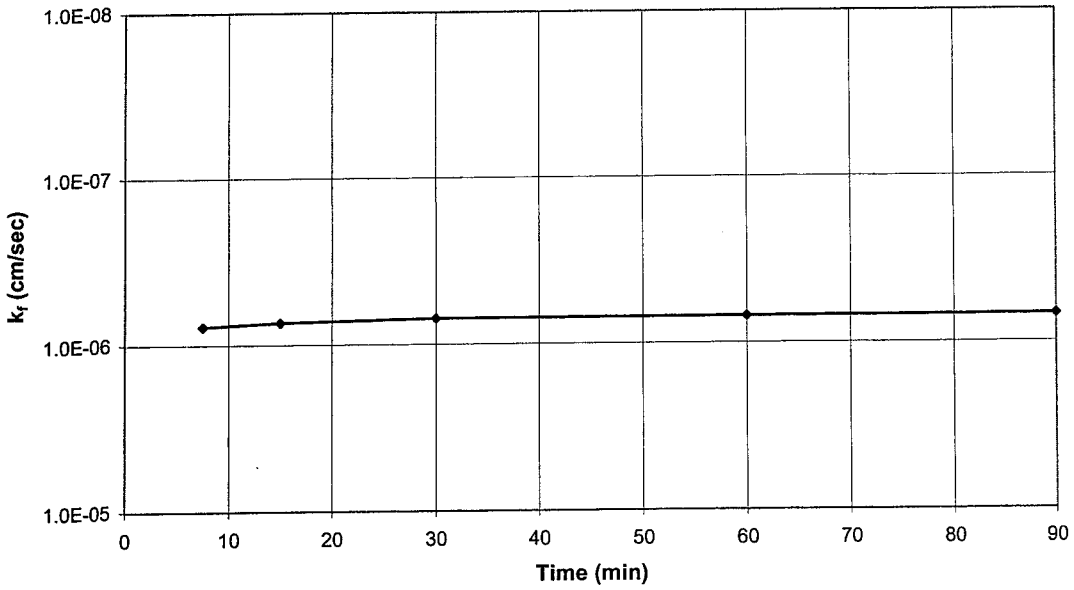

Field Permeablilty Testing Device

Test ID: I10-3
Date : 10/21/99

Phase III : Field Testing
Location : I-10, East Bound Lane - Jefferson County

Sieve Analysis

Sieve No.	Diameter (mm)	M_{sv} (g)	$M_{sv,s}$ (g)	M_s (g)	% Soil Retained	%Soil Passing
4	4.75	589.59	593.75	4.16	0.76	99.24
10	2.00	417.43	424.77	7.34	1.34	97.90
20	0.85	402.27	428.48	26.21	4.78	93.12
30	0.6	450.81	478.34	27.53	5.03	88.09
60	0.25	364.7	535.6	170.90	31.20	56.90
100	0.15	315.1	483.39	168.29	30.72	26.18
200	0.075	334.81	421.65	86.84	15.85	10.33
Pan	-	375.65	432.22	56.57	10.33	0.00
			Sum =	547.84		

Grain Size Distribution Curve

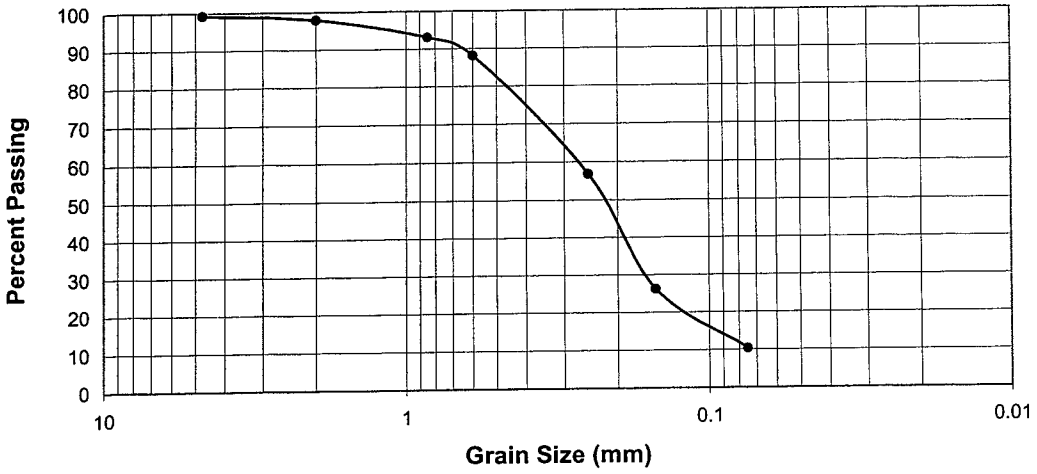

% Gravel :	0.76	D_{10} :	0.075
% Coarse Sand :	1.34	D_{30} :	0.16
% Medium Sand :	22.90	D_{60} :	0.26
% Fine Sand :	64.67	C_u :	3.47
% Fines :	10.33	C_z :	1.31

Field Permeablilty Testing Device

Phase III : Field Testing

Location : I-10, East Bound Lane - Jefferson County

Test ID: I10-4

Date : 10/21/99

Site Sketch

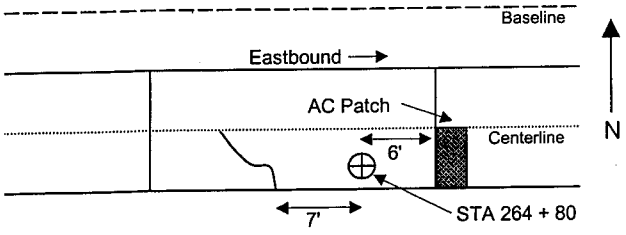

Profile

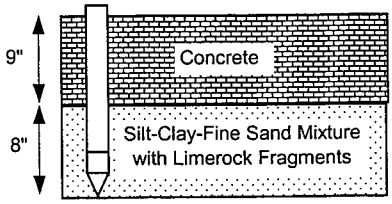

Falling Head Test

Sleeve Diameter (in):	0.775
Sleeve Length (in):	0.685
Shape Factor (cm):	8.208
Depth of Probe into Soil Layer (in):	8.0
Thickness of Concrete (in):	9.0
Standpipe Diameter (in):	0.25
Height of Water Above Concrete (in):	53.5

Time (min)	ΔH (in)	k_f (cm/sec)
7.5	0.81	1.01E-06
15	1.63	1.02E-06
30	3.25	1.03E-06
60	6.75	1.10E-06
90	10.06	1.13E-06

k_f (average): 1.06E-06

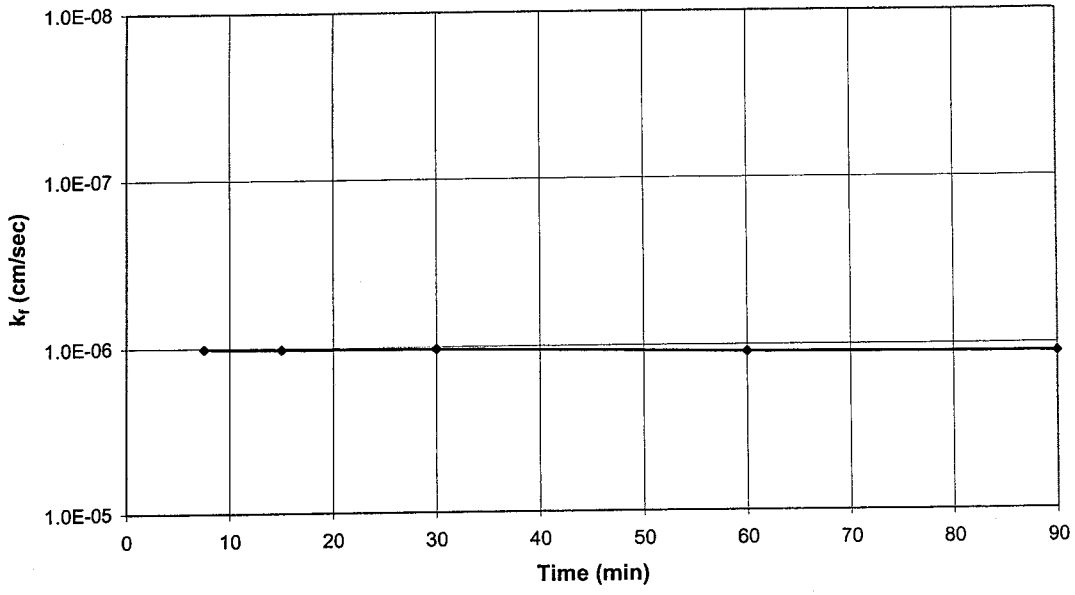

Field Permeablilty Testing Device

Test ID: I10-4
Date : 10/21/99

Phase III : Field Testing
Location : I-10, East Bound Lane - Jefferson County

Sieve Analysis

Sieve No.	Diameter (mm)	M_{sv} (g)	$M_{sv,s}$ (g)	M_s (g)	% Soil Retained	%Soil Passing
4	4.75	589.59	606.32	16.73	2.85	97.15
10	2.00	417.45	432.77	15.32	2.61	94.55
20	0.85	402.24	451.8	49.56	8.43	86.11
30	0.6	450.69	481.1	30.41	5.17	80.94
60	0.25	364.72	525.29	160.57	27.32	53.61
100	0.15	315.06	466.84	151.78	25.83	27.78
200	0.075	334.81	440.78	105.97	18.03	9.75
Pan	-	375.62	432.92	57.30	9.75	0.00
			Sum =	587.64		

Grain Size Distribution Curve

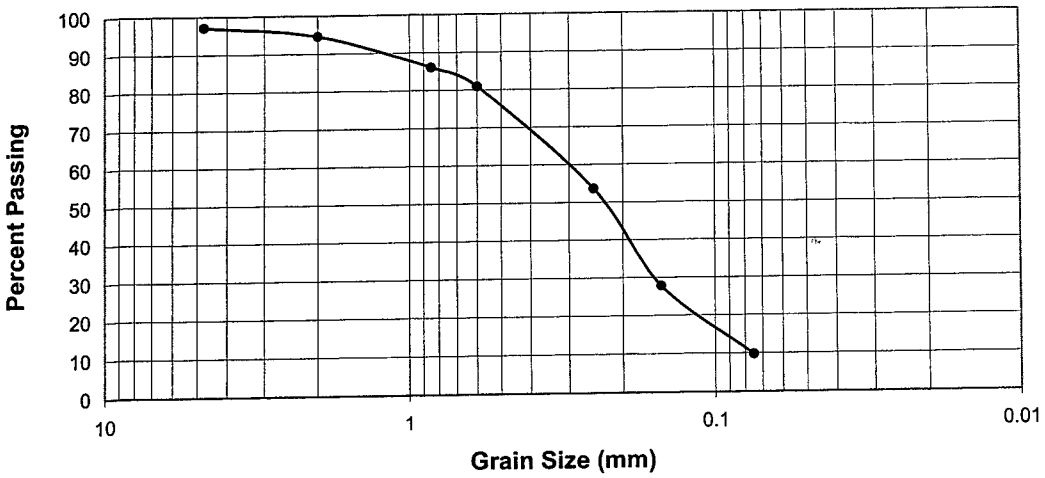

% Gravel :	2.85	D_{10} :	0.075
% Coarse Sand :	2.60	D_{30} :	0.16
% Medium Sand :	24.55	D_{60} :	0.3
% Fine Sand :	60.25	C_u :	4.0
% Fines :	9.75	C_z :	1.14

Field Permeablilty Testing Device

Phase III : Field Testing

Location : I-10, West Bound Lane - Jefferson County

Test ID: I10-5

Date : 10/26/99

Site Sketch

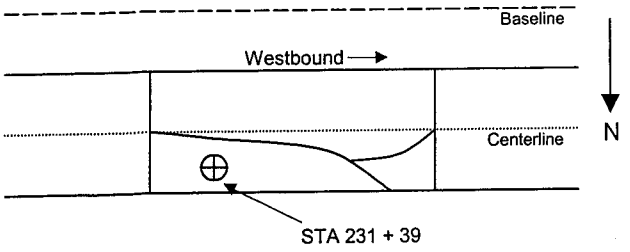

Profile

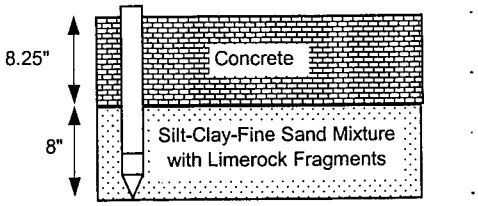

Falling Head Test

Sleeve Diameter (in):	0.775
Sleeve Length (in):	0.685
Shape Factor (cm):	8.208
Depth of Probe into Soil Layer (in):	8.0
Thickness of Concrete (in):	8.25
Standpipe Diameter (in):	0.25
Height of Water Above Concrete (in):	55

Time (min)	ΔH (in)	k_f (cm/sec)
7.5	1.88	2.34E-06
15	3.63	2.29E-06
30	6.88	2.22E-06
60	13.69	2.34E-06
90	19.88	2.40E-06

k_f (average): 2.32E-06

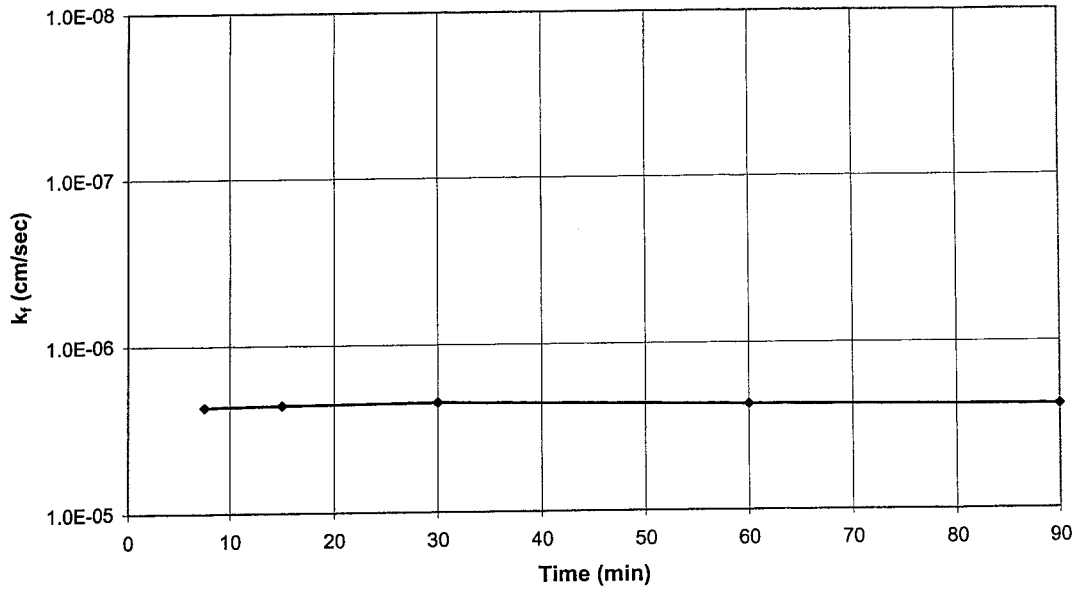

Field Permeablilty Testing Device

Test ID: I10-5
Date : 10/26/99

Phase III : Field Testing
Location : I-10, West Bound Lane - Jefferson County

Sieve Analysis

Sieve No.	Diameter (mm)	M_{sv} (g)	$M_{sv,s}$ (g)	M_s (g)	% Soil Retained	%Soil Passing
4	4.75	589.59	593.88	4.29	0.81	99.19
10	2.00	417.46	421.61	4.15	0.78	98.41
20	0.85	402.05	432.8	30.75	5.79	92.62
30	0.6	450.65	477.2	26.55	5.00	87.61
60	0.25	364.65	533.99	169.34	31.90	55.71
100	0.15	315.03	472.65	157.62	29.70	26.02
200	0.075	334.81	421.32	86.51	16.30	9.72
Pan	-	375.71	427.29	51.58	9.72	0.00
			Sum =	530.79		

Grain Size Distribution Curve

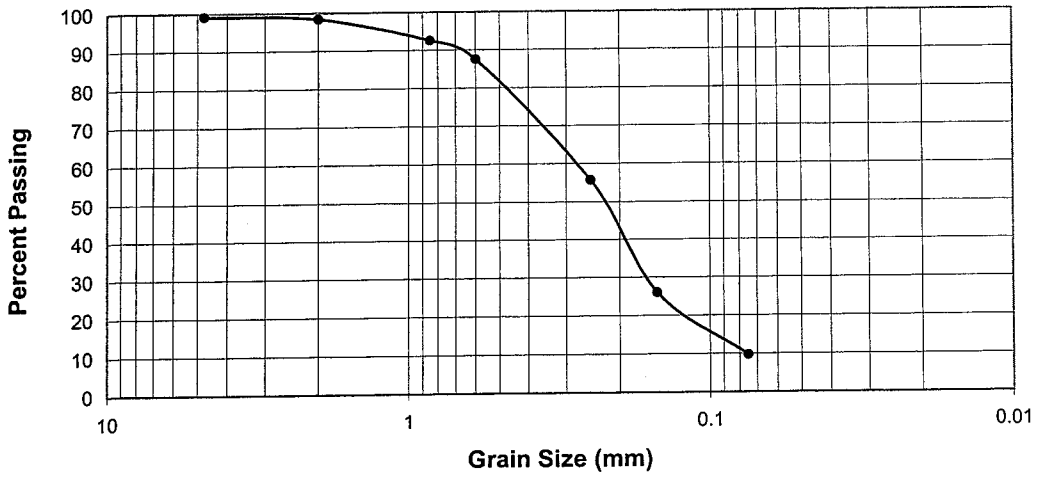

% Gravel :	0.81	D_{10} :	0.075
% Coarse Sand :	0.78	D_{30} :	0.16
% Medium Sand :	23.41	D_{60} :	0.28
% Fine Sand :	65.28	C_u :	3.73
% Fines :	9.72	C_z :	1.22

Field Permeablilty Testing Device

Phase III : Field Testing

Location : I-10, West Bound Lane - Jefferson County

Test ID: I10-6

Date : 10/26/99

Site Sketch

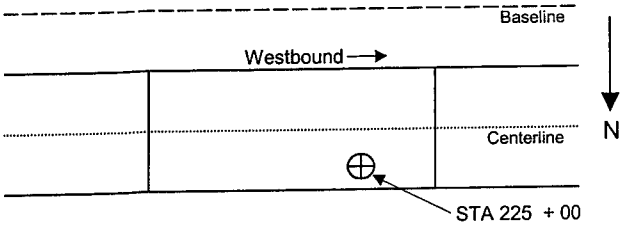

Profile

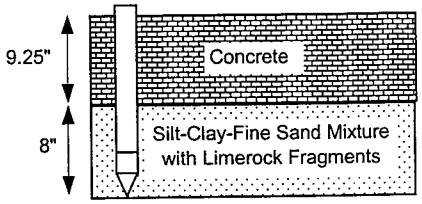

Falling Head Test

Sleeve Diameter (in):	0.775
Sleeve Length (in):	0.685
Shape Factor (cm):	8.208
Depth of Probe into Soil Layer (in):	8.0
Thickness of Concrete (in):	9.25
Standpipe Diameter (in):	0.25
Height of Water Above Concrete (in):	51.5

Time (min)	ΔH (in)	k_f (cm/sec)
7.5	0.88	1.12E-06
15	1.63	1.05E-06
30	3.25	1.06E-06
60	6.06	1.01E-06
90	9.00	1.03E-06

k_f (average): 1.05E-06

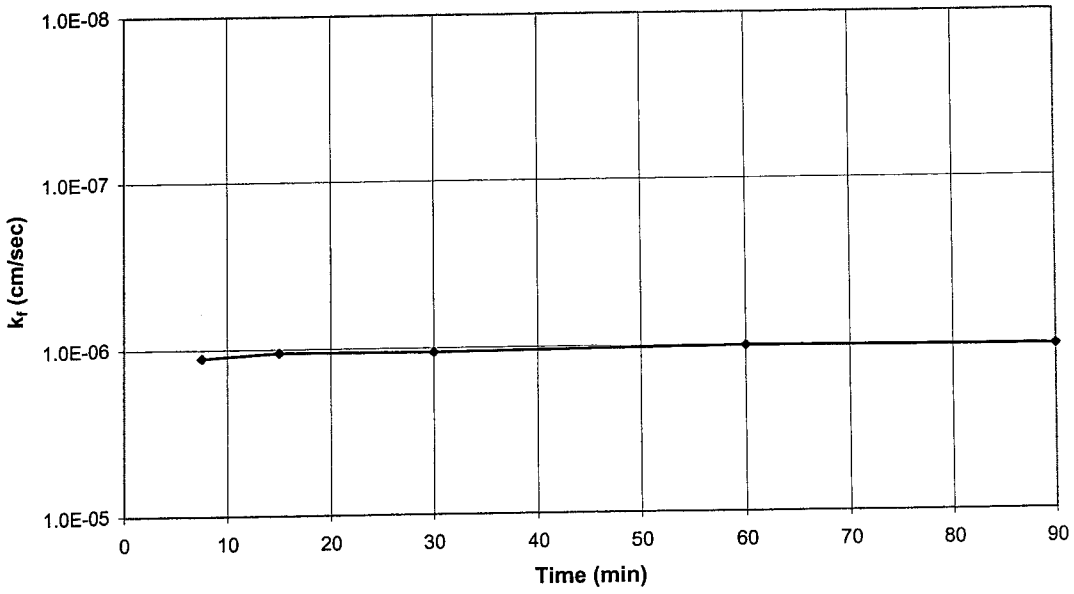

Field Permeablilty Testing Device

Test ID: I10-6
Date : 10/26/99

Phase III : Field Testing
Location : I-10, West Bound Lane - Jefferson County

Sieve Analysis

Sieve No.	Diameter (mm)	M_{sv} (g)	$M_{sv,s}$ (g)	M_s (g)	% Soil Retained	%Soil Passing
4	4.75	589.57	592.40	2.83	0.52	99.48
10	2.00	417.42	425.37	7.95	1.46	98.02
20	0.85	401.97	437.67	35.70	6.54	91.48
30	0.6	450.62	479.57	28.95	5.30	86.18
60	0.25	364.66	545.01	180.35	33.05	53.13
100	0.15	315.1	474.23	159.13	29.16	23.98
200	0.075	334.79	420.09	85.30	15.63	8.35
Pan	-	375.64	421.20	45.56	8.35	0.00
			Sum =	545.77		

Grain Size Distribution Curve

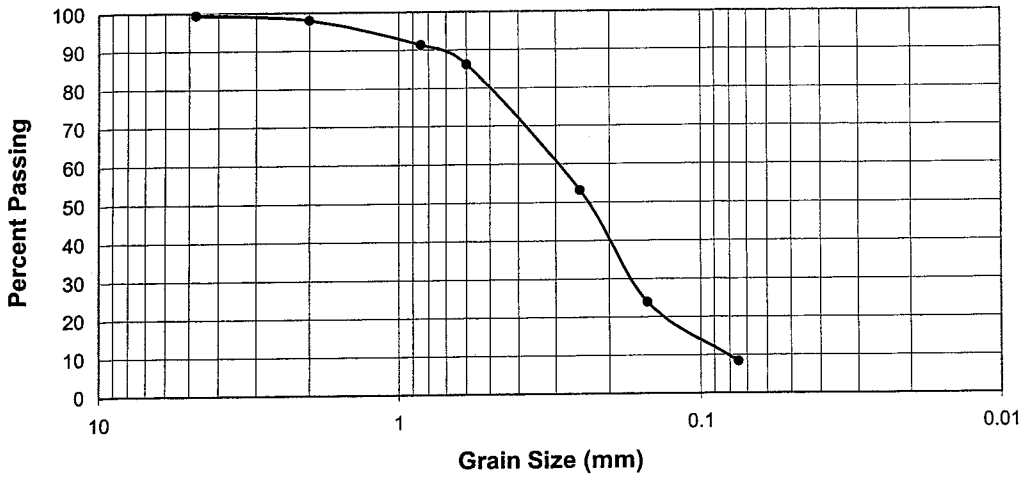

% Gravel :	0.52	D_{10} :	0.8
% Coarse Sand :	1.46	D_{30} :	0.17
% Medium Sand :	26.02	D_{60} :	0.3
% Fine Sand :	63.65	C_u :	0.38
% Fines :	8.35	C_z :	0.12

Field Permeablilty Testing Device

Test ID: I10-7
Date : 11/2/99

Phase III : Field Testing
Location : I-10, West Bound Lane - Jefferson County

Site Sketch

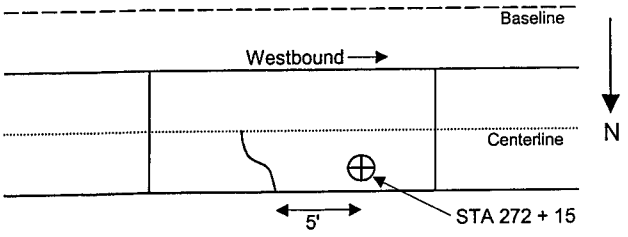

Profile

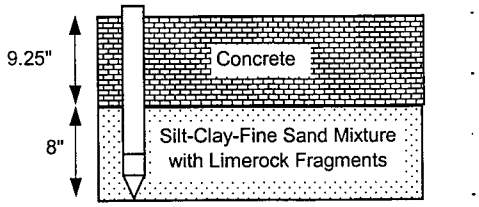

Falling Head Test

Sleeve Diameter (in):	0.775
Sleeve Length (in):	0.685
Shape Factor (cm):	8.208
Depth of Probe into Soil Layer (in):	8.0
Thickness of Concrete (in):	9.25
Standpipe Diameter (in):	0.25
Height of Water Above Concrete (in):	54.125

Time (min)	ΔH (in)	k_f (cm/sec)
7.5	9.5	1.25E-05
15	17.3125	1.22E-05
	Re-established Head	
7.5	9.75	1.29E-05
15	18	1.28E-05
	Re-established Head	
7.5	9.75	1.29E-05
15	18	1.28E-05

k_f (average): 1.27E-05

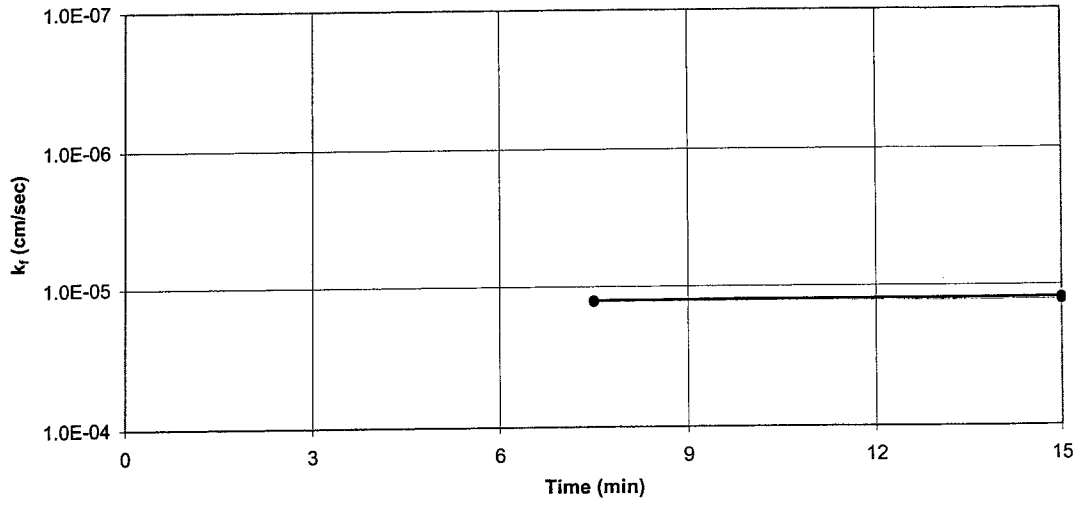

Field Permeablilty Testing Device

Phase III : Field Testing

Location : I-10, West Bound Lane - Jefferson County

Test ID: I10-7

Date : 11/2/99

Sieve Analysis

Sieve No.	Diameter (mm)	M_{sv} (g)	$M_{sv,s}$ (g)	M_s (g)	% Soil Retained	%Soil Passing
4	4.75	589.58	612.76	23.18	3.56	96.44
10	2.00	417.48	430.95	13.47	2.07	94.37
20	0.85	401.97	450.99	49.02	7.53	86.85
30	0.6	450.64	476.47	25.83	3.97	82.88
60	0.25	364.59	555.22	190.63	29.27	53.61
100	0.15	315.10	487.68	172.58	26.50	27.11
200	0.075	334.82	452.01	117.19	17.99	9.12
Pan	-	375.62	434.99	59.37	9.12	0.00
			Sum =	651.27		

Grain Size Distribution Curve

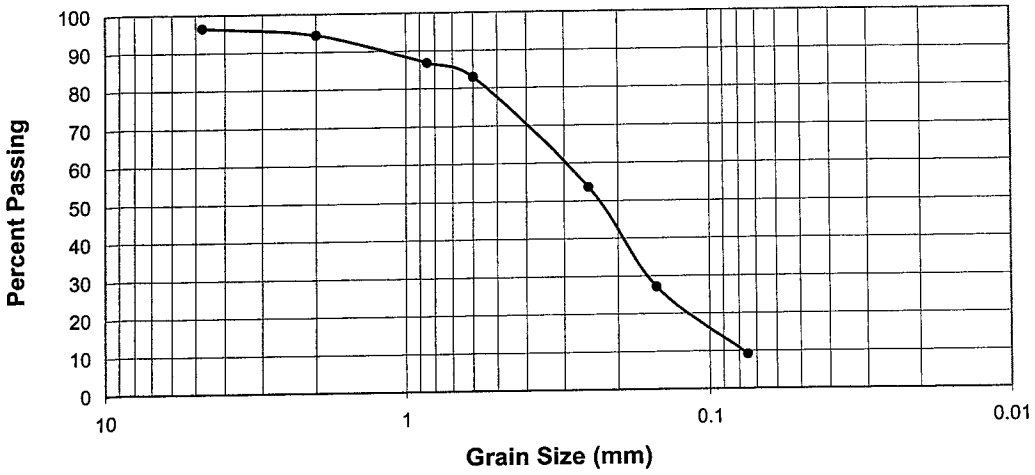

% Gravel :	3.56	D_{10} :	0.075
% Coarse Sand :	2.07	D_{30} :	0.16
% Medium Sand :	24.37	D_{60} :	0.3
% Fine Sand :	60.88	C_u :	4.0
% Fines :	9.12	C_z :	1.14

Field Permeablilty Testing Device

Phase III : Field Testing

Location : I-10, West Bound Lane - Jefferson County

Test ID: I10-8

Date : 11/2/99

Site Sketch

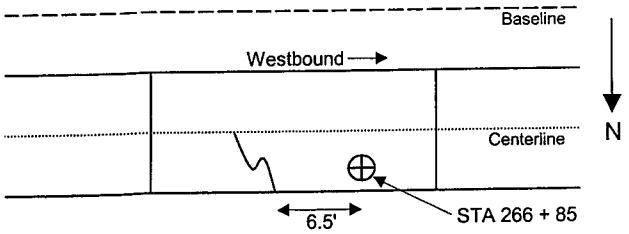

Profile

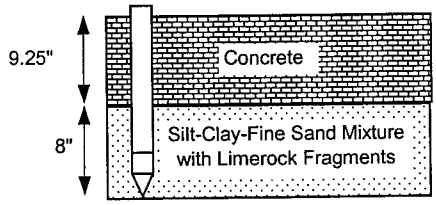

Falling Head Test

Sleeve Diameter (in):	0.775
Sleeve Length (in):	0.685
Shape Factor (cm):	8.208
Depth of Probe into Soil Layer (in):	8.0
Thickness of Concrete (in):	9.25
Standpipe Diameter (in):	0.25
Height of Water Above Concrete (in):	53.88

Time (min)	ΔH (in)	k_f (cm/sec)
7.5	1.19	1.48E-06
15	2.31	1.45E-06
30	4.44	1.41E-06
60	8.88	1.46E-06
90	13.13	1.49E-06

k_f (average): 1.46E-06

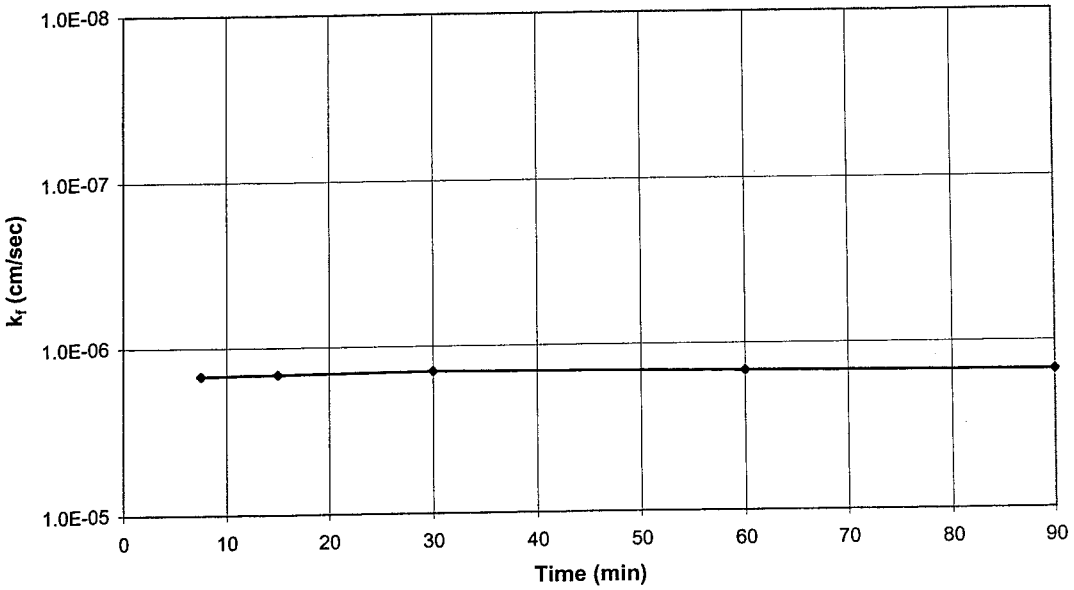

Field Permeablilty Testing Device

Test ID: I10-8
Phase III : Field Testing
Date : 11/2//99
Location : I-10, West Bound Lane - Jefferson County

Sieve Analysis

Sieve No.	Diameter (mm)	M_{sv} (g)	$M_{sv,s}$ (g)	M_s (g)	% Soil Retained	%Soil Passing
4	4.75	589.58	591.78	2.20	0.54	99.46
10	2.00	417.39	422.52	5.13	1.26	98.19
20	0.85	402.01	417.42	15.41	3.80	94.40
30	0.6	450.67	476.53	25.86	6.37	88.03
60	0.25	364.62	518.4	153.78	37.88	50.15
100	0.15	315.04	424.69	109.65	27.01	23.14
200	0.075	334.78	398.38	63.60	15.67	7.47
Pan	-	375.64	405.98	30.34	7.47	0.00
			Sum =	405.97		

Grain Size Distribution Curve

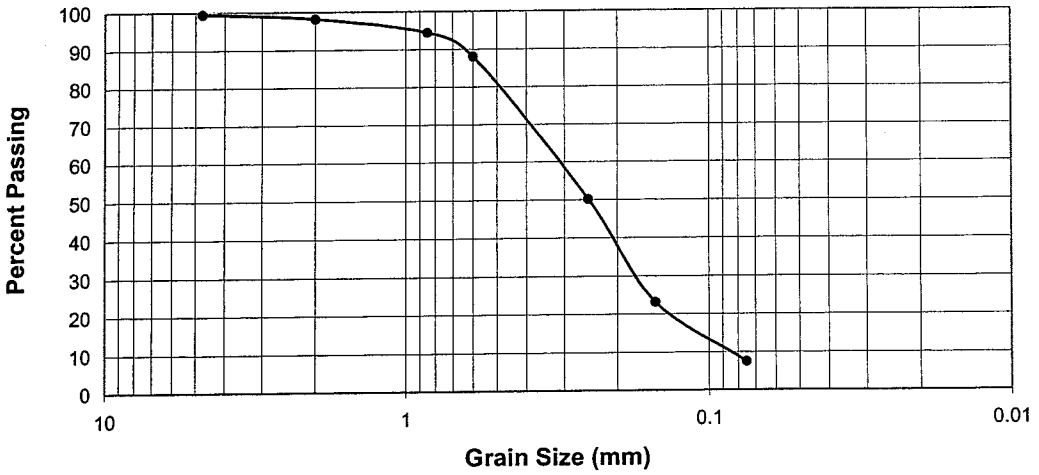

% Gravel :	0.54	D_{10} :	0.8
% Coarse Sand :	1.26	D_{30} :	0.17
% Medium Sand :	26.19	D_{60} :	0.3
% Fine Sand :	64.53	C_u :	0.38
% Fines :	7.47	C_z :	0.12

Field Permeablilty Testing Device

Phase III : Field Testing
Location : I-4 / Lakeland, FL

Test ID: I4
Date : 8/29/00

Test ID	STA	Pavement Condition	Depth (in)	k (cm/sec)
East Bound				
L1EA	851 + 98	bad	15.0	4.68E-05
L1EC	852 + 95	good	15.0	1.96E-06
L4EA	613 + 00	bad	15.0	9.41E-05
L4EC(a)	614 + 12	good	15.0	2.22E-05
L4EC(b)	614 + 12	good	23.5	4.95E-04
L5EA1(a)	676 + 76	bad	15.0	1.11E-05
L5EA1(b)	676 + 76	bad	23.0	1.96E-07
L5EC2	677 + 84	good	15.0	1.43E-06
L6EC2	718 + 78	bad	15.0	3.70E-06
L9EC1	650 + 86	bad	15.0	1.14E-04
L9EC2	651 + 36	good	15.0	2.76E-06
L10EC1	700 + 50	bad	15.0	3.07E-03
L10EC2	701 + 00	good	15.0	1.13E-05
L11EC	801 + 50	good	15.0	7.49E-06
L11EA	802 + 75	bad	15.0	8.34E-07
West Bound				
L1WC	852 + 00	good	15.0	2.84E-06
L1WA	848 + 00	bad	15.0	3.88E-05
L2WC	840 + 45	good	15.0	1.11E-04
L2WA	839 + 00	bad	15.0	2.37E-05

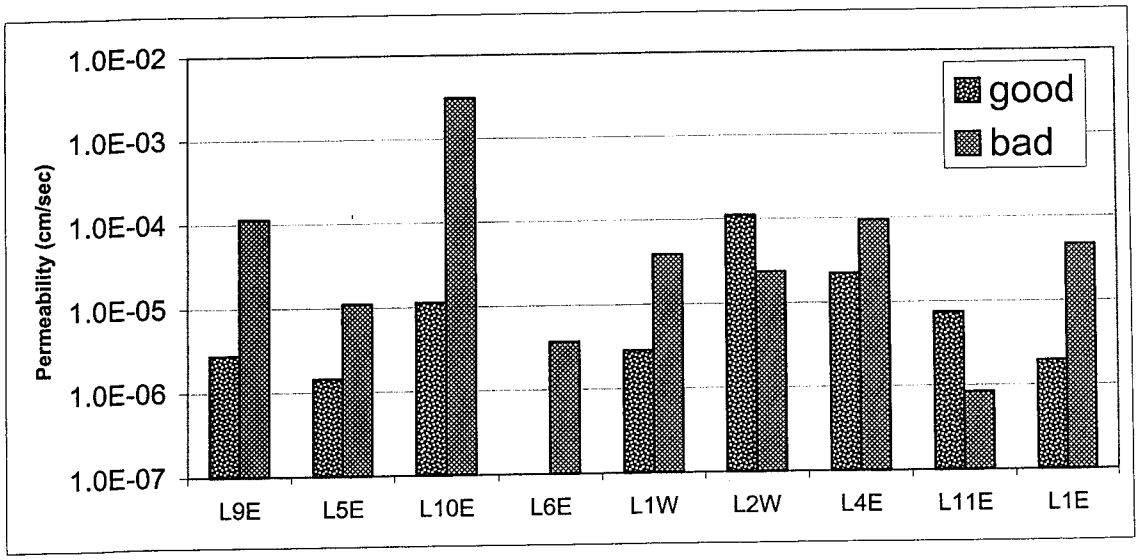

APPENDIX B
STANDARD OPERATING PROCEDURE

The procedure for operating the Field Permeability Testing Device is described in this appendix. The sequential observance of these guidelines is critical for proper operation of the device.

Towing Procedure

- A two-inch ball is required to properly secure the towing vehicle to the trailer.
- The towing vehicle must be able to accept a 7-pin male brake light cable connection.
- The towing vehicle must have a hauling capacity in excess of 7500 pounds.
- Prior to departure, check the following:
  - Brake lights function properly.
  - Tow hitch is securely locked.
  - Tires have sufficient air pressure.
  - Safety chains and the emergency brake chain are attached to the tow vehicle.
  - Hydraulic jacks are raised in the traveling position.
  - Center swivel plate is locked down with the traveling pin.
  - Probe guide is raised and shaft collars are tightened.

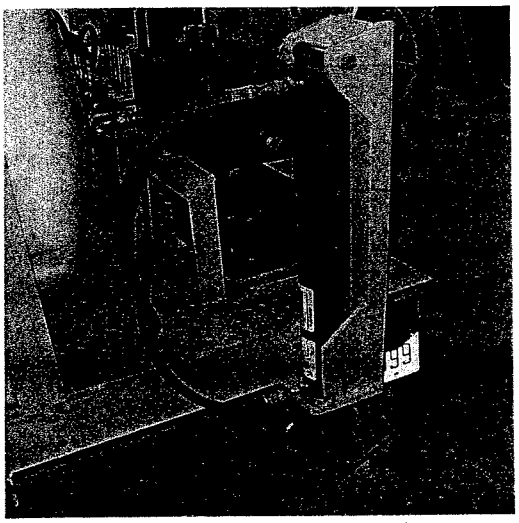

Hydraulic Leveling Jack

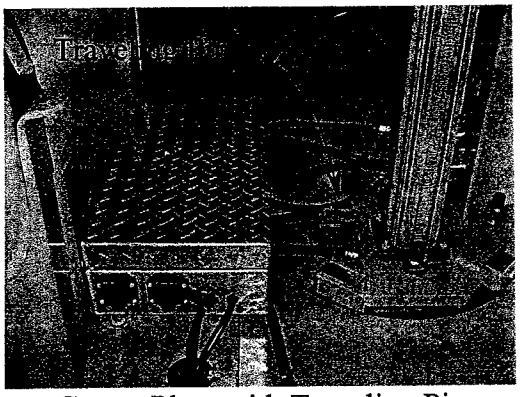

Center Plate with Traveling Pin

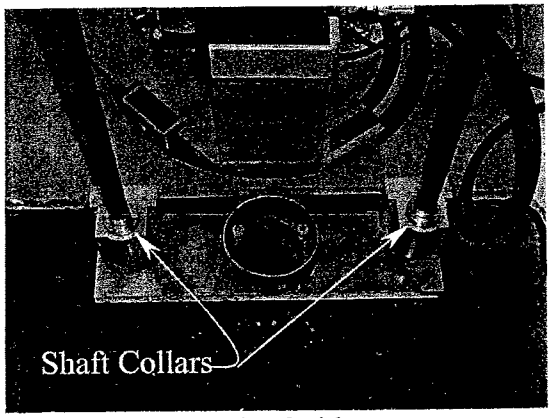

Probe Guide

Setup Procedure

- ❑ Loosen the hitch from the hitch ball.
- ❑ Connect the power supply cord from the trailer to the tow vehicle.
- ❑ Remove the traveling pin from the center swivel plate and lock the plate in position by raising the flat-jacks with the manual hand pump.
- ❑ Supply power to the hydraulic pump by turning the power switch near the pump to the ON position.
- ❑ Place the magnetic level on the center ram.
- ❑ Lower the jacks with the controls until all jacks touch the ground.
- ❑ Continue to raise and level the trailer until enough distance between the ground and the ram exists such that the probe can be attached. If the coring device is to be used, ensure that the core bit can be attached as well.
- ❑ Perform a final level check with the magnetic level.
- ❑ Turn the hydraulic power switch to the OFF position.

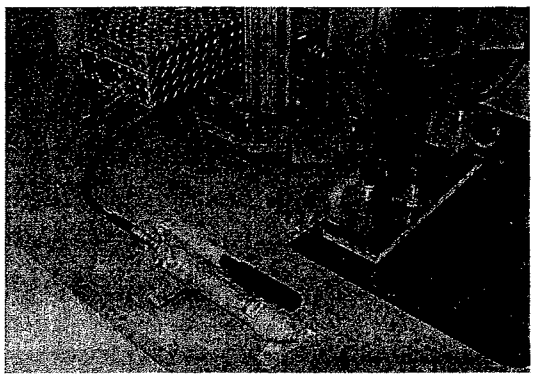

Manual Hand Pump

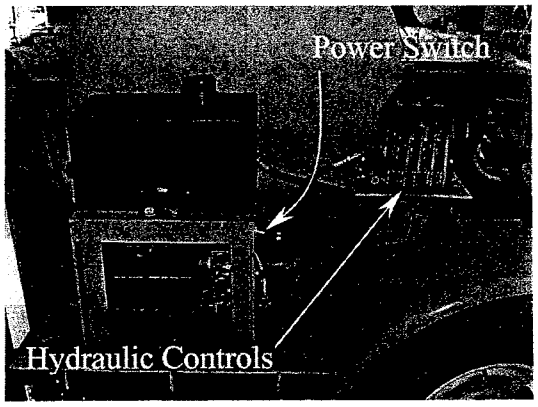

Hydraulic Pump and Controls

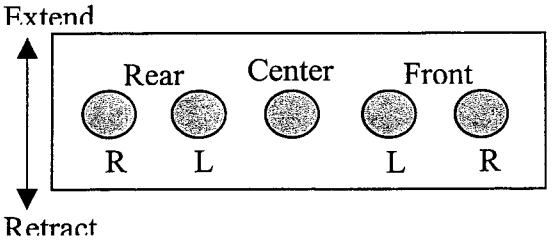

Hydraulic Control Diagram

Coring Procedure

- If a test is performed on an existing road, the coring device is required to provide access to the base and sub-base material.
- Attach the coring motor to the coring stand on the center swivel plate.
- Rotate the plate such that the coring device and stand is in the primary position.
- Lock the plate in position by raising the flat-jacks with the manual hand pump.
- Pass the coring bit through the center guide and attach to the coring motor.
- Connect a hose from the water tank to the water pump and then to the coring device.
- Connect the power cord of the coring motor to the transformer and the cord from the transformer to the generator.
- Turn the generator and the water pump on.
- Core through the road surface and remove.

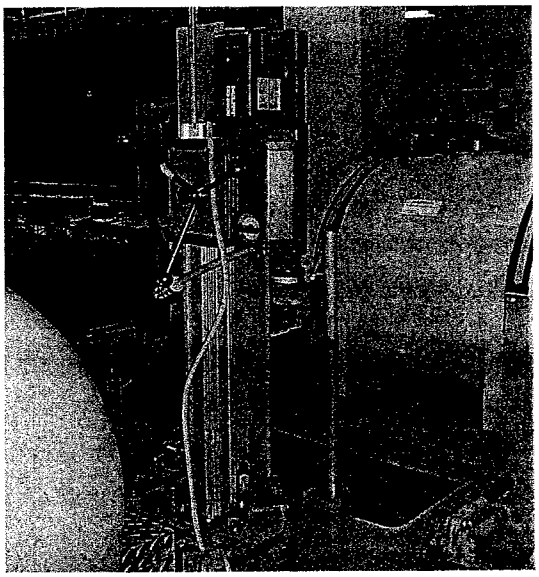

Coring Device on the Coring Stand

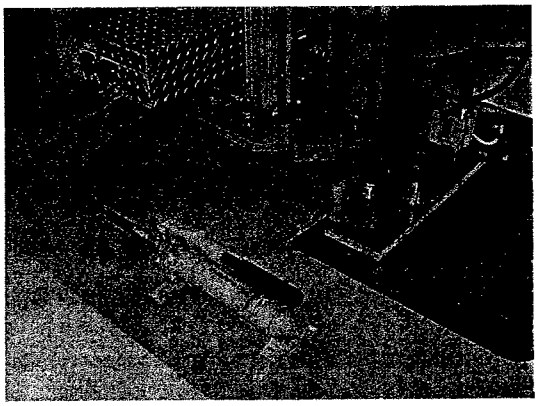

Manual Hand Pump

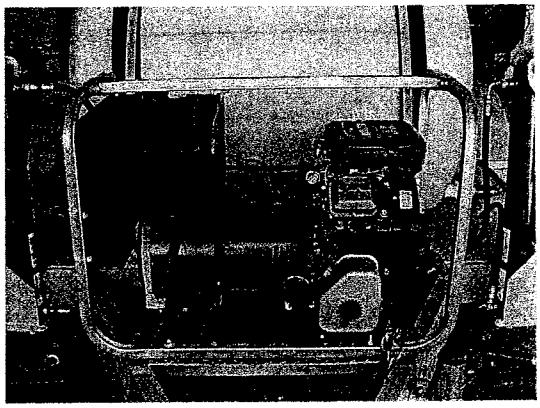

Generator

Test Preparation

- Connect the control box to the solenoid and flow meter housing box with the two 30 foot cables.
- Rotate the center plate until the ram is in the primary position. Lock the plate using the manual hand pump.
- Insert a porous element into the probe tip.
- Screw the probe tip onto the probe shaft.
- Slide the probe assembly through the guide sleeve and screw the probe into the hydraulic ram. Adjust the sleeve into the probe guide.
- Connect the water supply to the probe with the quick-connect.
- Determine the depth of penetration.
- Measure off the depth of penetration from a reference point on the probe guide and up the probe shaft. Place a mark at that point.
- Turn the hydraulic pump on and lower the probe until the mark is level with the reference point. Turn the hydraulic pump off.

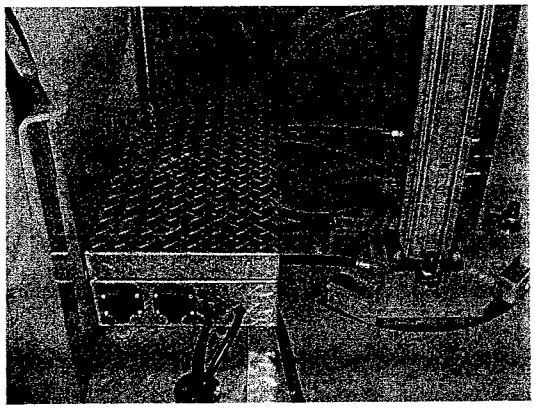

Solenoid and Flow Meter Housing

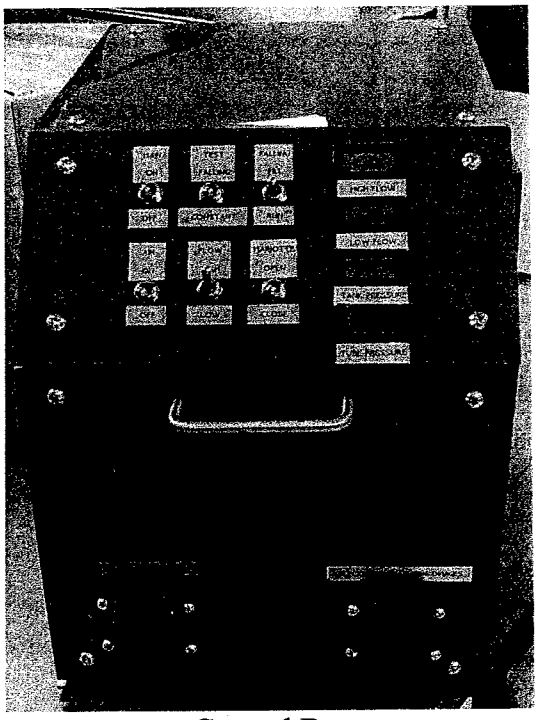

Control Box

- At the control panel turn the MAIN switch to the ON position, the TEST switch to CONSTANT, the FLOW switch to HIGH, and the MARIOTTE switch to OPEN.
- Ensure that the AIR switch is set to OFF and that the FALLING switch is at the center position.
- Open the bleed valve on the probe until the water fills the probe and exits the valve.
- Close the bleed valve. The system should now be air free.
- Verify that the pressure regulator is closed by turning the valve counterclockwise. Connect the air line to the nitrogen tank using the quick-connect.
- Open the valve on the nitrogen tank and set the tank regulator such that the exit pressure does not exceed 40-psi.
- Measure and record the height of the trailer bed.

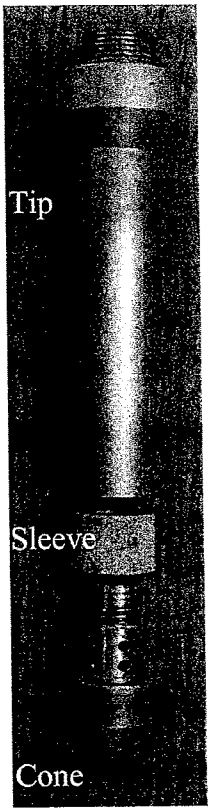

Probe Assembly

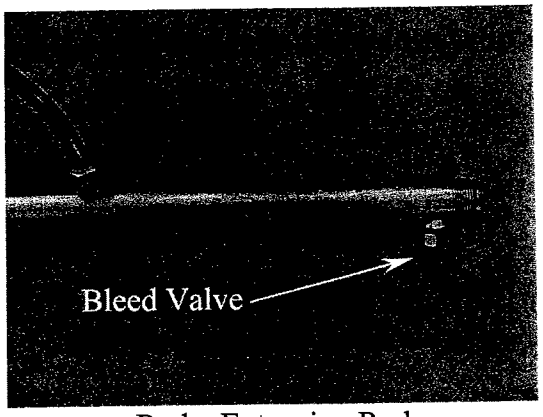

Probe Extension Rod

Constant Head Test Procedure

- Follow the Data Acquisition procedure before performing a test.
- At the Mariotte tank, ensure that the release valve is closed.
- At the control panel turn the MAIN switch to the ON position, the TEST switch to CONSTANT, the FLOW switch to HIGH, and the MARIOTTE switch to OPEN.
- Ensure that the AIR switch is set to OFF and that the FALLING switch is at the center position.
- If the flow rate is below 50 cm^3/min, then switch to the Falling Head Test Procedure.
- A real time graph of the flow and pressure values should be displayed on the laptop computer.
- When the flow rate has been stabilized for a period of 5 minutes (after a constant head of water has been applied), set the MARIOTTE switch to CLOSED.
- At the nitrogen controls, increase the pressure with the regulator such that an equivalent height of 15 inches of water has been added.
- Once the pressure in the Mariotte tank has stabilized, wait for the flow rate to stabilize for a period of five minutes.
- Return the MARIOTTE switch to OPEN and close the air supply.
- Continue until the pressure in the Mariotte tank has stabilized followed by the flow stabilizing for 5 minutes.
- The constant head test is complete.

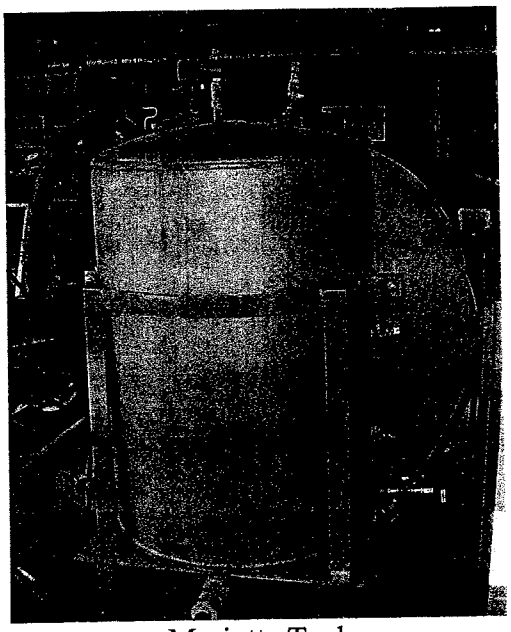

Mariotte Tank

Falling Head Test Procedure

- Setup the Data Acquisition system before performing a test.
- At the control panel turn the MAIN switch to the ON position, the TEST switch to FALLING, the FLOW switch to HIGH, and the MARIOTTE switch to CLOSED.
- Ensure that the release valve on the Mariotte tank is closed and add over 36 inches of equivalent pressure to the Mariotte tank using the nitrogen pressure system.
- Turn the FALLING switch to FILL.
- Fill the tube to the desired height. Note the height on the data acquisition display.
- If the tube is filling slowly or it does not fill to the desired height, supply more air pressure to the Mariotte tank.
- Turn the FALLING switch to the neutral position. Wait about 30 seconds to allow the computer to read the initial height.
- Turn the FALLING switch to the RUN position.
- After the desired time or water level has been reached, turn the FALLING switch to the neutral position.
- The time and change of height can be reduced from the data acquisition logger.
- Refill the tube and repeat the procedure for a minimum of 3 times.

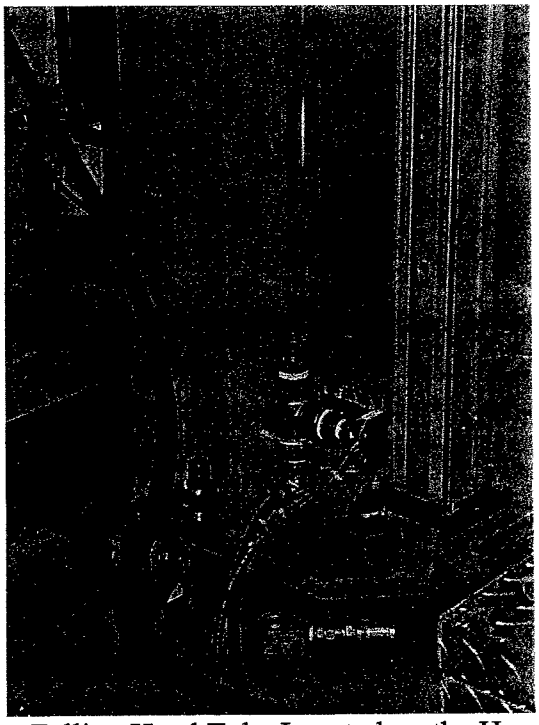

Falling Head Tube Located on the H-Beam.

Test Conclusion

After running the constant and/or falling head test, the probe can be pushed to another depth. Mark the incremental change on the probe first and record the new depth. Redo the procedure outlined for the constant and/or falling head test.

When the test is completed verify and perform the following:

- ☐ The pressure relief valve is open on the Mariotte tank.
- ☐ The MARIOTTE switch is on OPEN.
- ☐ Close and then disconnect the nitrogen tank.
- ☐ Turn the TEST switch to neutral.
- ☐ Set the MAIN switch OFF.
- ☐ Turn the hydraulic pump on and raise the probe.
- ☐ Remove the probe from the ram, raise the probe guide, and lower the trailer.
- ☐ Clean the probe assembly and the porous element.
- ☐ Refer to the Towing Procedure

Data Acquisition

- Connect the data acquisition cable from the control box to the PCMCIA card on the laptop computer.
- Turn the computer on.
- Select the LOGGER icon from the desktop
- When the program loads, select the EDIT pull down menu.
- Select SETTINGS.
- The LOGGER SETTING window should appear.
- Select the FILE CONFIG… button.
- The FILE CONFIGURATION window should appear.
- Under the FILE NAME, type the name of the file to be saved.
- Check the ENABLE LOGGING box.
- Check the BEGIN LOGGING ON START box.
- Select the OK button.
- Select the OK button from the LOGGER SETTING window.
- Select the START button at the bottom of the main screen.
- A real time graph of the pressure and flow rates should appear on the screen.
- Move the cursor on the graph to far right end.
- When the test is completed, select the STOP button on the main screen.
- Close the program.
- For data reduction, open the file in Excel.

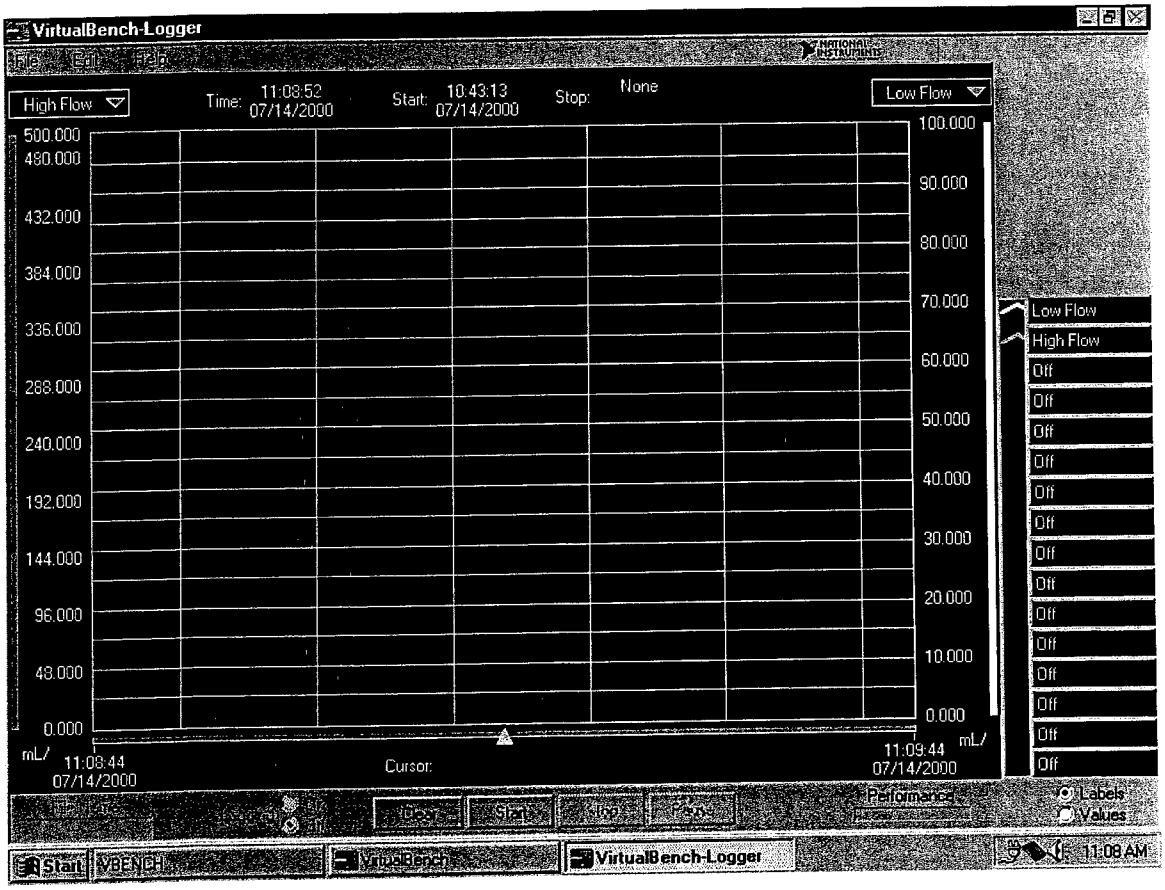

Start-up Screen

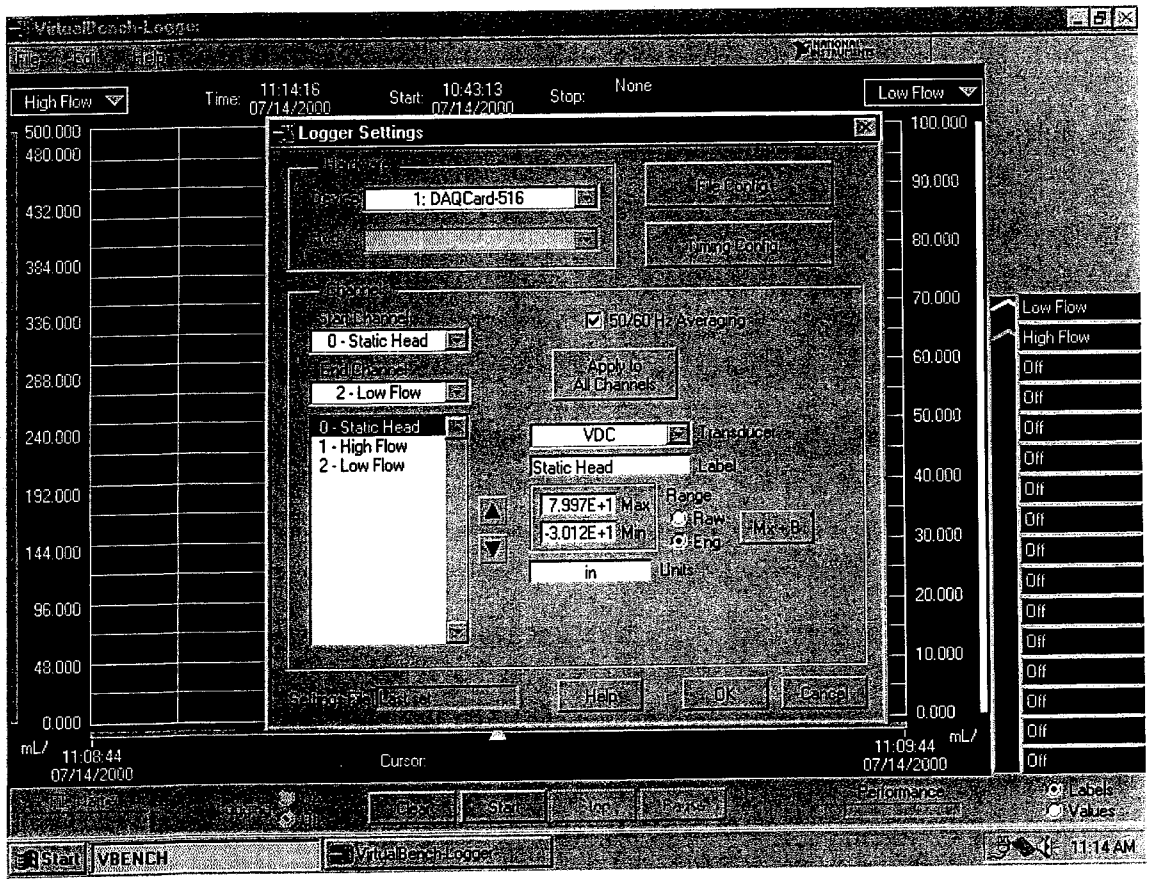

Logger Settings Window

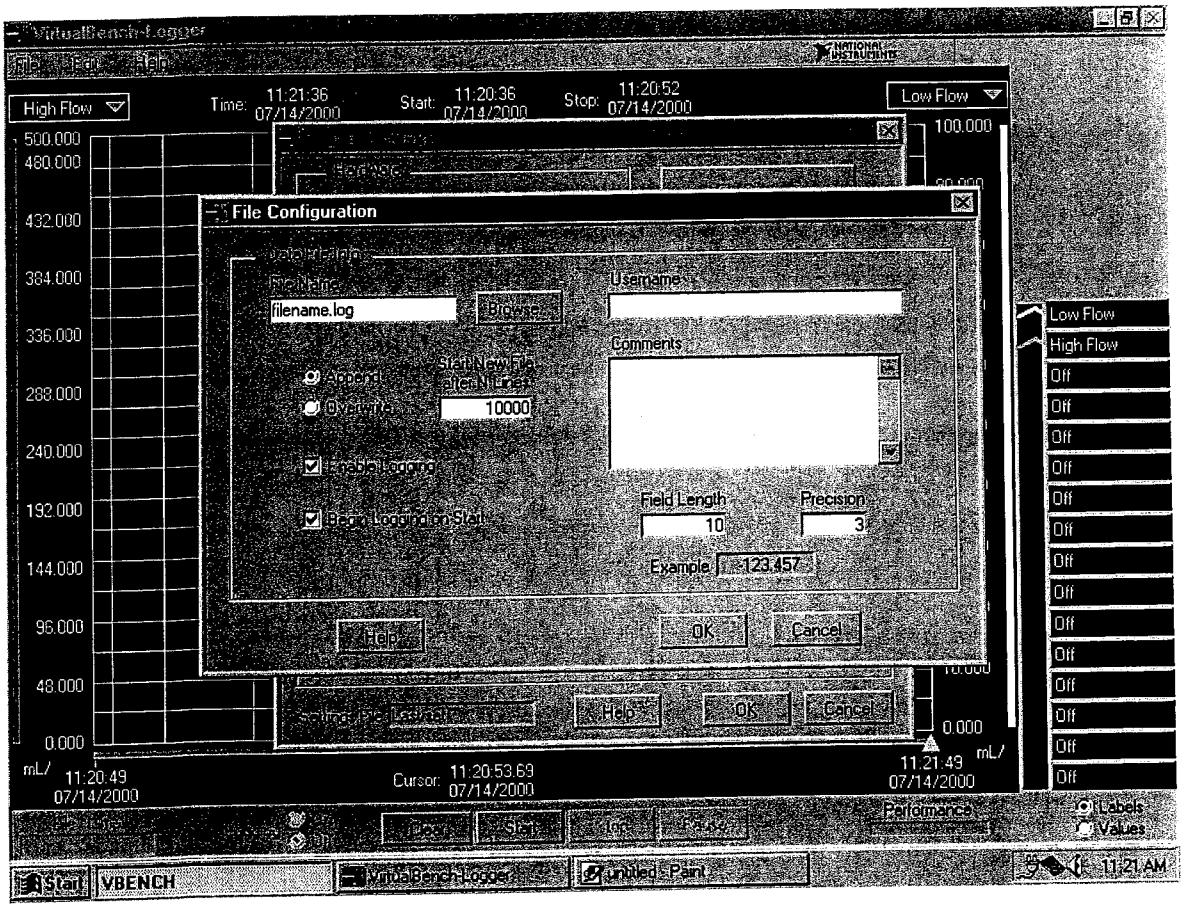

File Configuration Window

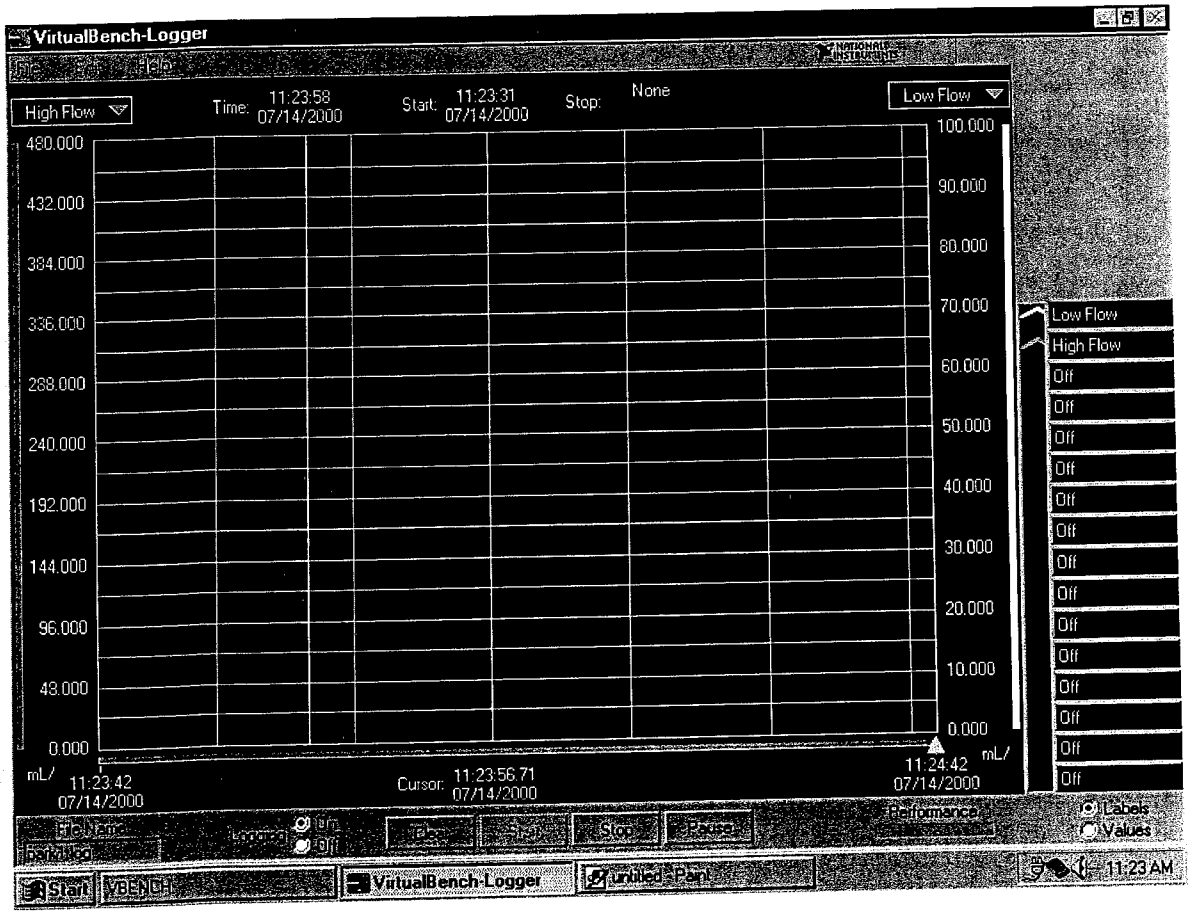

Final Screen

Obtaining GPS Coordinates

- ❑ Connect the GPS receiver to the serial port on the back of the laptop computer.
- ❑ Turn on the computer.
- ❑ Insert the Street Atlas software in the CD drive.
- ❑ Select the Street Atlas icon from the Windows desktop.
- ❑ Select the GPS pull down menu.
- ❑ Select the INITIALIZE button.
- ❑ Click NEXT.
- ❑ Click NEXT.
- ❑ Click FINISH.
- ❑ The MONITOR GPS STATUS window should appear.
- ❑ Select the POSITION tab and wait for the GPS status to indicate the 3-D fix has been achieved.
- ❑ Coordinates are obtained from either the current window or the main screen.

APPENDIX C
CALCULATION SHEET

The formulas for calculating the permeability from the constant and falling head test are provided in this appendix.

Calculating the Permeability from the Constant Head Test

$$k = \frac{q}{F \cdot (h + h_h) \cdot \left(60 \frac{sec}{min}\right)}$$

where k = permeability (cm/sec)

q = flow rate (cm^3/min)

h = reading from the Mariotte pressure transducer (cm)

h_h = height from the pressure transducer to the porous stone (cm)

F = shape factor equal to 12.2 cm.

Calculating the Permeability from the Falling Head Test

$$k = \frac{A}{F \cdot t} \cdot \ln\left(\frac{h_i + h_h}{h_f + h_h}\right)$$

where k = permeability (cm/sec)

A = cross sectional area of the falling head tube (cm^2)

F = shape factor equal to 12.2 cm

h_i = initial height of the water above the falling head pressure transducer (cm)

h_f = final height of the water above the falling head pressure transducer (cm)

h_h = height from the falling head pressure transducer to the porous stone (cm)

t = duration of time for the water to fall from h_i to h_f (sec).

APPENDIX D
CONTROL BOX ELECTRICAL DIAGRAM

Control Box Electrical Diagram

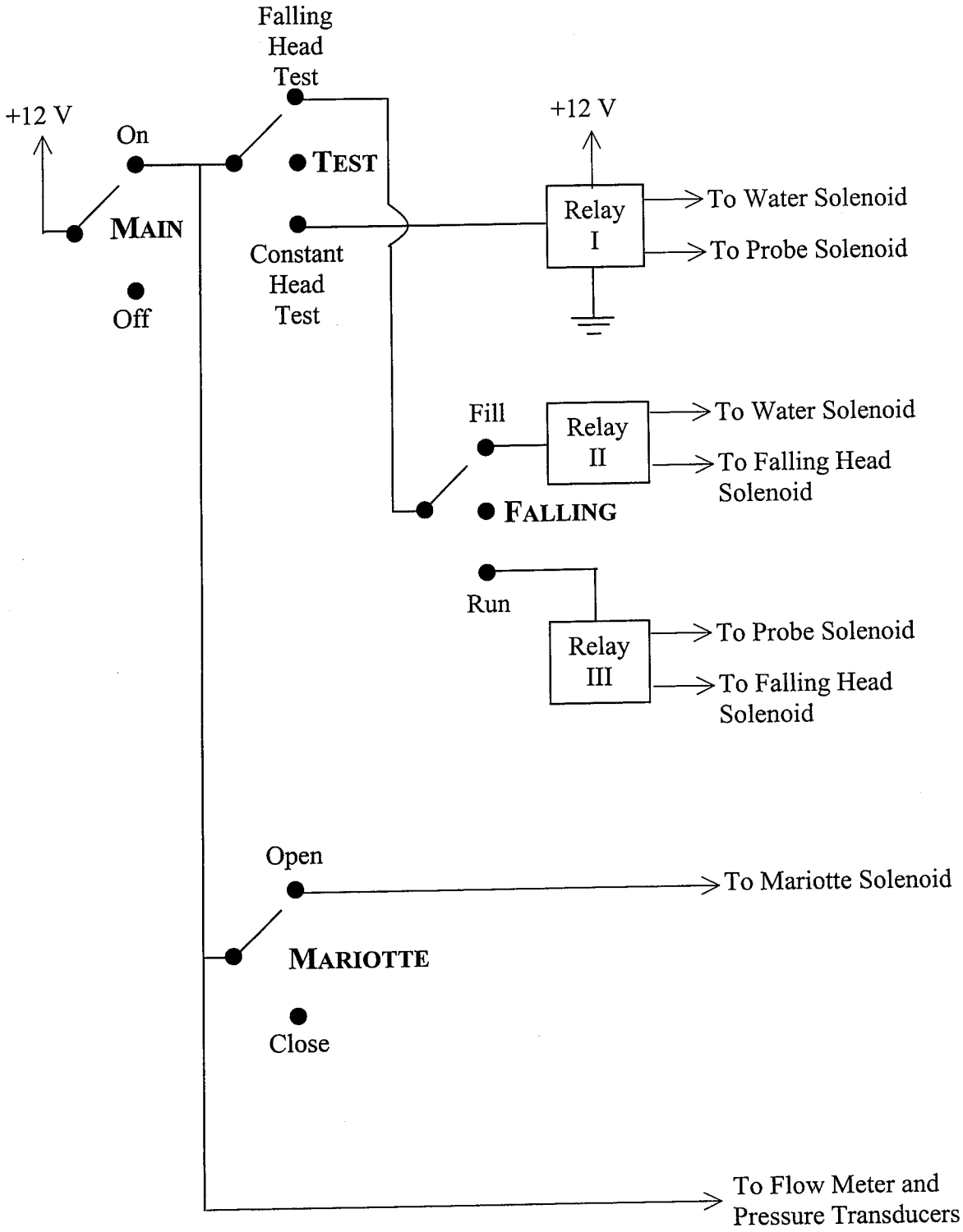

LIST OF REFERENCES

Cedergren, H.R., Drainage of Highways and Airfield Pavements, Robert E. Krieger Publishing Company, Malabar, Florida, 1987.

Cedergren, H.R., Seepage, Drainage, and Flow Nets (3rd ed.), Wiley-Interscience, New York, 1989.

Daniel, D.E., "In Situ Hydraulic Conductivity Tests for Compacted Clay," Journal of Geotechnical Engineering, ASCE, Vol. 115, No. 9, 1989, pp. 1205-1225.

Davidson, J.L., Soil Mechanics Laboratory Manual, University of Florida, Gainesville, Florida, Spring 1998.

Harr, M.E., Groundwater and Seepage, McGraw-Hill, New York, 1962.

Hvorslev, M.J., "Time Lag and Soil Permeability in Groundwater Observations," Bulletin No. 36, Waterways Experiment Station, Corps of Engineers, Vicksburg, Mississippi, 1951.

Meletiou, C.A., "Development of a Field Permeability Test for Assessing the Durability of Concrete in Marine Structures," University of Florida, Gainesville, Florida, 1991.

Olson, R.E., & Daniel, D.E., "Measurement of the Hydraulic Conductivity of Fine Grained Soils," ASTM STP 746, American Society for Testing and Materials, 1981,
pp. 18-64.

Sharma, H.D., & Lewis, S.P., Waste Containment Systems, Waste Stabilization, and Landfills Design and Evaluation, Wiley-Interscience, New York, 1994.